

Distribution Agreement

In presenting this thesis or dissertation as a partial fulfillment of the requirements for an advanced degree from Emory University, I hereby grant to Emory University and its agents the non-exclusive license to archive, make accessible, and display my thesis or dissertation in whole or in part in all forms of media, now or hereafter known, including display on the world wide web. I understand that I may select some access restrictions as part of the online submission of this thesis or dissertation. I retain all ownership rights to the copyright of the thesis or dissertation. I also retain the right to use in future works (such as articles or books) all or part of this thesis or dissertation.

Signature:

Adeiye Ayodele Pilgrim

Date

The Yes-Associated Protein (YAP) promotes resistance to anti-GD2 immunotherapy in neuroblastoma through downregulation of *ST8SIA1*

By

Adeiye Ayodele Pilgrim

Doctor of Philosophy

Graduate Division of Biological and Biomedical Sciences

Cancer Biology

Kelly C. Goldsmith, MD
Advisor

Melissa Gilbert-Ross, PhD
Committee Member

Adam Marcus, PhD
Committee Member

Chrystal Paulos, PhD
Committee Member

Steven Sloan, MD PhD
Committee Member

Accepted:

Kimberly Jacob Arriola, PhD, MPH
Dean of the James T. Laney School of Graduate Studies

The Yes-Associated Protein (YAP) promotes resistance to anti-GD2 immunotherapy in neuroblastoma through downregulation of *ST8SIA1*

By

Adeiyé Ayodele Pilgrim

B.S., Hollins University, 2015

Advisor: Kelly C. Goldsmith, MD

An abstract of
A dissertation submitted to the faculty of the James T. Laney School of Graduate Studies of
Emory University
in partial fulfillment of the requirements for the degree of
Doctor of Philosophy
in
Graduate Division of Biological and Biomedical Sciences
Cancer Biology

2023

Abstract

The Yes-Associated Protein (YAP) promotes resistance to anti-GD2 immunotherapy in neuroblastoma through downregulation of *ST8SIA1*

By

Adeiyeye Ayodele Pilgrim

Pediatric patients with high-risk neuroblastoma often relapse with chemotherapy-resistant, incurable disease. Relapsed neuroblastomas harbor chemo-resistant mesenchymal tumor cells and increased expression/activity of the transcriptional co-regulator, the Yes-Associated Protein (YAP). Patients with relapsed neuroblastoma are often treated with immunotherapy such as the anti-GD2 antibody, dinutuximab, in combination with chemotherapy. Since YAP mediates both chemotherapy and MEK inhibitor resistance in relapsed *RAS* mutated neuroblastoma, we posited that YAP might also be involved in anti-GD2 antibody resistance. We now show that YAP inhibition significantly enhances sensitivity of mesenchymal neuroblastomas to dinutuximab and gamma delta ($\gamma\delta$) T cells both *in vitro* and *in vivo*. Mechanistically, YAP inhibition induces increased GD2 cell surface expression through upregulation of *ST8SIA1*, the gene encoding GD3 synthase, the rate-limiting enzyme in GD2 biosynthesis. The mechanism of *ST8SIA1* suppression by YAP is independent of *PRRX1* expression, a mesenchymal master transcription factor, suggesting YAP may be the downstream effector of mesenchymal GD2 resistance. These results therefore identify YAP as a potential therapeutic target to augment GD2 immunotherapy responses in patients with neuroblastoma.

The Yes-Associated Protein (YAP) promotes resistance to anti-GD2 immunotherapy in neuroblastoma through downregulation of *ST8SIA1*

By

Adeiyé Ayodele Pilgrim

B.S., Hollins University, 2015

Advisor: Kelly C. Goldsmith, MD

A dissertation submitted to the faculty of the James T. Laney School of Graduate Studies of
Emory University
in partial fulfillment of the requirements for the degree of
Doctor of Philosophy
in
Graduate Division of Biological and Biomedical Sciences
Cancer Biology

2023

Acknowledgments

My path to the MD PhD program at Emory has been circuitous. I am so thankful for the love and support of my friends from childhood, high school, college, and here at the EUSOM. I started the journey to a career in science and medicine when, right out of St. Augustine Girls' High School (SAGHS), I entered the Bachelor of Medicine, Bachelor of Surgery (MBBS) program in 2005 at the University of West Indies, Mona in Kingston, Jamaica. I was devastated when I was diagnosed with a severe case of clinical depression which required that I take a medical leave of absence. During that time, my psychologist, Dr. Dianne Douglas, my family, and friends, helped me to a healthier place until I was able to return to my academic pursuits through the Horizons program for non-traditional students at Hollins University in Roanoke, VA in 2011.

At Hollins University, I met my first scientific mentor, Dr. Jonathan Stoltzfus, who encouraged me to always ask questions and be open to answers that are unexpected. Thank you, Jonathan, for believing in my intelligence when I lacked confidence, for always encouraging me to do and be better, both personally and professionally. I consider you an amazing mentor, example, and friend. While at Hollins, I also met a friend for life, Dr. Mennatallah Albarqi, who has seen me at my best and at my worst and has accepted, encouraged, and consistently supported me through thick and thin. I am so grateful to have you in my life, Menna!

Throughout my PhD, I have been supported by many individuals without whom this would have been impossible. My first dissertation project in Dr. Robert Schnepf's lab examined the role of the RNA-binding protein MSI2 in neuroblastoma, providing a strong foundation for the dissertation in Dr. Kelly Goldsmith's lab that you see before you now. I am so grateful for your examples as physician scientists, Bob and Kelly! Kelly - I learned how my future career could look by observing the strong clinical trial portfolio, research program and balance of work/life that you have robustly established. During both projects, I had the privilege of working and learning alongside and from a group of talented and enthusiastic individuals including, but not limited to: Cara, Claire, Dailia, Hunter, Jenny, Jodi, Julie, Leon, Raaven, and Selma – amazing scientists and people (and for some of you, excellent clinicians as well).

My family has been at my side from the very start – thanks to my mother, Garthlyn, father, Clyde, sister, Alake, and brother, Chike and more recent additions to our family - my nephew and niece, Chiedu and Onyedikachi. From you, mummy, I learned what it looks like to be a mother and a physician, thank you for caring for and loving us unconditionally. Daddy – you inspired me to always seek knowledge, thank you. When I could barely make it over the finish line while writing this dissertation, you sat with me and helped pull me along (you have been my rock all my life) – thank you, Alake. I have always felt supported, protected by and ready to laugh with you, big brother, Chike, thank you! My in-laws have been at my side as though we were born into the same family. Thank you, Barbara and Thelbert; Regina, Eric and Michael for your continuous presence and love in my life. To my aunties who are like mummies – Auntie Monica: you took care of me from infancy to adulthood (almost!) and then have been doing the same for my son. Your example of sacrifice and caring is amazing. Auntie Selva – we connected later in life, but you have shown me how to live your true self unabashedly and to embrace creativity – thank you. I couldn't have asked for better loved ones – the Craig, Pilgrim, Hicks, Henry, and extended families!

At EUSOM, I met and married my best friend, Dr. Curtis James Henry. Together, we have built a beautiful life. I love you and I am inspired by you as a scientist, father, friend, and life partner. I

can't wait to see what we do together! To my son, Chidi who said "You've got this, mama!" at my toughest moments this year, you motivate me to be my best self. I love you all.

Table of Contents

Chapter I: Introduction	1
1.1 Definition, diagnosis, risk stratification, and treatment of neuroblastoma.....	1
1.1.1 Clinical presentation and diagnosis of neuroblastoma	1
1.1.2 Risk stratification and classification of neuroblastoma	2
1.1.3 Treatment of neuroblastoma.....	3
1.2 Genetic alterations in neuroblastoma	4
1.2.1 <i>MYCN</i> amplification.....	5
1.2.2 <i>ALK</i> mutations	6
1.2.3 Telomere maintenance mechanisms and chromosomal segmental alterations.....	8
1.2.4 RAS/MAPK pathway activation.....	11
1.3 Developmental origins and phenotypic plasticity of neuroblastoma	13
1.3.1 Developmental origins of neuroblastoma	13
1.3.2 Phenotypic plasticity of neuroblastoma.....	14
1.4 Summary of the content of this dissertation	18
Chapter II: The role of the Yes-Associated Protein (YAP) and its paralog, transcriptional co-activator with PDZ-binding motif (TAZ) in cancer	19
2.1 Structure, signaling, and function of YAP and TAZ.....	19
2.1.1 Structure of YAP/ TAZ	19
2.1.2 Regulation of YAP/ TAZ.....	20
2.1.3 Mechanisms of transcriptional control by YAP/TAZ.....	26
2.2 Cell-autonomous and tumor microenvironmental functions of YAP/TAZ in tumorigenesis.....	29
2.2.1 Tumor cell-autonomous functions of YAP/TAZ in cancer	30
2.2.2 The tumor microenvironmental role of YAP/TAZ in cancer.....	32
2.3 Therapeutic targeting of YAP/TAZ	35
2.4 The role of YAP/TAZ in neuroblastoma.	36
Chapter III: $\gamma\delta$ T cell biology, GD2 and GD2-targeting immunotherapies ..	38
3.1 The biology of $\gamma\delta$ T cells	38
3.1.1 Development, structure and function of $\gamma\delta$ T cells	38
3.1.2 $\gamma\delta$ T cells in cancer	40
3.1.3 $\gamma\delta$ T cells as an immunotherapy	43
3.2 The glycosphingolipid GD2 and its biological significance	46
3.2.1 Glycobiology and biosynthesis of GD2	46
3.2.2 GD2 expression in cancers including neuroblastoma	48
3.3 GD2-targeting immunotherapies	49
3.3.1 GD2 as a cancer immunotherapeutic target	49
3.3.2 Optimizing response to anti-GD2 immunotherapy	51

Chapter IV: The Yes-Associated Protein (YAP) promotes resistance to anti-GD2 immunotherapy in neuroblastoma through downregulation of <i>ST8SIA1</i>.	55
4.1 Introduction	55
4.2 Materials and Methods	58
4.3 Results	64
4.4 Discussion	76
4.5 Supplementary figures and tables	80
Chapter V: Conclusions and Future Directions	92
5.1 Summary of findings and implications of this study	92
5.2 Limitations of this work and future directions	93
5.2.1 Mechanism of YAP-GD2 regulation in neuroblastoma	93
5.2.2 The role of TAZ in regulation of GD2 in neuroblastoma.....	95
5.2.3 Role of YAP inhibition in sensitization to $\gamma\delta$ T cell cytotoxicity.....	96
5.3 Overall Conclusions	97
References	99

List of Figures

Figure 1.1. Treatment schema for high-risk neuroblastoma

Figure 1.2. Summary figure of important neuroblastoma genetic alterations

Figure 1.3. Phenotypic plasticity in neuroblastoma.

Figure 2.1. The structures of YAP and its paralog, TAZ.

Figure 2.2. The Hippo Pathway signaling cascade.

Figure 2.3. Transcriptional regulation by YAP/TAZ.

Figure 3.1. Expression of cell surface receptors and ligands on V δ 1 and V δ 2 $\gamma\delta$ T cell subsets.

Figure 3.2. Antitumorigenic effects of $\gamma\delta$ T cells.

Figure 3.3. Ganglioside biosynthesis.

Figure 3.4. Structures of GD2-targeting monoclonal antibodies.

Figure 4.1. YAP expression is high in neuroblastoma cell lines that are resistant to anti-GD2/ $\gamma\delta$ T cell immunotherapy.

Figure 4.2. Genetic inhibition of YAP increases in vitro response to anti-GD2/ $\gamma\delta$ T cell immunotherapy with corresponding upregulation of GD2 surface expression in SK-N-AS.

Figure 4.3. YAP inhibition mediates significantly increased gene expression of the GD2 biosynthetic enzyme, *ST8SIA1*.

Figure 4.4. GD3S (*ST8SIA1*) inhibition reverses the phenotypes of increased GD2 surface expression and sensitivity to anti-GD2/ $\gamma\delta$ T cell immunotherapy when YAP is inhibited in SK-N-AS cells.

Figure 4.5. *YAP* and *ST8SIA1* expression are negatively correlated in primary neuroblastoma tumors, low *ST8SIA1* expression is associated with worse overall survival and *YAP* and GD2 are inversely correlated in neuroblastoma patient derived xenografts (PDXs).

Figure 5.1. Model showing the role of YAP in response to $\gamma\delta$ T cell/dinutuximab immunotherapy in neuroblastoma.

Supplementary Figure S4.1. Representative gating strategy for apoptotic cells in neuroblastoma cytotoxicity assays (at 1:1 effector:target ratio).

Supplementary Figure S4.2. Representative gating strategy for GD2 cell surface expression in neuroblastoma cell lines by flow cytometry.

Supplementary Figure S4.3. Early degranulation (CD107a) is unchanged in $\gamma\delta$ T cells post-co-culture with SK-N-AS control and shYAP1 cells with or without dinutuximab treatment.

Supplementary Figure S4.4. Immunophenotyping of $\gamma\delta$ T cells co-cultured with SK-N-AS control, shYAP1 and shYAP2 cells for 24 hours.

Supplementary Figure S4.5. YAP does not affect expression of tumor stress antigens, DNAM-1 ligands, and death receptors on SK-N-AS cells

Supplementary Figure S4.6. IFN γ release $\gamma\delta$ T cells is increased when co-cultured with SK-N-AS shYAP cells in the presence of dinutuximab.

Supplementary Figure S4.7. Ectopic expression of YAP 5SA and YAP S94A in SMS-SAN cells reduces GD2 cell surface expression.

Supplementary Figure S4.8. Genetic inhibition of TAZ in SK-N-AS neuroblastoma cells does not cause increased cell surface expression of GD2.

Supplementary Figure S4.9. Genetic ablation of YAP in SK-N-AS neuroblastoma cells does not cause increased cell surface expression of GD2 but results in compensatory TAZ binding to TEAD2.

Supplementary Figure S4.10. Inhibition of YAP in SK-N-AS NB cells prolongs survival of mice treated with cyclophosphamide (CYCLO)/ dinutuximab (DIN)/ $\gamma\delta$ T cell ($\gamma\delta$ T) chemoimmunotherapy.

Supplementary Figure S4.11. Gene expression of enzymes in the biosynthetic pathway of GD2.

Supplementary Figure S4.12. Gene expression of *YAP* and *ST8SIA1* in dually transduced control or *YAP/ST8SIA1* knockdown models.

The figures in chapters 1, 2, 3, and 5 were created with BioRender.com.

List of Tables

Table 1.1. List of genes encoding the transcription factors in the core regulatory circuitry of neuroblastoma cells

Supplementary Table S4.1. Antibodies used for western blot and co-immunoprecipitation.

Supplementary Table S4.2. Antibodies used to profile $\gamma\delta$ T cells for use in cytotoxic assays.

Supplementary Table S4.3. Antibodies used for determination of *in vitro* or *in vivo* GD2 surface expression of neuroblastoma cells.

Supplementary Table S4.4. Antibodies used for in-depth characterization of expanded $\gamma\delta$ T cells pre- and post-cytotoxicity assay.

Supplementary Table S4.5. Primer sequences

Chapter I: Introduction

1.1 Definition, diagnosis, risk stratification, and treatment of neuroblastoma

1.1.1 Clinical presentation and diagnosis of neuroblastoma

Neuroblastomas develop in the sympathetic nervous system. Although they may present in any portion of the peripheral nervous system, the most common primary sites are the adrenal gland, followed by abdominal, thoracic, cervical, and pelvic sympathetic ganglia. While neuroblastomas may be localized to sympathetic chain ganglia and the adrenal gland, they may also rapidly metastasize to multiple organs including the bone, bone marrow, liver, and lymph nodes.¹

To make a definitive diagnosis of neuroblastoma, biopsy of the primary tumor, followed by histology, is recommended. Additionally, elevation of urinary catecholamine metabolites such as homovanillic acid and vanillylmandelic acid is indicative of neuroblastoma disease. More extensive imaging such as computed tomography or magnetic resonance imaging is the next step in the process as this gives further resolution of the mass(es) and reveals whether metastasis has occurred.¹ Upon confirmation of a neuroblastoma diagnosis, an ¹²³I-metaiodobenzylguanidine (MIBG) scan is performed to detect additional lesions, particularly if there is bony metastatic disease. In contrast, the higher dose radioactive isotope of ¹³¹I-MIBG is reserved for treatment of neuroblastoma.

The clinical presentation of neuroblastoma is highly heterogeneous, with some patients experiencing spontaneous regression of their disease and others succumbing to rapid disease progression, multi-organ metastasis or relapse after initial response to multimodal therapy. To standardize the approach to the patient with neuroblastoma, systems of risk stratification and staging have been established in geographical regions in which neuroblastoma has been extensively studied.

1.1.2 Risk stratification and classification of neuroblastoma

A consensus group consisting of representatives from Europe, Japan, and the United States, formulated the initial system for neuroblastoma risk stratification/classification and staging, the International Neuroblastoma Staging System (INSS).^{2,3} The purpose of the INSS was to standardize classification systems to allow for comparison of clinical trials and biologic studies, informing diagnostic and potential treatment approaches. One of the major premises underlying the INSS was the degree of surgical resection of the neuroblastoma that was performed.

Two decades after the INSS was established, based on significant advancements in understanding of neuroblastoma tumor genetics and biology, the International Neuroblastoma Risk Group (INRG) Task Force established updated risk classification and staging systems called the INRG Classification System and International Neuroblastoma Risk Group Staging System (INRGSS).^{4,5} The updated staging system was necessary to transition from the surgically-based INSS to a system based on image-defined risk factors.⁵ Instead of post-surgical staging, pre-operative images were implemented to define a patient's stage of neuroblastoma disease. Using the INRGSS allowed for pretreatment risk classification for treatment planning and clinical trial assignment.

The first iteration of the INRGSS risk classification/stratification is extensive; briefly, it combines INRG stage, age at diagnosis, tumor histology and differentiation, *MYCN* amplification state, 11q alteration, and ploidy to stratify patients into pretreatment risk groups from very low risk to high risk.⁴ Finally, the Children's Oncology Group (COG) has, in parallel, established a risk classifier system that was initially based on the INSS and other genomic and biologic neuroblastoma markers. The most recent iteration of the COG risk classifier incorporates the INRGSS and considers the significant role of segmental chromosomal aberrations (SCAs) as a biomarker in neuroblastoma.⁶ These parameters are used to define neuroblastoma as low-, intermediate-, or high-risk.

1.1.3 Treatment of neuroblastoma

The treatment plan for a patient with neuroblastoma is based on an integration of the risk classification that was described in 1.1.2 and incorporates the following: disease stage, age of the patient, INRGSS, presence of *MYCN* amplification and/or segmental chromosome alterations, and histologic appearance. The most intensive treatment approach is employed for patients with high-risk neuroblastoma. This regimen includes a combination of surgery, chemotherapy, autologous hematopoietic stem cell transplantation, radiation, differentiation therapy, and immunotherapy (**Figure 1.1**).

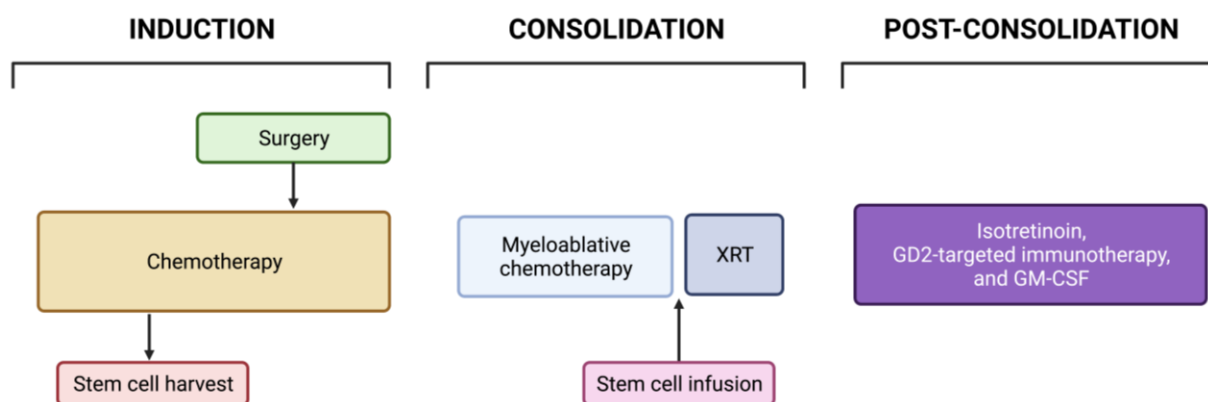


Figure 1.1. Treatment schema for high-risk neuroblastoma including the induction, consolidation, and post-consolidation (maintenance) phases of treatment. This image is adapted from Pinto *et al.*, 2015⁷

The induction phase of treatment includes multiagent chemotherapy, measures of local control such as cytoreductive surgery; followed by consolidation with high-dose chemotherapy, autologous stem cell harvest and radiation therapy, and a post-consolidation period with immunotherapy and differentiation therapy.¹ The induction regimen includes five cycles of multiagent chemotherapy with topotecan, cyclophosphamide, vincristine, doxorubicin, cisplatin, and etoposide.⁸ Autologous hematopoietic stem cell transplantation follows induction chemotherapy and cytoreductive surgery.⁹ Patients with high-risk neuroblastoma are typically

apheresed at the end of 2 cycles of chemotherapy. The stem cell product is re-infused during the consolidation phase of treatment. Finally, the role of the post-consolidation phase is to target minimal residual disease, and this typically consists of dinutuximab, a monoclonal antibody targeting the disialoganglioside, GD2, granulocyte-macrophage colony-stimulating factor (GM-CSF), as well as differentiation therapy, isotretinoin.⁷

Despite this aggressive approach, there is a subset of patients who either do not initially respond that is, are primary refractory, or patients with tumor recurrence or relapsed neuroblastoma. Next-generation sequencing efforts have mapped the targetable mutations that are enriched in relapsed neuroblastoma.¹⁰⁻¹² Indeed, in models that recapitulate relapsed neuroblastoma in mice, patient derived xenograft (PDX) neuroblastoma tumors were enriched for mesenchymal gene signatures and closely resembled immature Schwann cell precursors transcriptionally.¹³

Chemoimmunotherapy, a combination of irinotecan, temozolomide, dinutuximab, and GM-CSF, has been effective in patients with multiply relapsed neuroblastoma, recommending its integration into standard up-front therapeutic regimens.^{14,15} However, there is still minimal understanding of the biomarkers of response, mechanisms of resistance to chemoimmunotherapy, and the potential approaches to overcoming these resistance mechanisms.

1.2 Genetic alterations in neuroblastoma

Neuroblastoma tumors have a paucity of somatic mutations when compared to adult cancers.¹⁶ However, there are genetic alterations which are characteristic of neuroblastoma, at diagnosis and relapse, which inform the establishment of potential therapeutic targets. These genetic alterations include, at diagnosis, amplification of the v-myc myelocytomatosis viral related oncogene, neuroblastoma derived (*MYCN*) gene,¹⁷⁻¹⁹ telomerase maintenance mechanisms (TMMs)^{20,21} and

segmental chromosomal alterations.^{1,22,23} Although activating mutations of the receptor tyrosine kinase, anaplastic lymphoma kinase (*ALK*) are also present at diagnosis, they are enriched at relapse.²⁴⁻²⁸ In contrast, activating mutations of the rat sarcoma virus (*RAS*) are rarely present at diagnosis but significantly enriched at relapse.^{11,29}

1.2.1 MYCN amplification

The *MYC* family of genes consists of *MYC* (which encodes c-MYC or MYC), *MYCL* (which encodes L-MYC), and *MYCN* (which encodes N-MYC or MYCN). All MYC transcription factors have a basic helix-loop-helix/leucine zipper structure and bind to the MYC Associated Factor X (MAX), forming a heterodimer which recognizes the consensus sequence, E-box, 5'-CANNTG-3', to regulate expression of target genes.^{30,31} *MYCN* is located on chromosome 2p24.3 and was identified and cloned in 1983.^{17,19} While MYC is ubiquitously expressed, the tissue distribution of L-MYC is less well understood, and MYCN is restricted to central and peripheral nervous system tissues.³² The repressive functions of MYC are well-established as it forms a ternary complex with MAX and the Myc-interacting zinc finger protein (MIZ1, also known as ZBTB17) to block the induction of cell cycle inhibitors *CDKN2B* and *CDKN1A* (p21^{WAF1}) by antimetogenic stimuli.^{33,34} However, interactions of MYCN with MIZ1 are weaker and few examples of transcriptional repression occurring downstream of this interaction exist in the literature, except for regulation of the orphan receptor gene, neuronal leucine-rich repeat protein-3 (*NLRR3*).^{35,36} In contrast, MYCN mediates repression through an epigenetic mechanism by binding Enhancer Of Zeste homolog 2 (EZH2), an enzymatic catalytic subunit of the polycomb repressor complex 2 (PRC2).³⁷ *MYCN* is either overexpressed or amplified in several tumors of neuroendocrine origin including neuroblastoma, medulloblastoma, castration-resistant/neuroendocrine prostate cancer and small-cell lung cancer.^{38,39}

Amplification of *MYCN* is found in approximately 25% of cases of neuroblastoma and is the most well-characterized indicator of poor prognosis and high-risk neuroblastoma disease.^{39,40} However, *MYC* is also shown to drive tumorigenesis in some non-*MYCN*-amplified high-risk neuroblastomas through a phenomenon called enhancer hijacking.⁴¹ Primary non-*MYCN*-amplified and *MYCN*-amplified neuroblastoma tumors and cell lines generally have an inverse correlation between expression of *MYC* and *MYCN*, suggesting overlapping roles in neuroblastoma tumorigenesis.⁴¹ The non-*MYCN*-amplified neuroblastoma cell line, SK-N-AS, the model that is primarily used in this dissertation, expresses high levels of *MYC*, and has a highly aggressive, therapy-resistant phenotype as a result of oncogenic *MYC*-driven transcriptional programs.

The oncogenic function of *MYCN* in neuroblastoma was confirmed by forced expression in neural crest cells leading to formation of primitive neuroectodermal tumors including neuroblastoma.⁴² In neuroblastoma, *MYCN* has pleiotropic roles in regulation of angiogenesis, metabolic reprogramming, cell survival and proliferation, self-renewal and differentiation, metastasis, as well as immune surveillance.⁴³ *MYCN* also transcriptionally activates telomerase reverse transcriptase (*TERT*) and thus, its expression is correlated with *TERT* in neuroblastoma.^{44,45} Regardless of *MYCN* amplification state, high *MYCN* expression in neuroblastoma tumors is associated with worse prognosis; indicating its involvement in neuroblastoma progression and solidifying it as a clinical determinant of risk stratification for patients with neuroblastoma.⁴⁶

1.2.2 *ALK* mutations

In 2000, the receptor tyrosine kinase (RTK), *ALK*, which is located on chromosome 2p23, was shown to be highly expressed through amplification in neuroblastoma cell lines.⁴⁷ The structure of *ALK* includes an N-terminal glycine-rich extracellular ligand-binding domain, a hydrophobic

transmembrane domain, and an intracellular kinase domain.^{48,49} The extracellular domain of ALK also consists of a heparin-binding domain (HBD), 2 membrane-proximal meprin A5 protein and receptor protein tyrosine phosphatase mu (MAM) domains which flank a low-density lipoprotein class A (LDL_A) motif and closest to the plasma membrane is a glycine-rich motif which it shares with its closest relative within the insulin receptor superfamily, leukocyte tyrosine kinase (LTK).⁴⁹ Although the structure of ALK has been long elucidated, its ligands have not been recognized until more recently; these include the cytokines ALK And LTK Ligand 1/2 (ALKAL1/2) and FAM150A/B.⁵⁰⁻⁵²

Fusion proteins between ALK and nucleophosmin-1 (NPM1) or echinoderm microtubule-associated protein-like 4 (EML4), which cause constitutive signaling of the kinase domain, were discovered in ALK-positive anaplastic large cell lymphoma and non-small-cell lung cancer, respectively.⁵³⁻⁵⁵ However, although rearrangements of ALK in neuroblastoma also lead to increased activity of the protein, these are rare.^{56,57} More commonly, aberrant ALK activation in neuroblastoma is linked to hotspot mutations in its kinase domain.²⁴⁻²⁷ The functional consequence of these hotspot mutations in *ALK* are substitutions at amino acid residues R1275 (43%), F1174 (30%), and F1245 (12%), among others, which lead to constitutive activity because of loss of the autoinhibitory ALK protein conformation.⁵⁸ The oncogenic role of ALK mutations was established through the ability of its F1174L and R1275Q variants to transform interleukin-3-dependent murine haematopoietic Ba/F3 cells to cytokine-independent growth.²⁷ The resultant ligand-independent signaling of ALK through its downstream pathways such as Janus kinase-signal transducer and activator of transcription protein (JAK/STAT) and RAS/mitogen-activated protein kinase (MAPK) signaling, leads to increased proliferation and decreased apoptosis of cells with these mutations.⁵⁹ Additionally, one of the recently discovered ALK ligands, ALKAL2, independently potentiates oncogenic growth in *MYCN*-amplified neuroblastoma in the absence of ALK mutations.⁶⁰

Familial neuroblastoma, although rare, is inherited in an autosomal dominant pattern and most often linked to *ALK* mutations as well as mutations in the paired-like homeobox 2B gene (*PHOX2B*).^{25,61,62} *ALK* mutations occur equally in *MYCN*-amplified and *MYCN*-non-amplified neuroblastoma.²⁵ Since *ALK* and *MYCN* are genomic neighbors on chromosome 2p, it is possible that co-amplification may occur. There are several generations of *ALK* inhibitors that were synthesized to inhibit this oncogene, including the first-generation (crizotinib), second-generation (ceritinib, alectinib, brigatinib, and ensartinib), and third-generation (lorlatinib).⁶³ Inhibition of *ALK* either genetically or pharmacologically has shown promise in preclinical models of neuroblastoma.⁶⁴ The first-generation *ALK* inhibitor, crizotinib, showed greater efficacy in the treatment of tumors harboring an *ALK* translocation versus *ALK*-mutated tumors in patients with anaplastic large cell lymphoma, non-small cell lung cancer (NSCLC), inflammatory myofibroblastic tumors, and neuroblastoma.⁶⁵

Unfortunately, mechanisms of resistance to the first generation of *ALK* inhibitors evolved, requiring the development of combination treatment approaches or use of later generation *ALK* inhibitors with alternative mechanisms of action.⁶⁶ Indeed, neuroblastoma cells have developed resistance mechanisms to even the most recent generation of *ALK* inhibitor, lorlatinib.⁶⁷ Inhibition of *ALK* with or without chemotherapy is of significant therapeutic interest for neuroblastoma as a phase I clinical trial showed that the response rate in combination with chemotherapy for patients with relapsed/refractory neuroblastoma under 18 years old was 63%.⁶⁸ Consequently, targeting of *ALK* remains a promising approach for treatment of high-risk *ALK*-driven neuroblastoma at diagnosis and relapse.

1.2.3 Telomere maintenance mechanisms and chromosomal segmental alterations

Telomeres are complex structures located at the end of chromosomes which maintain chromosomal structural integrity and genome stability. In the setting of cancer, telomeres are

maintained primarily by the increased activity of the telomerase enzyme and more rarely, by alternative lengthening of telomeres (ALT).^{69,70} Mechanisms of telomere maintenance are commonly present in high-risk neuroblastoma.⁷¹ The critical catalytic subunit of telomerase is encoded by *TERT* which is located on chromosome 5p15.33.⁷² Dysregulation of TERT occurs in up to 90% of cancers as it enabled replicative immortality, one of the hallmarks of cancer.⁷³⁻⁷⁵

Telomere maintenance mechanisms (TMMs) are a determinant of clinical outcome in neuroblastoma given that patients with neuroblastoma tumors with low *TERT* expression and no alternative lengthening of telomeres have significantly better overall survival than those with high *TERT* expression or ALT.⁷¹ Increased *TERT* expression is the main mechanism of telomerase activation and this is accomplished in multiple ways in most cancers including *TERT* promoter mutations, *TERT* rearrangements, and *TERT* amplification.⁷⁶ However, the major mechanism of increased *TERT* expression in neuroblastoma is *TERT* rearrangement.^{20,21} These rearrangements approximate enhancer elements with the *TERT* coding sequence, resulting in massive overexpression of *TERT*.²¹ Furthermore, telomerase activation, through *TERT* rearrangements or *MYCN* amplification leading to increased *TERT* expression, is prognostic of the worst overall survival outcomes in high-risk neuroblastoma and enriched in recurrent neuroblastoma, nominating inhibition of TERT as a potential therapeutic strategy in these contexts.^{77,78} Indeed, recent studies have leveraged bromodomain and extraterminal domain (BET) family inhibitors in combination with proteasome inhibition to epigenetically inhibit *TERT* and such inhibitors are being investigated in clinical trials of heavily pre-treated patients with pediatric solid tumors ([NCT03936465](#)).⁷⁹⁻⁸¹

Alternative lengthening of telomeres (ALT) is the other TMM that is employed in neuroblastoma.⁸² While ALT-positive neuroblastomas more commonly exist in the high-risk subset of the disease, there are ALT-positive tumors which do not fall into this group. ALT leads

to resistance to irinotecan and temozolomide, chemotherapeutic drugs commonly used in neuroblastoma salvage therapy, which can be reversed by inhibition of Ataxia-telangiectasia mutated (ATM) as a synthetic lethal pairing.⁷¹ Around 55-60% of all ALT-positive tumors have loss-of-function mutations of alpha-thalassemia/mental retardation, X-linked (ATRX) and/or low abundance of ATRX protein.^{71,83} Alpha-thalassemia/mental retardation, X-linked (ATRX) is involved in transcriptional regulation and chromatin remodeling as a member of the SWItch/Sucrose Non-Fermentable (SWI/SNF) family of proteins.⁸⁴ Loss of function mutations in the *ATRX* gene that lead to truncations of ATRX protein have been found in up to 10% of neuroblastoma tumors.^{23,85,86} Interestingly, *ATRX* inactivating mutations and *MYCN* amplification, another indicator of poor prognosis in neuroblastoma, are mutually exclusive in both engineered murine models of neuroblastoma and human neuroblastoma tumors.⁸⁶ These data suggest a role for TMM in neuroblastoma disease progression and relapse.

Chromosomal instability is a feature of cancer. This instability may lead to alterations in total number of chromosomes, or aneuploidy, as well as gain, loss, or rearrangement of chromosomal arms, segmental chromosomal alterations (SCAs). In neuroblastoma, chromosomal instability may be a consequence of telomere maintenance mechanisms.⁷¹ In neuroblastoma, aneuploidy is often associated with better prognosis; whereas, SCAs generally are associated with worse prognosis.⁸⁷ Furthermore, chromothripsis, massive genomic rearrangement which occurs in a single event, is found to occur in almost 20% of high-risk neuroblastomas and is associated with worse prognosis.⁸⁸ Thus, methods of analyzing these events such as copy number profiling of cell-free DNA is of clinical value in neuroblastoma.⁸⁹

Many recurrent SCAs have been reported in neuroblastoma tumors including, but not limited to, loss of chromosomes 1p,⁹⁰⁻⁹² 3p,⁹³ 4p,⁹⁴ 9p,⁹⁵⁻⁹⁷ 11q,^{98,99} and 14q^{98,100} and gain of 1q, 2p and 17q.^{91,92,101,102} Loss of 1p and 11q has specifically been associated with worse outcomes and have

recently been recommended to assist in risk stratification of specific subsets of patients with metastatic spread of *MYCN*-NA neuroblastoma.⁶ For some of these SCAs, there is a clear loss of tumor suppressor or gain of oncogene function.^{103,104} However, in other cases, it is less well-defined how these changes affect neuroblastoma tumor aggressiveness, although it is likely because of the compounding effects of multiple genomic alterations.

1.2.4 RAS/MAPK pathway activation

The RAS family of proteins consists of HRAS, KRAS, and NRAS. Like *MYCN*, the structure and sequence of NRAS was discovered in 1983.¹⁰⁵⁻¹⁰⁹ RAS proteins cycle between a GTP-bound and GDP-bound state; GTP-bound RAS is formed by guanine nucleotide exchange factors (GEFs) and GTPase activating proteins (GAPs) catalyze the conversion from active RAS-GTP to inactive RAS-GDP.¹¹⁰ The RAS family member that is predominantly expressed in neuroblastoma is NRAS. Autophosphorylation of RTKs on the cell surface membrane results in binding and signaling through adaptor proteins such as SHC and growth factor receptor-bound protein 2 (GRB2), leading to activation of GEFs like SOS, which convert RAS to its active RAS-GTP form.¹¹⁰ Each of the five isoforms of NRAS have differential downstream effects on its canonical pathways, including activation of phosphatidylinositol 3-kinase (PI3K)/AKT and rapidly accelerated fibrosarcoma (RAF)/MAPK signaling to varying degrees (**Figure 1.2**).¹¹¹ Early indications of the oncogenic role of RAS signaling in neuroblastoma arose because forced HRAS expression using the dopamine-beta-hydroxylase promoter in mouse neuroblasts led to the development of neuroblastomas *in vivo*.¹¹²

Although RAS mutations are rare in neuroblastoma at diagnosis, a genetic signature indicative of RAS hyperactivation has been shown to be involved in neuroblastoma tumor progression.²⁹ Indeed, activation of the RAS-MAPK pathway and its upstream drivers is characteristic of a large proportion of recurrent neuroblastoma tumors.¹⁰⁻¹² The presence of RAS mutations in

neuroblastoma is also associated with poor patient outcomes regardless of *MYCN* amplification state.⁸²

Upstream mediators of RAS signaling which are also mutated in neuroblastoma include the RTK, ALK, neurofibromin (*NF1*), and protein tyrosine phosphatase non-receptor type 11 (*PTPN11*) which encodes src homology region 2 domain phosphatase (SHP2). The role of ALK in neuroblastoma is described in an earlier section. Neurofibromin (*NF1*) encodes a GAP and loss of *NF1* occurs in several neuroblastoma cell lines, inducing hyperactive RAS signaling and resistance to retinoic acid or differentiation therapy which is commonly used in the post-consolidation phase of treatment of patients with neuroblastoma (**Figure 1.1**).^{113,114} Loss of *NF1* and hyperactive RAS signaling, particularly through the *NRAS*^{Q61K} recurrent mutation led to an increased susceptibility of neuroblastoma cells to SHP2 inhibition.^{115,116} Activating mutations in *PTPN11* (encodes SHP2) occur in about 3% of neuroblastomas.^{23,117} The consequence of *PTPN11* activating mutations, like loss of *NF1*, is hyperactive RAS signaling. Since these alterations converge on downstream oncogenic signaling pathways, their effects similarly lead to more aggressive neuroblastoma disease.

In RAS-mutated neuroblastoma,^{118,119} rhabdomyosarcoma,¹²⁰ and pancreatic ductal adenocarcinoma tumors,¹²¹ there is increased expression of the Yes-associated protein (YAP), mediating resistance to targeted inhibitors and chemotherapy. The enrichment of RAS mutations and increased YAP expression in relapsed neuroblastoma provide a basis for YAP inhibition in this clinical context and the role of YAP will be further explored in chapter 2 of this dissertation.

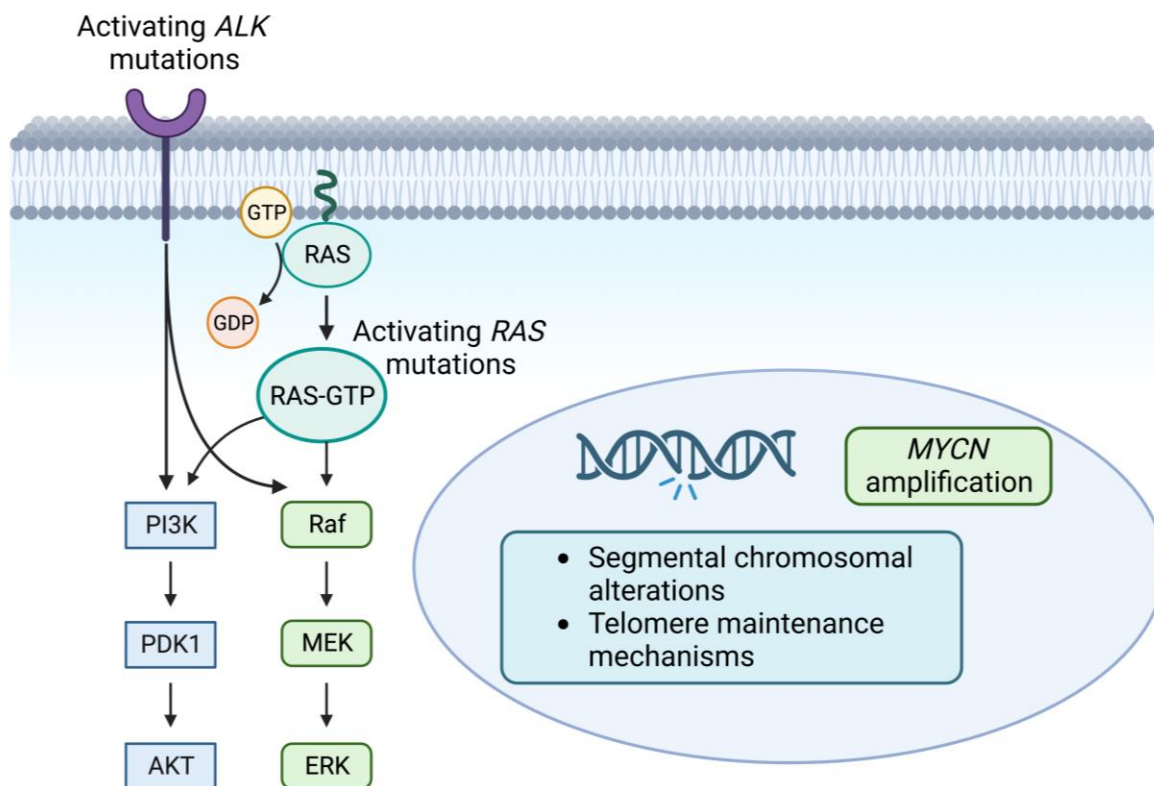


Figure 1.2. Summary figure of important neuroblastoma genetic alterations modified from Matthay *et al.*, 2016.¹

1.3 Developmental origins and phenotypic plasticity of neuroblastoma

1.3.1 Developmental origins of neuroblastoma

Studies to determine the neuroblastoma cell of origin have been very recently accelerated by technologies such as single-cell RNA sequencing (scRNA-seq) which examine gene expression programs at high resolution. One hypothesis in the field is that the developmental origin of neuroblastoma can be traced to cells arrested at various precursor stages of the mature human sympathetic nervous system including neural crest cells.^{122,123} Spatiotemporal tracing of neural crest developmental programs in mouse embryos using scRNA-seq, revealed that many of these precursors closely resembled neuroblastoma cells.^{124,125} In humans, a comparative approach was adopted which analyzed single-cell transcriptomics of malignant cells from patient-derived, treatment-naive, neuroblastoma tumors relative to putative cells of origin from early human

embryos and fetal adrenal glands.¹²⁶⁻¹²⁹ These studies determined that neuroblastoma tumor cells most closely resemble fetal noradrenergic chromaffin cells in their transcriptional programs. Further studies combining lineage tracing and assessment of epigenetic and transcriptional states may be necessary to unequivocally identify neuroblastoma cancer-initiating cells.

Cell-of-origin studies provide a mechanistic basis for understanding neuroblastoma tumor development and progression. However, after the tumor-initiating genetic changes have occurred, there are divergent phenotypes of neuroblastoma cells. Thus, recent study has been focused on studying neuroblastoma phenotypic plasticity and how underlying molecular circuitry may explain the heterogeneity of clinical presentations of neuroblastoma.

1.3.2 Phenotypic plasticity of neuroblastoma

The intratumoral and inter-individual heterogeneity of neuroblastoma led to the hypothesis that neuroblastoma cells may be differentially sensitive to the therapies.¹³⁰ The first evidence for phenotypic plasticity of neuroblastoma cells arose from studies in 1983 of morphologically distinct neuroblast-like and epithelial cells in the same culture of a neuroblastoma cell line.¹³¹ Other research has since validated phenotypic plasticity in neuroblastoma by identifying and characterizing the presence of two major subtypes - a (nor)adrenergic subtype and mesenchymal/neural crest-like cells, with a fleeting transitional state that is intermediate (**Figure 1.3**).¹³²⁻¹³⁴ Phenotypic plasticity is the newest addition to the paradigm of cancer hallmarks and in the last decade, there have been multiple recent research studies focused on understanding phenotypic plasticity in neuroblastoma.⁷⁵

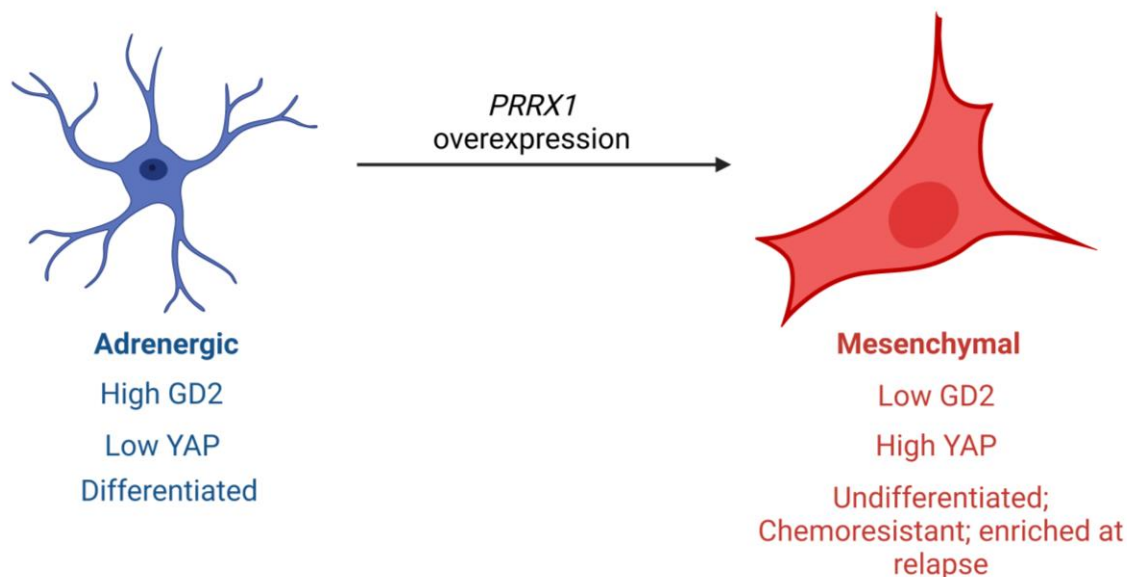


Figure 1.3. Phenotypic plasticity in neuroblastoma. Adrenergic and mesenchymal phenotypes are representative of the intratumoral heterogeneity of neuroblastoma.

To elucidate the regulatory landscape of neuroblastoma cells, H3K27Ac chromatin immunoprecipitation and sequencing (ChIP-Seq) was performed on neuroblastoma cell lines and primary tumors.^{132,133} H3K27Ac is a marker of active transcription and the largest collection of H3K27Ac peaks occur at active groups of enhancers called super-enhancers.^{135,136} Together, these transcription factors regulated by super-enhancers, make up the core regulatory circuitry of the cell. In cancer, super-enhancers often regulate oncogenes and disruption of these leads to cancer cell death.¹³⁷ The core regulatory circuitry of neuroblastoma adrenergic cells includes paired homeobox 2B (PHOX2B), heart and neural crest derivatives expressed 2 (HAND2), and GATA binding protein 3 (GATA3).^{132,133} In the mesenchymal subset of neuroblastoma cells, core transcription factors include paired related homeobox 1 (PRRX1).¹³³ The full list of transcription factors in the core regulatory circuitry of adrenergic and mesenchymal neuroblastoma cells is documented in **Table 1.1**.

Table 1.1. List of genes encoding the transcription factors in the core regulatory circuitry of neuroblastoma cells

Adrenergic core regulatory circuitry transcription factors	Mesenchymal core regulatory circuitry transcription factors
Achaete-Scute Family BHLH Transcription Factor (<i>ASCL1</i>)	AE Binding Protein 1 (<i>AEBP1</i>)
Dachshund Family Transcription Factor (<i>DACH1</i>)	Core binding factor beta (<i>CBFB</i>)
EYA transcriptional coactivator and phosphatase 1 (<i>EYA1</i>)	Cellular Repressor of E1A Stimulated Genes (<i>CREG1</i>)
GATA binding protein 2 (<i>GATA2</i>)	DDB1 And CUL4 Associated Factor 6 (<i>DCAF6</i>)
GATA binding protein 3 (<i>GATA3</i>)	Early growth response 3 (<i>EGR3</i>)
Heart And Neural Crest Derivatives Expressed 1 (<i>HAND1</i>)	ETS Transcription Factor ELK4 (<i>ELK4</i>)
Hairy/enhancer-of-split related with YRPW motif protein 1 (<i>HEY1</i>)	Inhibitor of DNA Binding 1 (<i>ID1</i>)
ISL LIM Homeobox 1 (<i>ISL1</i>)	Interferon Alpha Inducible Protein 6 (<i>IFI6</i>)
KLF Transcription Factor 7 (<i>KLF7</i>)	Mastermind Like Transcriptional Coactivator 2 (<i>MAML2</i>)
KLF Transcription Factor 13 (<i>KLF13</i>)	Mesenchyme Homeobox 1 (<i>MEOX1</i>)
PBX Homeobox 3 (<i>PBX3</i>)	Mesenchyme Homeobox 2 (<i>MEOX2</i>)
Paired Like Homeobox 2A (<i>PHOX2A</i>)	Neurogenic locus notch homolog protein 2 (<i>NOTCH2</i>)
Paired Like Homeobox 2B (<i>PHOX2B</i>)	Paired Related Homeobox 1 (<i>PRRX1</i>)
SATB Homeobox 1 (<i>SATB1</i>)	SIX Homeobox 1 (<i>SIX1</i>)
SIX Homeobox 3 (<i>SIX3</i>)	SIX Homeobox 4 (<i>SIX4</i>)
SRY-Box Transcription Factor 11 (<i>SOX11</i>)	SMAD family member 3 (<i>SMAD3</i>)
Transcription Factor AP-2 Beta (<i>TFAP2B</i>)	SRY-Box Transcription Factor 9 (<i>SOX9</i>)
Zinc Finger Protein 536 (<i>ZNF536</i>)	WW Domain Containing Transcription Regulator 1 (<i>WWTR1</i>)
	ZFP36 Ring Finger Protein Like 1 (<i>ZFP36L1</i>)
	Zinc Finger Protein 217 (<i>ZNF217</i>)

Adrenergic neuroblastoma is a sympathetic lineage-committed or fully differentiated state in which neuroblastoma cells morphologically and, to some extent, functionally resemble normal embryonal neuroblasts (**Figure 1.3**). The adrenergic markers that are highly expressed at the protein level include delta-like non-canonical notch ligand 1 (DLK1), dopamine beta-hydroxylase (DBH), and members of the core regulatory circuitry such as GATA2, GATA3, PHOX2A, and PHOX2B.^{133,138} Neuroblastoma cells can be converted from an adrenergic to a mesenchymal state by overexpression of *PRRX1* (**Figure 1.3**).¹³³

Markers of neural crest cell-like or mesenchymal neuroblastoma identity include fibronectin (FN1), vimentin (VIM), snail family transcriptional repressor 2 (SNAI2), the Yes-associated protein (YAP) and core regulatory circuitry members, *PRRX1*, and WW domain containing transcription regulator 1 (*WWTR1* which encodes transcriptional co-activator with PDZ-binding motif (TAZ)).¹³³ Mesenchymal neuroblastoma is more resistant to therapy as the mesenchymal subtype is enriched in relapsed neuroblastomas and can be induced by RAS activation.¹³⁹

In addition to defining cell state and fate, the core regulatory circuitry of neuroblastoma presents a potential dependency which may be therapeutically targeted as exemplified by recent design of chimeric antigen receptor (CAR) T cells targeting a peptide derived from *PHOX2B*.¹³⁹⁻¹⁴¹ Additionally, mesenchymal cells have been demonstrated to be more immunogenic than adrenergic cells as they express genes involved in innate immune recognition, antigen presentation and processing.¹⁴² In another study, neuroblastoma mesenchymal cells were demonstrated to have an inflammatory response gene signature that might suggest their increased vulnerability to immunotherapy.¹⁴³ These data contradict some of the observations in this dissertation and suggest the importance of studying the relationship between intratumoral heterogeneity/ phenotypic plasticity and resistance to immunotherapy in neuroblastoma.

1.4 Summary of the content of this dissertation

The current understanding of how neuroblastoma is diagnosed, subdivided into risk groups, and its genetic alterations and developmental origins influence treatment paradigms. Patients with high-risk neuroblastoma have a 50% survival rate and often relapse is fatal. Thus, this dissertation seeks to explore a role for the Yes-associated protein (YAP), which is typically increased in relapsed neuroblastomas, in mediating resistance to a combination of $\gamma\delta$ T cell/GD2-targeted immunotherapy for neuroblastoma (Chapter 4). While Chapter 4 of this dissertation elucidates the mechanism of resistance to $\gamma\delta$ T cell/GD2-targeted immunotherapy in neuroblastoma, the preceding chapters 1-3 aim to contextualize this mechanism in the larger body of literature which has been published on each aspect of this project: YAP and its paralog, TAZ (chapter 2), and $\gamma\delta$ T cells, GD2 and GD2-targeting therapies in neuroblastoma (chapter 3). Finally, chapter 5 reiterates the significance of this work, including main conclusions, limitations, and future directions.

Chapter II: The role of the Yes-Associated Protein (YAP) and its paralog, transcriptional co-activator with PDZ-binding motif (TAZ) in cancer

2.1 Structure, signaling, and function of YAP and TAZ

2.1.1 Structure of YAP/ TAZ

The Yes-associated protein (YAP/YAP1/YAP65; henceforth referred to as YAP) was first discovered because of its ability to bind to the Src family protein tyrosine kinase, Yes.¹⁴⁴ There are 8 isoforms of YAP that each vary in modular structure and consequently, function. The common structures in each isoform are, from N-terminus to C-terminus, the TEA-domain (TEAD)-binding domain (TBD), 14-3-3 binding domain, WW domain (named because of the characteristic presence of consecutive tryptophan (W) amino acids),¹⁴⁵ Src homology-3 (SH3)-binding domain, transcriptional activation domain (TAD), and PDZ binding domain (**Figure 2.1**).¹⁴⁶ Since YAP does not have a DNA-binding domain, it is dependent on a DNA-binding partner to function as a regulator of transcription.

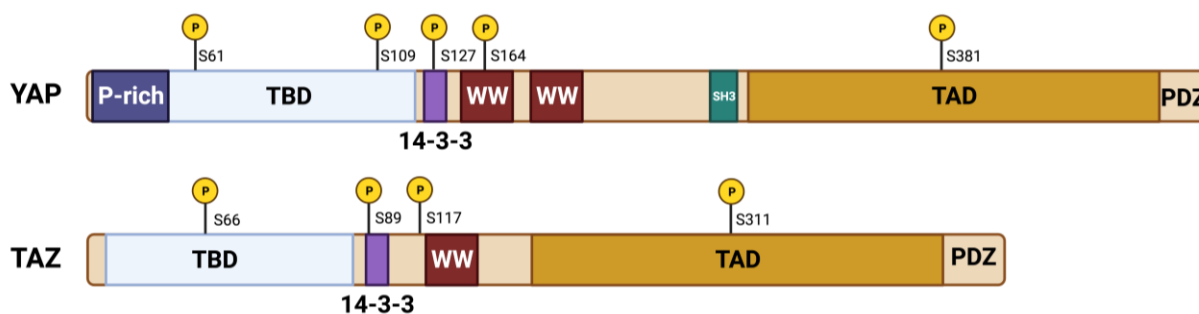


Figure 2.1: The structures of the Yes-Associated Protein (YAP) and its paralog, transcriptional co-activator with PDZ-binding motif (TAZ). YAP has an N-terminal proline-rich domain (P-rich), a second WW domain, and a Src homology 3 (SH3) domain that are absent in TAZ. The structure of both YAP and TAZ includes a TEAD-binding domain (TBD), 14-3-3 binding domain, transcriptional activation domain (TAD), and PDZ-binding motif (PDZ). This figure was adapted from Piccolo *et al.*, 2014 and Zhao *et al.*, 2010.^{147,148}

These isoforms vary based on the number of WW domains present (either 1 or 2) and the presence of additional amino acids within the leucine zipper of the TAD that occurs because of alternative splicing.¹⁴⁶ The biological and functional significance of the 8 YAP isoforms is that downstream transcriptional activity is altered by the varying locations of leucine zippers within these C-terminal sequences.¹⁴⁹ The paralog of YAP, transcriptional co-activator with PDZ-binding motif (TAZ, encoded by *WWTR1*), which exists only in vertebrates, has 60% sequence identity to YAP and was discovered primarily because of its binding to 14-3-3.¹⁵⁰ A few key structural differences between TAZ and YAP are: the existence of the SH3 domain in YAP, and not TAZ (which allows the binding of the Src kinase, Yes), and a proline-rich N-terminal region; TAZ contains a second phosphodegron that renders it more susceptible to degradation than YAP (**Figure 2.1**).¹⁵⁰ YAP and TAZ form distinct complexes when they interact with TEAD based on the differences in their TBD structures.¹⁵¹ A primary mode of regulation of both YAP and TAZ is post-translational modification, specifically phosphorylation, and the phosphorylation sites of large tumor suppressor homolog 1/2 (LATS1/2) are depicted in **Figure 2.1**. There are number of regulatory inputs upstream of YAP/TAZ and these are outlined in section 2.1.2.

2.1.2 Regulation of YAP/ TAZ

The Hippo Pathway

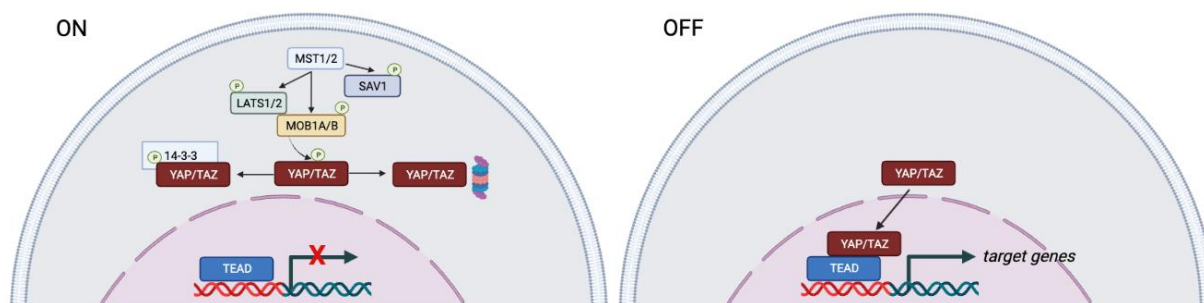


Figure 2.2. The Hippo Pathway signaling cascade consists of sequential kinase modules that regulate subcellular localization and function of YAP/TAZ.

The Hippo pathway was first elucidated in *Drosophila melanogaster* and the mammalian equivalent of this sequential kinase cascade which regulates the subcellular localization, stability, and function of YAP/TAZ is summarized in **Figure 2.2**. The mammalian sterile 20-like kinases (MST1/2) bind the regulatory protein, Salvador Family WW Domain Containing Protein 1 (SAV1), forming an enzyme which phosphorylates LATS1/2 kinases as well as MOB Kinase Activator 1A/B (MOB1A/B) regulatory subunits. Together, LATS1/2 and MOB1A/B form a complex which phosphorylates YAP and TAZ (**Figure 2.2**). Phosphorylation of YAP by LATS1/2 occurs at 5 consensus sites (S61, S109, S127, S164, and S381) and the 4 sites in TAZ are S66, S89, S117, and S311 (**Figure 2.1**).¹⁴⁷ The primary residues for regulation of the subcellular localization of YAP are S127 and S381 (of TAZ: S89 and S311).¹⁴⁷ Phosphorylation at S127 (S89 in TAZ) creates a consensus sequence for binding of the adaptor protein, 14-3-3 that allows for sequestration of YAP in the cytoplasm. Phosphorylation of S381 (S311 in TAZ) creates a phosphodegron, a sequence of phosphorylated amino acid residues that acts as a recognition and binding site for ubiquitin ligases, allowing for polyubiquitination and proteasomal degradation of YAP/TAZ.¹⁴⁷ In the absence of these phosphorylation events, YAP/TAZ shuttle into the nucleus, bind co-factors and elicit downstream transcriptional functions. Non-phosphorylatable and thus, constitutively active forms of YAP/TAZ have been generated which replace the 5 (for YAP) and 4 (for TAZ) serine residues at the LATS1/2 consensus sites by alanine residues, generating YAP5SA/TAZ4SA constitutively active constructs. In Chapter 4 of this dissertation, a YAP 5SA plasmid is introduced by lentiviral transduction into the neuroblastoma cell line, SMS-SAN, to generate a cell line with constitutively active YAP.

Wnt signaling

Another important regulator of YAP/TAZ is Wnt signaling. In the canonical Wnt pathway, in the absence of external stimuli, β -catenin is ubiquitinated and degraded by a destruction complex consisting of adenomatous polyposis coli (APC), Axin, casein kinase-1 (CK-1) (that independently

phosphorylates YAP), E3-ubiquitin ligase β -TrCP, glycogen synthase kinase 3 (GSK-3), and protein phosphatase 2A (PP2A).¹⁵² The effect of Wnt signaling on YAP/TAZ is context dependent. When Wnt signaling is active, Wnt binds to LRP5/6 and Frizzled (Frz) at the membrane, preventing the assembly of the destruction complex, allowing β -catenin accumulation. After translocation to the nucleus, β -catenin binds the TCF/LEF family of transcription factors, regulating transcription of target genes. Another downstream consequence of Wnt signaling is stabilization of TAZ – in the absence of Wnt signaling, phosphorylated β -catenin binds TAZ and bridges an association with E3-ubiquitin ligase β -TrCP, resulting in degradation of TAZ.¹⁵³ The regulation of YAP/TAZ discussed in this section 2.1.2 is primarily through post-translational mechanisms. However, Wnt regulation of YAP in colorectal cancer cells is transcriptional, the β -catenin/TCF4 complex binds an enhancer element within the first intron of *YAP*, driving its expression.¹⁵⁴ Additionally, there are feedback mechanisms through which YAP/TAZ bind β -catenin, antagonizing Wnt signaling.¹⁵⁵

G-protein coupled receptor (GPCR)-mediated signaling and YAP/ TAZ

G-protein coupled receptors (GPCRs) are membrane-bound, ubiquitously expressed receptors in eukaryotes. They consist of seven transmembrane α -helices which upon binding of their cognate ligands, undergo conformational changes and thus, interact with their associated G-proteins.¹⁵⁶ G-proteins associated with GPCRs are heterotrimeric, consisting of membrane-linked α and γ subunits, and an intermediary β subunit.¹⁵⁶ In their inactive state, these G-proteins are guanosine diphosphate (GDP)-bound. However, their association with GPCRs results in guanosine triphosphate (GTP) exchanged for GDP resulting in various intracellular signaling cascades initiated by second messengers such as cyclic adenosine monophosphate (cAMP), diacylglycerol (DAG), and inositol 1,4,5-triphosphate (IP3).¹⁵⁶ The complexity of combinations of G-proteins with GPCRs is vast given that there are several families of each subunit: $G\alpha$, $G\beta$, and $G\gamma$.

Here, we focus on the four families of G α subunits, G α_s , G α_i , G α_q , and G α_{12} , which interact with LATS1/2 to regulate YAP/TAZ either agonistically or antagonistically. The G α_i -, G α_q -, and G α_{12} -coupled receptors inhibit LATS1/2; thus, decreasing YAP/TAZ phosphorylation, consequently increasing its nuclear accumulation and activity.¹⁵⁷ On the other hand, G α_s -coupled GPCRs inhibit YAP/TAZ by activating LATS1/2.¹⁵⁷ In uveal melanoma, activating mutations of the G α_q family activate YAP through LATS1/2 inhibition.¹⁵⁸ However, there are Hippo pathway-independent mechanisms of YAP regulation by GPCRs which depend upon the stimulation of Trio, a GEF by G α_q and G α_{11} (G α_q family members), leading to the consequent activation of Rho and RAC small GTPases which cause dissociation of angiominin (AMOT)-YAP complexes in the cytoplasm, causing nuclear translocation of YAP.^{159,160}

Mechanotransduction and YAP/TAZ

In its normal physiological role, YAP is responsible for sensing extracellular mechanical signals, integrating these, and responding through transcriptional control of genes. The detection of these signals occurs at the interface between the plasma membrane and extracellular environment. The primary mechanical signals which are detected include extracellular matrix (ECM) stiffness, cytoskeletal tension, shear stress, cell density, and cellular geometry.¹⁶¹ When these mechanical signals are highest, that is, a stiff ECM or external substrate, high cytoskeletal tension, shear stress, low cell density and deformation of the cell, YAP/TAZ are activated, localizing to the nucleus.¹⁶²

The molecules on the surface of the cell that mediate cell-to-cell and cell-to-matrix adhesion are integrins. Integrins, through associated vinculin and talin molecules, connect to filamentous actin (F-actin) in the cytoplasm as components of structures called focal adhesions and this is mediated by focal adhesion kinase (FAK), integrin-linked kinase (ILK), and SRC. Increased ECM stiffness specifically activates FAK which activates SRC; SRC inhibits LATS1/2, and independently of the

Hippo pathway, directly phosphorylates and activates YAP.¹⁶¹ When extracellular forces are exerted on a cell, there is remodeling of the cytoskeleton that is facilitated by Rho GTPases, Rho-associated protein kinase (ROCK), and actomyosin activity and formation.¹⁶¹

The complete mechanistic link between F-actin, actomyosin formation and cytoplasmic-to-nuclear shuttling of YAP/TAZ has not been fully elucidated. Loss or inactivation of F-actin capping and severing proteins, and the resulting stress fiber/excessive F-actin filament formation, is sufficient to induce translocation of YAP/TAZ to the nucleus, regardless of other external forces and signaling inputs such as the Hippo pathway.¹⁶³ One proposed mechanism relates to the linker of the nucleoskeleton and cytoskeleton (LINC) complex which connects the nucleus to the cytoskeleton.¹⁶⁴ Changes in actomyosin contractility transfer force to the nucleus via the LINC complex and this leads to opening of nuclear pores, allowing for import of YAP/TAZ.¹⁶⁵ Another additional mechanism is that, under low mechanical stress conditions, in a TEAD-independent manner, the AT-Rich Interaction Domain 1A (ARID1A) subunit of the SWI/SNF complex binds to and competitively prevents YAP/TAZ/TEAD binding in the nucleus.¹⁶⁶ In contrast, under high mechanical stress, F-actin is formed and binds ARID1A-SWI/SNF, preventing its association with YAP/TAZ and allowing YAP/TAZ to thus, bind to cis-regulatory elements and regulate gene expression.¹⁶⁶ As previously noted, low cell density signals nuclear localization of YAP/TAZ; however, at higher density, YAP/TAZ is situated in the cytoplasm mediating contact inhibition of proliferation.¹⁶⁷ At high cell density, a plasma membrane-associated molecule ANXA2, forms a complex with MST2 and YAP, further maintaining its cytoplasmic localization.¹⁶⁸ The Hippo pathway is also integrated into this process and a canonical target of YAP, cysteine-rich angiogenic inducer 61 (CYR61) is secreted and has been shown to reduce density-dependent apoptosis.¹⁶⁹ These mechanotransductive properties of YAP are especially relevant in the solid tumor microenvironment, including in neuroblastoma, and will be further explored in sections 2.2.2 and 2.4.

Stress signaling and metabolic regulation of YAP/TAZ

Various forms of stress including energy stress through nutrient deprivation, endoplasmic reticulum (ER) stress, heat stress, hypoxia, osmotic stress, and oxidative stress regulate YAP/TAZ.¹⁷⁰ Adenosine monophosphate (AMP)-activated protein kinase (AMPK) is an enzyme which senses energy changes through detection of AMP and ATP levels by binding of AMP. Under low energy (particularly, glucose) levels, AMPK phosphorylates YAP at the S94 residue, essential for YAP-TEAD interaction; thus, directly inhibiting YAP transcriptional activity.^{171,172} Regulation of YAP by AMPK also occurs indirectly through phosphorylation of angiomotin-like 1 (AMOTL1) which promotes LATS1/2 activity and directly binds YAP, sequestering it to the cytoplasm.¹⁷³ Prolonged ER stress leads to the activation of the unfolded protein response as protein kinase RNA-like ER kinase (PERK) detects ER stress and inhibits translation by phosphorylating eukaryotic translation initiator factor 2 α (eIF2 α), inducing translation of ATF4, a transcription factor that binds the promoter of *YAP*, driving its transcription.¹⁷⁴ Heat stress induced by hyperthermia activates a YAP/TAZ regulated heat shock gene and cell survival response.¹⁷⁵

Hypoxic stimuli activate the E3 ubiquitin ligase, seven in absentia homolog 2 (SIAH2), resulting in the formation of a ternary complex with the scaffold protein, Zyxin, and LATS2, leading to LATS2 degradation, disinhibition of YAP/TAZ and activation of downstream transcriptional activity.^{176,177} Osmotic stress is induced by a higher extracellular than intracellular solute concentration and when this occurs, phosphorylation of YAP S128 by Nemo-like kinase (NLK) disrupts 14-3-3 binding and enables the translocation of YAP to the nucleus and activation of its downstream signaling.^{178,179} An intracellular excess of reactive oxygen species leads to oxidative stress; in response, YAP-FOXO1 forms a complex at the promoters of antioxidant genes like catalase and manganese superoxide dismutase (MnSOD), increasing cell survival in these contexts.¹⁸⁰ Conversely, oxidative stress also leads to MOB1 acetylation by cAMP response

element-binding protein (CREB)-binding protein (CBP), causing LATS1 activation, YAP phosphorylation, decreased nuclear localization of YAP, and cell apoptosis.¹⁸¹

In breast cancer cells that are dependent on glutamine, YAP/TAZ are shown to mediate the expression of genes that regulate amino acid metabolism, including glutamic–oxaloacetic transaminase (*GOT1*) and phosphoserine aminotransferase (*PSAT1*), increasing their dependence on glutamine for survival.¹⁸² High intracellular levels of glucose lead to the post-translational modification of YAP at S109, the addition of *O*-linked β -*N*-acetylglucosamine (*O*-GlcNAc), *O*-GlcNAcylation, preventing LATS1 phosphorylation and resulting in inhibition of YAP.¹⁸³ Lipid and cholesterol metabolites/ intermediates are also known to regulate YAP. The free fatty acid, palmitate, induces MST1 phosphorylation and consequent YAP phosphorylation and inhibition.¹⁸⁴ Additionally, stearoyl-CoA-desaturase 1 (*SCD1*), a fatty acid synthesis enzyme increases YAP/TAZ stability through the inactivation of the β -catenin destruction complex.¹⁸⁵ The autopalmitoylation of TEAD at cysteine residues facilitates YAP/TAZ binding.¹⁸⁶ Mevalonate is an intermediate in cholesterol biosynthesis. Mevalonate leads to post-translational modification and activation of Rho small GTPases by geranylgeranylation; the consequence of this is YAP/TAZ nuclear localization and activation.¹⁸⁷ There are innumerable signaling inputs that regulate YAP/TAZ and the consequence of these signals is regulation of transcription by these co-regulators as described in 2.1.3.

2.1.3 Mechanisms of transcriptional control by YAP/TAZ

The lack of a DNA-binding domain in the structure of YAP/TAZ necessitates binding to transcription factor or co-activator partners. Some of the DNA-binding partners of YAP/TAZ include Erb-B2 Receptor Tyrosine Kinase 4 (*ERBB4*),¹⁸⁸ early growth response factor 1 (*EGR-1*),¹⁸⁹ p73,¹⁹⁰ Runt-related transcription factor family (*RUNX1/2/3*),¹⁹¹ and Suppressor of Mothers against Decapentaplegic family (*SMADs*).¹⁹² However, the most common binding partners of

YAP/TAZ are the members of the TEA-domain (TEAD) family (TEAD1/2/3/4).^{193,194} Through ChIP-Seq experiments, a large majority (>90%) of YAP/TAZ/TEAD complexes have been shown to bind to enhancers.¹⁹⁵ The recruitment of YAP/TAZ/TEAD complexes to enhancers occurs through the formation of a transcriptional complex with the transcription factor, activator protein 1 (AP-1: FOS/JUN heterodimer) leading to enhancer activation as evidenced by an increase in acetylation of histone H3 at lysine 27 (H3K27Ac) (**Figure 2.3**).^{195,196} These enhancers form classical chromatin loops with promoters of YAP/TAZ target genes to control their expression.

The epigenetic mechanism described in the preceding paragraph is TEAD-dependent; that is, TEAD mediates the binding of YAP/TAZ to AP1. Further complicating these models, however, is the reality that YAP/TAZ directly binds to other components or regulators of the transcriptional machinery. Additionally, the functions of YAP and TAZ are cell- and context-dependent and are thus, not always interchangeable.¹⁹⁷ The TAZ/TEAD complex interacts with BRG1 and BRM subunits of the SWI/SNF complex, controlling epithelial cell lineage commitment in breast tissue through transcriptional control mediated by binding to BRM specifically while in this context, YAP is found to be dispensable.¹⁹⁸ A small portion of YAP/TAZ enhancer interactions demonstrate features of super-enhancers with increased binding of mediator complex (MED1) and cyclin-dependent kinase-9 (CDK9), resulting in markers of enhanced transcription of target genes through release of RNA polymerase II (PolII) pausing (**Figure 2.3**).¹⁹⁹ Additionally, YAP/TAZ has been determined to bind to chromatin modifiers and readers such as bromodomain-containing protein 4 (BRD4), histone acetyltransferases like p300 and p400 and histone methyltransferases like lysine methyltransferase 2D (KMT2D).^{195,198,200,201} Analogous to the stabilization of YAP/TAZ in the cytoplasm by lack of phosphorylation, cyclin-dependent kinase 7 (CDK7), a component of the basal transcriptional machinery, stabilizes YAP/TAZ in the nucleus by phosphorylation, preventing its degradation.²⁰² Together, these data indicate a model in which

YAP/TAZ recruits PolIII to transcriptional start sites by approximating YAP/TAZ-bound enhancers to the promoters of target genes (**Figure 2.3**).²⁰⁰

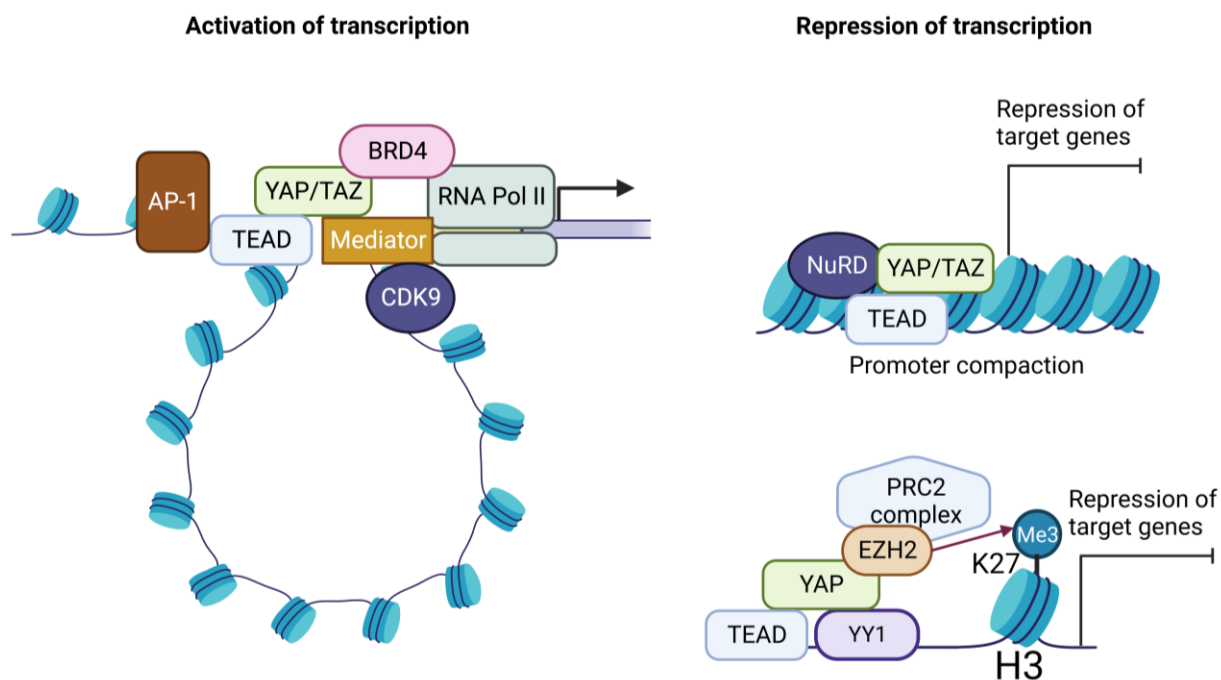


Figure 2.3. Transcriptional regulation by YAP/TAZ results in activation and repression of target genes. Image adapted from Hoxha *et al.*, 2020, Kim *et al.*, 2015, and Piccolo *et al.*, 2023.
203-205

Thus far, we have described the role of YAP/TAZ in driving transcription of target genes; however, transcriptional repression by YAP is an important aspect of its function that is particularly relevant to this dissertation. In human Schwann cells, YAP suppresses CDKN1B/p27 expression through binding of YAP, YY1 and EZH2 to the CDKN1B/p27 promoter and placement of repressive marks such as H3K27me3 (**Figure 2.3**).²⁰³ Another mechanism of gene repression by YAP/TAZ/TEAD is through histone deacetylation by the nucleosome remodeling and deacetylase (NuRD) complex at the promoters of target genes such as *DDIT4*, *NR4A1*, and *Trail* (**Figure 2.3**).^{204,206} Additionally, a YAP/TAZ/TEAD/SMAD2/3/OCT4 complex forms at promoters of

pluripotency genes such as *OCT4* and *NANOG*, suppressing genes that lead to mesoendodermal differentiation and thus, maintaining pluripotency.²⁰⁷

These highly organized mechanisms of transcriptional control by YAP/TAZ are dependent on their ability to localize to the nucleus. However, YAP forms both cytoplasmic and nuclear condensates under varying intracellular conditions.²⁰⁸ In the nucleus, YAP condensates allow for interaction and localization of YAP with key players, such as TEAD and RNAPolIII, to control transcription.²⁰⁸ The pleiotropic effects of YAP that are mediated through its effects on transcription of target genes are too abundant to completely review in this dissertation; thus, in section 2.2, I focus on cancer-related functions of YAP/TAZ in tumor cells and the tumor microenvironment.

2.2 Cell-autonomous and tumor microenvironmental functions of YAP/TAZ in tumorigenesis.

The regulatory inputs to YAP/TAZ expression and function are modified in the context of cancer. There are few activating YAP/TAZ mutations that directly lead to increased tumorigenesis, oncogenic alterations primarily lead to increased expression of YAP/TAZ by affecting its regulators or rarely, through YAP fusions that eliminate the C-terminal S381 site which is needed to mediate proteasomal degradation.²⁰⁹ These functions of YAP/TAZ are modulated either through tumor cell-autonomous mechanisms or in the tumor microenvironment (TME) by regulation of immune cell populations, stromal cells, extracellular matrix, and soluble mediators/signaling.

2.2.1 Tumor cell-autonomous functions of YAP/TAZ in cancer

Cell survival

The role of YAP/TAZ in regulation of cell proliferation and apoptosis is well-established. Increased expression and/or activity of YAP/TAZ results in hallmarks of cancer including sustained proliferative signaling and resisting cell death, nominating them as oncogenes almost two decades ago.²¹⁰⁻²¹⁵ The mechanisms by which YAP/TAZ control proliferation include regulation of cell cycle-promoting genes that drive S-phase entry such as cyclin A2 (*CCNA2*), *CCND1*, and forkhead box protein M1 (*FOXM1*),^{196,216} co-operation with E2F transcription factors in RAS-mutant cancers,¹²¹ and activation of Notch signaling by induction of jagged-1 (*JAG1*) gene expression.²¹⁷ YAP has both pro- and anti-apoptotic functions that can be dysregulated in cancer. Another binding partner of YAP/TAZ, as mentioned in Section 2.1.3, is p73. YAP promotes apoptosis through its interaction with p73 and increased expression of the pro-apoptotic protein, B-cell lymphoma 2 (*BCL2*)-associated protein X (*BAX*).²¹⁸⁻²²⁰ The anti-apoptotic mechanisms of YAP which are more congruent with its role as an oncogene include suppression of the pro-apoptotic genes, *Harakiri* (*HRK*),¹¹⁸ and *NR4A1* which normally binds *BCL2*,²⁰⁶ and upregulation of *BCL2*.²²¹

Metastasis

The classical metastatic cascade includes loss of apicobasal polarity, epithelial-to-mesenchymal transition (EMT), invasion, migration, extravasation, survival in circulation (anoikis resistance), intravasation, and micro- and macrometastasis establishment. Each of these steps is related to functions mediated by YAP/TAZ but apicobasal polarity and EMT, the initiation of metastasis, are regulated by YAP/TAZ. Apical proteins such as Crumbs Cell Polarity Complex Component 3 (*CRB3*), protein associated with LIN7 1 (*PALS1*), and AMOT-like proteins regulate subcellular localization of YAP/TAZ, and YAP/TAZ, in turn, lead to loss of integrity of the apex/polarity of

cells.²²² Additionally, a YAP/TAZ/TEAD4/AP1/SRC1-3 complex forms binding and driving invasion and migration through the transcription of genes regulating cytoskeletal structure and adhesion such as the DOCK family, *CDH2*, and *MACF1*.^{223,224} Indeed, YAP and KRAS cooperate to increase expression of mesenchymal genes such as fibronectin (*FN1*), Slug (*SNAI2*), vimentin (*VIM*), and zinc-finger E-box binding homeobox 1 (*ZEB1*) and reduce the expression of epithelial genes such as E-cadherin (*CDH1*) and occludin (*OCLN*), inducing EMT.²²⁵

Another cancer hallmark that is regulated by YAP/TAZ is the deregulation of cellular metabolism. Some of the major intersections between YAP/TAZ signaling and metabolism have already been covered in Section 2.1.2. Finally, another tumor cell-intrinsic function of YAP/TAZ is therapy resistance. Some mechanisms of therapy resistance may also be facilitated by tumor microenvironmental changes, and these will be described in Section 2.2.2.

Therapy resistance

Targeted therapy

Targeted inhibition of RTKs and downstream MAPK signaling has been an approach for treating cancers for two decades. Resistance to these targeted therapies is mediated by YAP/TAZ. For example, resistance to BRAF mutations and consequent hyperactivated MAPK signaling in melanoma lead to actin remodeling and YAP/TAZ nuclear localization, activation, and transcription of target genes that mediate cell survival such as E2F- and MYC-pathway related genes.²²⁶ Resistance to RAF- and MEK-targeted therapies in melanoma, non-small cell lung cancer, pancreatic adenocarcinoma, colon and thyroid cancer, and neuroblastoma, has been promoted by increased expression and downstream activity of YAP.^{119,227,228}

Chemotherapy

Chemotherapeutic drugs target and kill cancer cells based on their highly proliferative properties. Resistance to these drugs is either mediated by regulation of factors upstream of YAP/TAZ or of YAP/TAZ themselves, and thus, their downstream signaling. Genes encoding multidrug resistant transporters, *ABCB1* (encodes MDR1) and *ABCC1* (encodes MRP1) are transcriptional targets of YAP/TAZ/TEAD and these transporters mediate the efflux of chemotherapeutic drugs.^{229,230} Most commonly, however, as a resistance mechanism, YAP/TAZ regulate expression of genes involved in anti-apoptosis and survival including *BCL2L1* (encodes BCL-xL), *BIRC5* (encodes survivin), *CTGF*, *CYR61*, and inhibitor of apoptosis-1 (*IAP1*).²³¹⁻²³⁴

Immunotherapy

Checkpoint inhibitors, drugs that prevent T cell exhaustion, targeting the programmed cell death ligand -1 (PD-L1)/PD-1 axis are a commonly used immunotherapy. A complex of YAP/TAZ/TEAD directly binds the *CD274* (encodes PD-L1) promoter in tumor cells, driving expression of this target gene, potentially mediating resistance to these inhibitors as well as adoptive T cell therapies that depend upon T-cell fitness for optimal efficacy.²³⁵⁻²³⁹ Release of IFN γ after anti-PD1 immunotherapy for melanoma leads to YAP phase condensate formation, nuclear localization and resistance mediated by increased *CD155* (encodes poliovirus receptor (PVR)) expression.²⁴⁰ Many of the effects of YAP/TAZ on immunotherapy resistance are as a result of its influence on skewing to an immunosuppressive tumor microenvironment and thus, will be covered in the following section 2.2.2.

2.2.2 The tumor microenvironmental role of YAP/TAZ in cancer

There are multiple roles of YAP/TAZ in the TME that, for the purpose of this dissertation, will be subdivided into effects on immune cell populations, stromal cells, extracellular matrix, and soluble mediators/signaling.

Immune cell populations

Immune cell infiltration can be used as a prognostic factor for outcomes of patients with cancer.²⁴¹ T-regulatory (Treg) cells are generally considered to be associated with less favorable outcomes in patients with cancer because of their widely accepted role as an immunosuppressive population. In hepatocellular carcinoma and melanoma, high YAP expression in Treg populations was found to drive TGF β signaling, leading to Treg differentiation and immunosuppressive microenvironments in mouse models and in patients.^{242,243} Furthermore, clinical trial correlates from a study of patients with oral cavity squamous cell carcinoma demonstrated high YAP protein expression in tumors and a higher Treg/Th17 ratio in the pretreatment blood was correlated with innate resistance to neoadjuvant PD-1 checkpoint therapy.²⁴⁴ Paradoxically, the YAP paralog, TAZ, is found to decrease Treg differentiation by promoting degradation of FOXP3.²⁴⁵ Additionally, deletion of YAP in CD8⁺ T cells was found to promote their cytotoxic function and infiltration in murine models of melanoma, colon adenocarcinoma and lung adenocarcinoma.^{246,247} Assessment of YAP expression in the small cell lung cancer tumor microenvironment of patients using RNA sequencing determined that higher YAP expression was associated with a more T-cell inflamed gene signature and better patient outcomes.²⁴⁸ However, a study of 23 cancer types demonstrated a negative correlation between *YAP* expression and the infiltration of activated natural killer (NK) T cells, CD4⁺ Th1 cells, CD8⁺ T cells, $\gamma\delta$ T cells, myeloid dendritic cells, and T follicular helper cells.²⁴⁹ In contrast, *YAP* expression was positively correlated with infiltration of more immunosuppressive populations such as cancer-associated fibroblasts (CAFs), myeloid-derived suppressor cells (MDSCs), and neutrophils.²⁴⁹ Generally, higher expression of YAP is considered to be involved in driving an immunosuppressive TME.

Increased YAP expression in lung adenocarcinoma,²⁵⁰ prostate adenocarcinoma,²⁵¹ colorectal cancer,²⁵² and pancreatic adenocarcinoma²⁵³ has been demonstrated to lead to increased

expression of *CXCL5*, attracting CXCR2+ MDSCs, facilitating tumor progression. Tumor-associated macrophages (TAMs) have traditionally been subdivided into M1 (anti-tumorigenic) and M2 (pro-tumorigenic) phenotypes based on *in vitro* differentiation/polarizing conditions.²⁵⁴ However, there is greater complexity of function of TAMs than these distinct, non-overlapping phenotypes suggest. Thus, in discussing the role of YAP in macrophages within the TME, I avoid M1/M2 terminology and refer to the specific phenotypic differences elicited by YAP in these contexts. In glioblastoma multiforme, increased YAP expression in tumor cells was found to drive the expression of lysyl oxidase (*LOX*), recruiting pro-tumorigenic macrophages which sustained tumor growth.²⁵⁵ Finally, a neutrophil-specific YAP/TAZ knockout model showed that gastric cancer progresses more readily in the context of high expression of YAP/TAZ in tumor-specific neutrophils.²⁵⁶ These varying roles of YAP/TAZ in immunomodulation within the tumor microenvironment nominate them as targets for systemic pharmacological treatments since they may elicit their immunosuppressive effects both within the cancer cells and the TME.

Stromal cells/ECM/Soluble mediators

The mechanisms by which YAP/TAZ detect and transduce mechanical signals has been covered in section 2.1.2. The mechanotransductive properties of YAP/TAZ are particularly relevant to their role in stromal cells and the dynamic extracellular environment within solid tumors. In breast cancer, CAFs are dependent on high expression and nuclear localization of YAP/TAZ to be generated and maintained, resulting in expression of target genes that remodeled the extracellular matrix to increase cancer cell invasion.²⁵⁷ YAP/TAZ drive oncogenic reprogramming of normal cells to tumor-initiating populations in solid tumors through regulation of oncogene expression and mechanosignaling resulting from varying ECM stiffness.²⁵⁸ The effect of ECM structure and stiffness on YAP/TAZ expression is not restricted to cancer cells themselves. Increased ECM stiffness activates YAP and is found to reduce CD8 T cell activation and reprogram the metabolic fitness of these cells which has broad implications for its role in intratumoral as well as intranodal

T cell behaviors.²⁵⁹ On the other hand, increased ECM stiffness and YAP expression increase the pro-inflammatory properties of macrophages.²⁶⁰ YAP/TAZ may indirectly regulate differences in infiltration and pro-/ anti-tumorigenic skewing of immune cells discussed through soluble mediators such as CCL2, CSF1, CSF2, CSF3 CTGF, CXCL5, CYR61, and IL-6.²⁵⁰ YAP/TAZ, in many instances, drive increased transcription of genes encoding these soluble mediators.

2.3 Therapeutic targeting of YAP/TAZ

Direct pharmacological inhibition of YAP/TAZ is challenging given the many intrinsically disordered domains in their structures. Considering the inputs into YAP/TAZ regulation reviewed in Sections 2.1.2, there are multiple indirect means of targeting YAP being explored pharmacologically. The disadvantage of this indirect approach is that there are likely more off-target effects of these drugs. Inhibitors such as C19 activate MST/LATS1/2 to phosphorylate and degrade YAP/TAZ; however, C19 also suppresses TGF β and Wnt signaling.²⁶¹ The mechanism underlying the inhibition of YAP/TAZ by CA3 is not fully elucidated as it has been shown to globally reduce expression of LATS1/2, YAP, TAZ, and TEAD.^{262,263} One inhibitor of YAP/TAZ, verteporfin, disrupts the stability of the YAP/TAZ/TEAD complex by binding YAP.²⁶⁴ However, verteporfin has been demonstrated to exert cytotoxicity that is completely independent of YAP/TAZ expression.²⁶⁵⁻²⁶⁷ Since most of the functions of YAP/TAZ occur downstream of TEAD binding, most recent research has focused on the disruption of the YAP/TAZ binding to TEAD.

The stability of TEAD transcription factors and regulation of downstream transcriptional activity is dependent on autopalmitylation at cysteine residues within its structure.^{186,268} Inhibitors block TEAD autopalmitylation by forming either non-covalent or covalent interactions. Drugs that covalently bind cysteine and disrupt TEAD autopalmitylation and thus, YAP/TAZ interaction with TEAD and downstream YAP/TAZ signaling include DC-TEADino2,²⁶⁹ K-975,²⁷⁰ MYF-01-37,²⁷¹ and TED-374.²⁷² Another similar drug VT3989 has shown promise for treatment of NF2-

deficient mesothelioma by inhibiting TEAD palmitoylation ([NCT04665206](#)).²⁷³ Targeting the lipid pocket of TEAD that facilitates YAP binding with drugs like CPD3 is another approach that has had success.²⁷⁴⁻²⁷⁸ The vestigial-like (VGLL) protein family (VGLL1-4) competitively binds TEAD, inhibiting YAP/TAZ downstream function. Thus, a recent study investigated the role of a peptide, super-TDU, that mimics the structure of VGLL4, acting as an antagonist for YAP/TAZ binding to TEAD and inhibiting tumor proliferative activity.²⁷⁹ Although these drugs have promise for treatment of YAP/TAZ-mediated cancers, they have shown limited single treatment efficacy and thus, efforts to combine them with drugs inhibiting potential escape pathways such as AKT signaling are underway.²⁸⁰

2.4 The role of YAP/TAZ in neuroblastoma.

Next-generation sequencing of primary and relapsed neuroblastomas revealed relapse-specific protein tyrosine phosphatase non-receptor type 14 (PTPN14) inactivating mutations that lead to increased YAP expression and transcriptional activity.¹² This increased expression and transcriptional activity of YAP in relapsed neuroblastoma was confirmed in further studies of paired diagnosis/relapsed neuroblastoma cell lines and patient-derived xenografts.¹¹⁸ In this insightful study, YAP expression was determined to be increased post-chemotherapy treatment and to enable suppression of stress-induced apoptosis in a TME-dependent manner through repression of the apoptotic regulator, *HRK*.¹¹⁸ Additionally, YAP has been demonstrated to play a role in neuroblastoma metastasis. In a murine metastatic model, YAP/TAZ expression is elevated in metastatic versus primary tumors and dual genetic inhibition of YAP/TAZ reduced metastasis and increased survival.²⁸¹ The pre-mRNA processing factor 19 (Prp19) is involved in splicing and processing of pre-mRNAs and regulates *YAP* expression in neuroblastoma; higher Prp19 and YAP expression drive neuroblastoma bone marrow metastasis and were associated with worse outcomes in neuroblastoma.²⁸² YAP also mediates resistance to targeted inhibition of MEK1/2 in neuroblastomas with increased activation of RAS/MAPK signaling.^{118,119}

The paralog of YAP, TAZ also has proliferative and tumorigenic functions in neuroblastoma that are mediated by CTGF and PDGF- β .²⁸³ This TAZ-CTGF axis also mediates EMT, promoting metastasis in neuroblastoma.²⁸⁴ Additionally, the expression of TAZ in neuroblastoma cell lines was found to correlate with immunosuppressive activity against NK cells.²⁸⁵ Finally, immune infiltration is increased in tumors formed from mesenchymal neuroblastoma cell lines that express high levels of YAP and this was associated with a higher expression of antigen processing and presentation genes.¹⁴³ Given the known tumor microenvironmental roles of YAP/TAZ and the complexity of the neuroblastoma solid tumor TME, there is much that is still to be explored in this field that can improve current treatment paradigms.²⁸⁶

Chapter III: $\gamma\delta$ T cell biology, GD2 and GD2-targeting immunotherapies

3.1 The biology of $\gamma\delta$ T cells

3.1.1 Development, structure and function of $\gamma\delta$ T cells

T-lymphocytes can be subdivided into populations based on the T-cell receptor (TCR) that they express. Most T cells express an $\alpha\beta$ TCR and can be further classified as CD4+ or CD8+ based on their ability to recognize major histocompatibility complex (MHC) class II and I molecules expressed on immune and somatic cells respectively. The fortuitous discovery of the TCR γ and δ chains occurred when there was investigation into the role of gene rearrangement in antigen receptor generation in $\alpha\beta$ T cells and B cells.^{287,288} $\gamma\delta$ T cells are a small subset of T cells that are MHC-independent, recognize a wide range of molecular patterns and antigens, and possess properties of both the innate and adaptive immune responses. The $\gamma\delta$ T cell population matures in the thymus from the double negative (CD3-/CD4-/CD8-) thymocyte (thus named because of the lack of CD4 and CD8 receptors).^{289,290} After maturity, CD3+ $\gamma\delta$ T cells remain in the thymus, reside in secondary lymphoid organs, circulate in the peripheral blood, or become tissue-resident, with permanent surveillance roles in primarily mucosal sites and their surface layer/epithelium.²⁹¹

T-cell receptors (TCRs) are generated based on rearrangement of variable (V), diversity (D), and joining (J) gene segments. The γ chain is made as a result of a combination of V γ and J γ gene segments and the δ chain is from a combination of V δ , D δ , and J δ gene segments.²⁹² The diversity of the V gene segments in humans is currently most well-understood to determine $\gamma\delta$ T cell location and function and this will be our focus in classifying $\gamma\delta$ T cells moving forward. Although multiple V γ and V δ pseudogenes exist, in humans, the most commonly expressed V γ genes include: V γ 2, V γ 3, V γ 4, V γ 5, V γ 8 V γ 9, and V γ 11, and the functional V δ genes are V δ 1, V δ 2, and V δ 3.²⁹³

Subsets of $\gamma\delta$ T cells are classified based on their V δ expression, V δ 1, V δ 2 or V δ 3, with each subset demonstrating varying homing patterns and functions.²⁹⁴ The V δ 1 subset of $\gamma\delta$ T cells are the most prominent postnatal thymic population. However, V δ 1+ $\gamma\delta$ T cells only form a small portion of the $\gamma\delta$ T cells in the peripheral blood of healthy individuals; instead, in the blood, they expand in response to infection or remain tissue-resident in the gut and skin.²⁹⁵ V δ 1+ $\gamma\delta$ T cells show no preference for V γ pairing. In contrast, V δ 2 almost exclusively pairs with V γ 9 and although mature human V γ 9V δ 2 cells in the circulation constitute <10% of T cells in the blood, they account for up to 95% of the peripheral blood $\gamma\delta$ T cells.²⁹⁶ The final subset of $\gamma\delta$ T cells, V δ 3+ $\gamma\delta$ T cells form ~0.2% of circulating T cells but reside primarily in the liver.²⁹⁷

Since $\gamma\delta$ T cells are such a rare population in the blood, there are various *ex vivo* expansion protocols for each subtype that maximize the quantity of $\gamma\delta$ T cells that can be obtained for downstream applications. These expansion protocols depend on stimulation by natural ligands specific to each subset. Thus, we employed an expansion protocol which capitalizes on the ability of V γ 9V δ 2 cells to recognize and respond to metabolic intermediates of the mevalonate biosynthetic pathway which accumulate because of the inhibition of key enzymes by zoledronate, an aminobisphosphonate.²⁹⁸ Using this protocol, we expanded $\gamma\delta$ T cells, from healthy peripheral blood donors, which were previously shown by our group and others to possess cytotoxic activity against neuroblastoma.^{299,300}

In addition to the $\gamma\delta$ TCR, $\gamma\delta$ T cells express distinct cell surface molecules that enable them to perform their functions including NK cell receptors (NKR): natural killer group 2D (NKG2D) and DNAX accessory molecule 1 (DNAM-1/CD226); natural cytotoxicity receptor (NCR) family receptors including: NKp30 (natural cytotoxicity triggering receptor 3 (NCR3/CD337), NKp44 (NCR2/CD336), and NKp46 (NCR1/CD335), low-affinity IgG, Fc region receptor III (Fc γ RIII/CD16), and apoptosis-inducing ligands such as tumor necrosis factor-related apoptosis

inducing ligand (TRAIL/TNFSF10) and Fas Ligand (FasL/CD95L/TNFSF6) (**Figure 3.1**). Assessment and characterization of cell surface markers is essential for understanding the function of $\gamma\delta$ T cells and is shown in the results section of chapter IV of this dissertation (**Supplementary Figure S4.4**). In response to engagement of these receptors by various ligands on the surface of tumor cells, $\gamma\delta$ T cells produce cytolytic mediators such as granzyme and perforin as well as cytokines like tumor necrosis factor (TNF) and IFN γ .

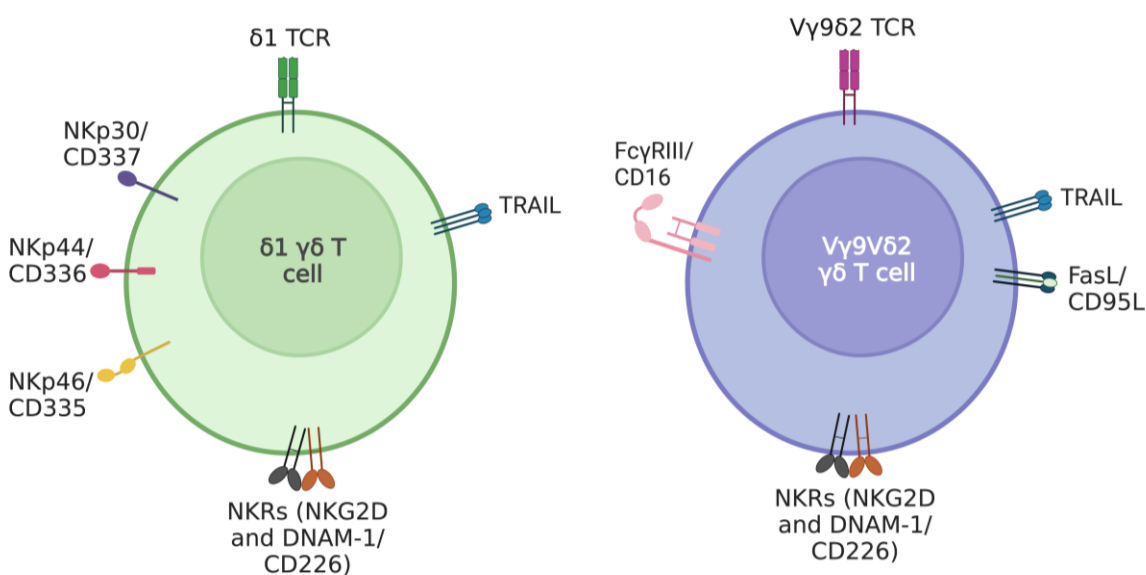


Figure 3.1. Expression of cell surface receptors and ligands on $V\delta 1$ and $V\gamma 9V\delta 2$ $\gamma\delta$ T cell subsets. Image adapted from Raverdeau *et al.*, 2019.³⁰¹

3.1.2 $\gamma\delta$ T cells in cancer

Many studies have sought to determine the prognostic value of assessing peripheral and tumor-infiltrating $\gamma\delta$ T cell populations in patients with cancer. An early work ascertained that tumor-infiltrating $\gamma\delta$ T cells were a poor prognostic indicator in patients with breast cancer.³⁰² However, a study of 39 different tumor types determined that, of all tumor-infiltrating immune cell populations, a $\gamma\delta$ T cell gene signature was associated with the most favorable prognosis.²⁴¹ In light of these contradictory data and the known distinct functions of $\gamma\delta$ T cell subsets, there is a necessity for further study into the contextual roles of $\gamma\delta$ T cells in cancer. Here, I first explore the

pro-tumorigenic roles of $\gamma\delta$ T cells, followed by anti-tumorigenic functions which recommend these cells as effective cellular immunotherapies (section 3.1.3).

The earliest insight into the protumorigenic function of $\gamma\delta$ T cells was a tumor-infiltrating V δ 1 population in breast cancer that reduced dendritic cell maturation and function and suppressed IL-2 secretion.³⁰³ Furthermore, tumor-promoting activity of $\gamma\delta$ T cells has also been linked to their production of interleukin-17 (IL-17) which does not typically occur at baseline in healthy individuals. Increased IL-17 production by $\gamma\delta$ T cells in patients with colorectal cancer leads to recruitment of immunosuppressive MDSCs and neutrophils to the TME.³⁰⁴ The excessive production of IL-17 by $\gamma\delta$ T cells has also been linked to increased angiogenesis, proliferation of tumor cells, and metastasis.^{305,306} The balance between IFN γ and IL-17 production in the TME is responsible for determining the degree to which there is skewing to an anti-tumorigenic or pro-tumorigenic milieu, respectively.³⁰⁷

Interactions between the receptors illustrated in **Figure 3.2** and ligands on the surface of tumor cells determine tumor cell recognition and killing by $\gamma\delta$ T cells. Tumor cells produce phosphoantigens in response to increased stress and dysregulation of the mevalonate pathway.³⁰⁸ Phosphoantigens bind intracellularly to butyrophilin subfamily 3 member A1 (BTN3A1/CD277),³⁰⁹ inducing a conformational change that results in interaction of the internal domains of BTN2A1/BTN3A1,³¹⁰ and their binding to the V γ 9 TCR chain on V γ 9V δ 2 T cells.³¹¹ The presence of phosphoantigens in stressed tumor cells mediates V γ 9V δ 2 T cell expansion and activation. Cytotoxic effector function of V γ 9V δ 2 T cells is also mediated by binding of NK cell receptors. Stress-induced molecules such as MHC class I chain-related proteins A and B (MICA and MICB), and UL16-binding proteins (ULBPs) bind NKG2D to mediate this cytotoxic function.^{312,313} Another NK cell receptor expressed on V γ 9V δ 2 T cells, DNAM-1, binds Nectin-2 (CD112) and poliovirus receptor (PVR/CD155).³¹⁴ Engagement of the NK receptors with tumor cells either

results in release of cytolytic granules with granzyme/perforin³¹⁵ or soluble TRAIL to induce apoptosis.³¹⁶ Ligation of death receptors by TRAIL and FASL/CD95L expressed on $\gamma\delta$ T cells is another mechanism of tumor cell killing.

Since these receptor-ligand interactions regulate effector function of V γ 9V δ 2 T cells, the expression of stress antigens and DNAM-1 ligands in SK-N-AS neuroblastoma cells is assessed in **Supplementary Figure S4.5** in the results section of Chapter IV. Finally, antibody-mediated cell-mediated cytotoxicity (ADCC) is another mechanism by which $\gamma\delta$ T cells interact with and kill tumor cells. The Fc region of therapeutic antibodies binds the Fc γ RIII (CD16) on V γ 9V δ 2 $\gamma\delta$ T cells, resulting in release of cytolytic mediators such as granzyme and perforin (**Figure 3.2**).^{317,318}

Finally, $\gamma\delta$ T cells mediate tumor cell killing indirectly by the release of IFN γ and TNF that stimulate CD8 T and NK cells. IFN γ released from $\gamma\delta$ T cells induces MHC I expression on tumor cells making them more targetable by CD8 T cells.³¹⁹ Although not the prototypical antigen-presenting cells, V γ 9V δ 2 $\gamma\delta$ T cells are capable of presenting tumor antigens, increasing tumor cell targeting by CD8+ cytotoxic T cells (**Figure 3.2**).³²⁰⁻³²² This process of antigen presentation by V γ 9V δ 2 $\gamma\delta$ T cells is licensed by their recognition and processing of antibody-opsonized tumor cells.³²³ Expression of 41BBL (CD137L/ TNFSF9) by $\gamma\delta$ T cells allows their interaction with 41BB (CD137/ TNFRSF9) on NK cells, stimulating NK cell-mediated cytotoxicity.³²⁴ Additionally, $\gamma\delta$ T cells promote B cell tumor-targeting antibody production and class switching through release of IL2, IL4, and IL10 (**Figure 3.2**).^{325,326}

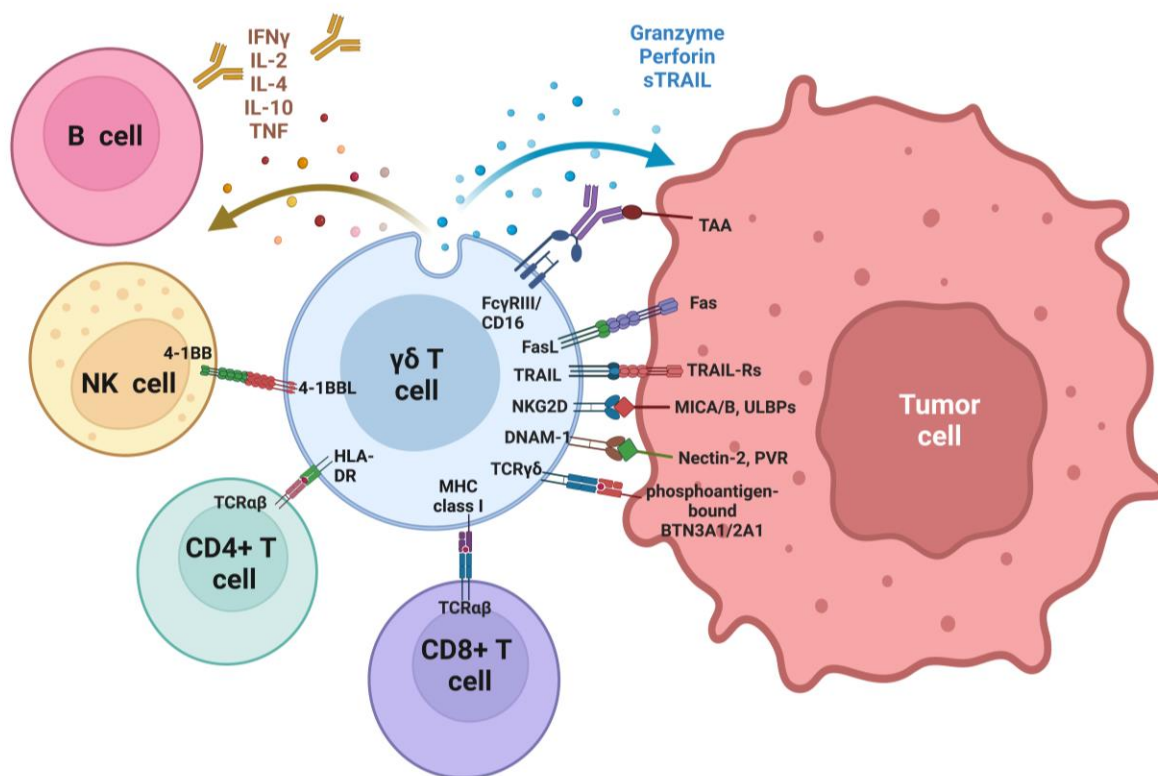


Figure 3.2. Antitumor effects of $\gamma\delta$ T cells are mediated through direct interaction with tumor cells or regulation of other immune cells including B cells, CD4 and CD8 T cells, and NK cells. Image adapted from Mensurado *et al.*, 2023.³²⁷

3.1.3 $\gamma\delta$ T cells as an immunotherapy

The utility of $\gamma\delta$ T cells as immunotherapeutic tools is illustrated by the numerous anti-tumorigenic functions in section 3.1.2. One advantage over their counterpart, $\alpha\beta$ T cells, is their MHC-independence, enabling allogeneic donors with potentially healthier immune systems to provide off-the-shelf therapeutic products. Much of the focus on developing $\gamma\delta$ T cells for immunotherapy has initially relied on V γ 9V δ 2 $\gamma\delta$ T cells. This dependence on the V γ 9V δ 2 $\gamma\delta$ T cell population is probably because of their abundance (when compared to V δ 1s) in peripheral blood. Initially, these studies attempted to stimulate *in vivo* expansion and activation of the V γ 9V δ 2 $\gamma\delta$ T cell compartment with IL-2, and bisphosphonates like pamidronate or zoledronate (or other synthetic phosphoantigens like bromohydrin pyrophosphate (BrHPP)) in patients with

neuroblastoma,³²⁸ prostate cancer,³²⁹ breast cancer,³³⁰ renal cell carcinoma,³³¹ and lymphoid malignancies.³³² These phase I clinical trials demonstrated the safety and general tolerability of *in vivo* expansion of V γ 9V δ 2 $\gamma\delta$ T cells; however, there was little to no clinical response in corresponding phase II trials.³³³

The relative ease of *ex vivo* expansion of V γ 9V δ 2 $\gamma\delta$ T cells using stimulants such as zoledronate and IL-2 allowed for allogeneic donors to be considered for $\gamma\delta$ T cell immunotherapy. This was an important development considering the likelihood that patients with cancer are immunocompromised and their *in vivo* expanded $\gamma\delta$ T cells may be ineffective as antitumorigenic agents. An additional advantage of the adoptive transfer of $\gamma\delta$ T cells is their ability to be modified *ex vivo* to be drug-resistant,³³⁴ to express CARs targeting tumor-associated antigens,^{335,336} including GD2,³³⁷ or to express a CAR of the external domain of NKG2D.³³⁸ Of these approaches, the phase I clinical trial of TMZ-resistant $\gamma\delta$ T cells ([NCT04165941](#)) for treatment of glioblastoma multiforme showed little or no dose-limiting toxicities and promising trends in progression-free survival; this trial continues to recruit patients through 2023.³²⁷ Data are not yet available for the NKG2DL-targeting phase I clinical trial ([NCT04107142](#)).

The limitations surrounding a clinically translatable V δ 1 expansion product have been recently overcome by the development of two Good Manufacturing Practices (GMP)-compliant methods that deplete the V δ 2+ populations in PBMCs and expand V δ 1+ cells using a combination of cytokines.^{339,340} As such, CAR V δ 1 $\gamma\delta$ T cells have been generated to target CD123 in acute myeloid leukemia (AML),³⁴¹ CD20 in B-cell malignancies ([NCT04735471](#)), and glypican-3 (GPC3) in hepatocellular carcinoma.³⁴²

Another immunotherapy that employs $\gamma\delta$ T cells or their TCR machinery are cell engagers. Cell engagers are antibody constructs that are typically designed to bring immune and target cells into

proximity to allow for targeted cancer cell killing. Bispecific T-cell engagers (BiTEs) are bispecific antibodies with a fused anti- $\gamma\delta$ TCR and anti-tumor antigen have been designed to target CD123 in AML,³⁴³ CD1d and CD40 in chronic lymphocytic leukemia (CLL),³⁴⁴⁻³⁴⁶ EGFR in colon cancer,³⁴⁷ and ERBB2 in pancreatic adenocarcinoma.³⁴⁸ Since V γ 9V δ 2 $\gamma\delta$ T cells are stimulated by BTN2A1/BTN3A1 engagement and the conformational change that results from phosphoantigen accumulation in tumor cells, another engager, a BTN3A1 agonist was designed to induce the same conformational change, rendering tumor cells more recognizable to V γ 9V δ 2 $\gamma\delta$ T cells.³⁴⁹ $\gamma\delta$ TCR anti-CD3 bispecific molecules (GABs) are another class of engagers which are designed to express an anti-CD3 (single-chain, variable fragment) scFV and a tumor-reactive V γ 9V δ 2 TCR to enable phosphoantigen-dependent tumor recognition by $\alpha\beta$ T cells.³⁵⁰ Finally, a recent PD-L1/CD3 BiTE-secreting HLA-G-expressing CAR V γ 9V δ 2 $\gamma\delta$ T cell was designed to effectively target NSCLC and triple negative breast cancer (TNBC) cells, directly killing tumor cells and recruiting other immune populations such as NK cells and CD8+ cytotoxic T cells to the TME.³⁵¹

Recent developments in immunotherapy seek to combine the advantages of persistence, helper activity, and robust effector function of $\alpha\beta$ T cells with the broad recognition of tumor cells by $\gamma\delta$ T cells. This approach generates autologous T cells engineered with defined $\gamma\delta$ TCRs (TEGs) and counteracts the downregulation of tumor-associated antigens, a well-established mechanism of tumor escape of CAR $\alpha\beta$ T cell therapies.³²⁷ These engineered T cells were generated for testing in models of acute myeloid leukemia, high-risk myelodysplastic syndrome, and multiple myeloma.³⁵²⁻³⁵⁴ A clinical phase I trial of TEG002 ([NCT04688853](https://clinicaltrials.gov/ct2/show/study/NCT04688853)) for relapsed/refractory multiple myeloma is estimated to be completed in 2024.

Currently, several combination treatments that either enhance innate $\gamma\delta$ T cells or synergize with infused $\gamma\delta$ T cell products are being explored. In cancers with HLA class I defects, $\gamma\delta$ T cells were found to be the effectors of checkpoint inhibitor immunotherapy.³⁵⁵ There is also precedent for $\gamma\delta$

T cell immunotherapy in neuroblastoma. Human $\gamma\delta$ T cells in combination with IL-2 (or zoledronate, IL-15, and IL-18) were found to recognize and kill neuroblastoma cell lines and tumor-initiating cells, respectively in *in vitro* models.^{356,357} Additionally, a combination immunotherapy with $\gamma\delta$ T cells, hu14.18, a GD2-targeting antibody, and Fc-IL7 immunocytokine extended survival in a disseminated neuroblastoma mouse model.³⁵⁸ The V δ 1 T cell subset was also effective in cytolysis of neuroblastoma cells.³⁵⁹ These studies were performed almost 20 years prior to the writing of this dissertation. More recently, a combination of $\gamma\delta$ T cells (from neuroblastoma patient apheresis products), TMZ and dinutuximab was found to effectively regress subcutaneous neuroblastoma tumors in murine models.²⁹⁹ Another elegant publication established a robust pipeline for selection of potent donor $\gamma\delta$ T cell products for use in neuroblastoma immunotherapy trials.³⁰⁰ Based on this and other work, there is currently a phase I clinical trial recruiting patients with refractory, relapsed, or progressive neuroblastoma to be treated with an allogeneic $\gamma\delta$ T cell product in combination with dinutuximab, irinotecan, temozolomide, and zoledronate ([NCT05400603](#)). The results in chapter IV of this dissertation examine a role for YAP inhibition in improving the efficacy of a combination of GD2-targeting antibodies and $\gamma\delta$ T cells. Thus, in section 3.2, GD2 and its role as an immunotherapeutic target in neuroblastoma is covered.

3.2 The glycosphingolipid GD2 and its biological significance

3.2.1 Glycobiology and biosynthesis of GD2

Glycosphingolipids are a class of lipids that have a ceramide backbone (sphingosine with a fatty acid residue) to which carbohydrate groups are added.³⁶⁰ Ceramide (Cer) is synthesized on the cytosolic surface of the ER and transported to the Golgi complex.³⁶¹ Gangliosides are a specific class of sialic acid-containing glycosphingolipids that consist of a Cer tail, glucose (Glc) is linked to the Cer, followed by galactose (Gal) and N-acetylgalactosamine (GalNAc) (**Figure 3.3**). The

number of sialic acid (NeuAc) residues attached to the Gal residue determines classification into series: 0, 1, 2, and 3 NeuAc residues are 0-, a-, b-, and c-series respectively (**Figure 3.3**).

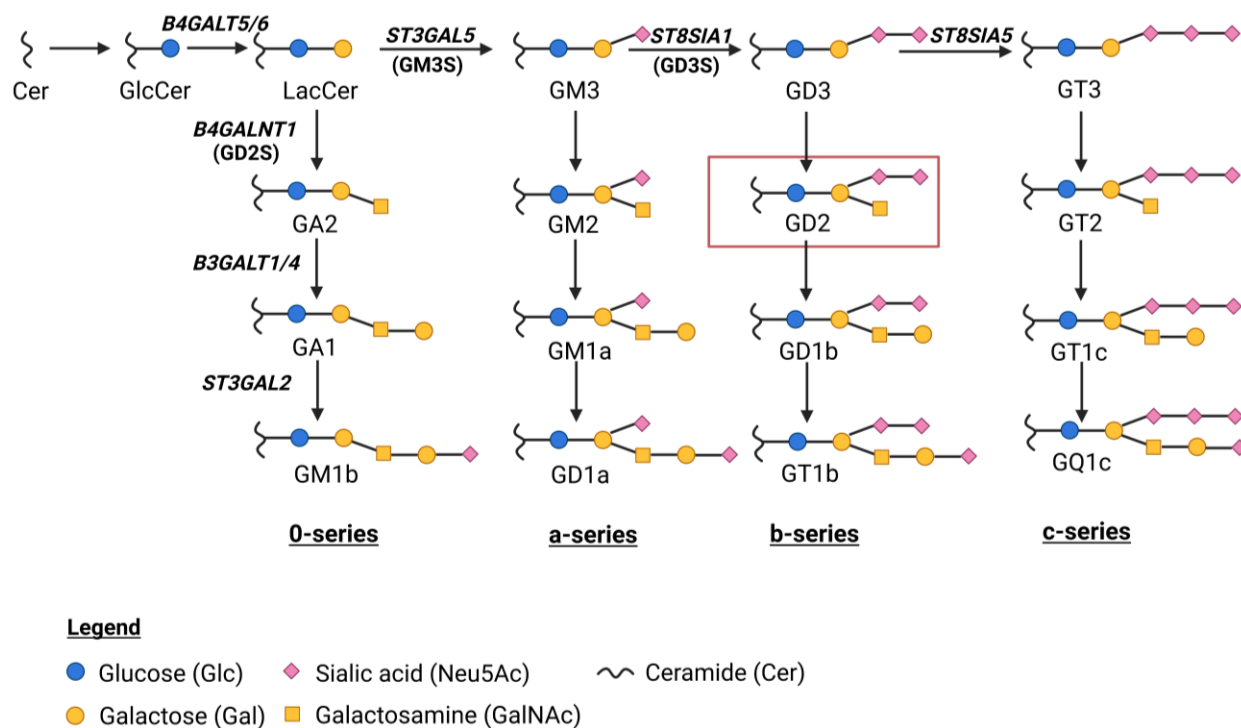


Figure 3.3. Ganglioside biosynthesis. Adapted from Sterner *et al.*, 2017.³⁶²

The addition of sugar groups to construct a ganglioside consists of consecutive reactions catalyzed by enzymes, membrane-bound sialyltransferases and glycosyltransferases, that reside in the Golgi complex. The regulation of these enzymes is mainly through transcriptional mechanisms; however, post-translational modifications have also been demonstrated to alter their activity.³⁶³ Gangliosides are then trafficked in vesicles to the cell surface and are distributed on the plasma membrane, with glycan moieties pointed externally, clustering with cholesterol in structures called glycolipid enriched microdomains (GEMs) or lipid rafts.

Gangliosides are expressed in every mammalian tissue; however, they are specifically enriched in the brain and nervous tissue. Genetic defects in ganglioside biosynthesis are rare and constitute

mutations in GM3 synthase (*ST3GAL5*) and GM2/GD2 synthase (*B4GALNT1*) that lead to infantile-onset epilepsy and complex hereditary spastic paraplegia, respectively.³⁶⁴⁻³⁶⁶ Glycosphingolipid storage disorders are slightly less rare and are caused by defects in glycosphingolipid (including ganglioside) catabolism, leading to glycosphingolipid accumulation in lysosomes. Ganglioside metabolic errors are also implicated in neurodegenerative disease.³⁶⁷ Gangliosides function as signaling molecules at the surface of the cell, mediating adhesion, and cell-to-cell recognition. Furthermore, gangliosides protect host cells from autoimmunity but may be exploited as recognition sites for pathogens including bacteria, parasites, and viruses.³⁶⁷ Intracellularly, gangliosides regulate calcium homeostasis, affecting the ER stress response; when this process is dysregulated, apoptosis is triggered.³⁶⁸

The structure of the disialoganglioside GD2, as its name suggests, consists of 2 sialic acid residues and is highlighted in the red box in **Figure 3.3**. The discovery of GD2 was initially made because of the antibodies that were generated in response to its expression on the surface of fetal brain and melanoma cells.^{369,370} GD2 was later detected on neuroblastoma cells by targeting with GD2-specific monoclonal antibodies.³⁷¹

3.2.2 GD2 expression in cancers including neuroblastoma

Changes in glycosylation and sialylation at the cell surface may lead to generation of tumor-associated antigens, including gangliosides.³⁷² The increased expression of gangliosides is not inert; because of their residence in lipid rafts, gangliosides have been determined to regulate RTK signaling by rearrangement of RTK intracellular domains to allow for dimerization and activation, or through direct ganglioside-RTK binding.³⁷³ The complex ganglioside GD2 leads to increased proliferation in breast cancer through activation of the RTK, c-Met.³⁷⁴ Increased expression of gangliosides, particularly GD2 and GD3, is reported to occur in numerous cancers including breast cancer,³⁷⁵ Ewing Sarcoma,³⁷⁶ glioma,³⁷⁷ melanoma,³⁷⁸ neuroblastoma,³⁷⁹ small cell lung

cancer,³⁸⁰ and osteosarcoma.³⁸¹ Moreover, gangliosides may be shed into the extracellular environment where they can act as immunosuppressive factors.³⁸²

In solid tumors other than neuroblastoma, GD2 has been determined to modulate a wide variety of oncogenic functions ranging from proliferation and invasion,³⁸³ to immune evasion but the mechanisms underlying these phenotypes have not been fully elucidated.³⁸⁴ While the body of literature validating GD2 as a ubiquitously expressed neuroblastoma antigen is vast, there is limited data on its functional role in the disease. The ability of GD2 to mediate attachment of neuroblastoma cells to the extracellular matrix may nominate it as a regulator of invasion, leading to metastasis but this has not been proven directly.³⁸⁵ Instead of functional studies, much of the initial focus on the role of GD2 in neuroblastoma was on its expression being of clinical prognostic value, later shifting to spotlight its potential as a therapeutic target. Cultured neuroblastoma cell lines and primary tumors from patients were determined to express high levels of GD2; additionally, serial assessment of serum levels of GD2 were positively correlated with neuroblastoma disease progression.^{379,386} Another study determined that patients with localized neuroblastoma who had GD2-positive cells in their bone marrow had worse overall survival than those who did not.³⁸⁷ These and other publications established interest in determining whether GD2 was a promising therapeutic target in neuroblastoma.

3.3 GD2-targeting immunotherapies

3.3.1 GD2 as a cancer immunotherapeutic target

The first GD2-targeting therapies to be approved for clinical use were monoclonal antibodies (mAbs). Murine, humanized, and chimeric (human/murine) antibodies have been tested in clinical trials including murine 3F8 (m3F8), naxitamab/humanized 3F8 (Hu3F8), murine 14G2a, humanized 14.18K322A (hu14.18K322A) (not depicted),³⁸⁸ dinutuximab (ch14.18), and dinutuximab-beta (**Figure 3.4**).³⁸⁹ The difference between dinutuximab and dinutiximab-beta is

the organism in which these antibodies are raised: dinutuximab is generated in mice and dinutuximab-beta, hamsters. Although these mAbs have similar specificity to GD2, to date, the mAb with the greatest binding affinity is humanized 3F8.³⁶²

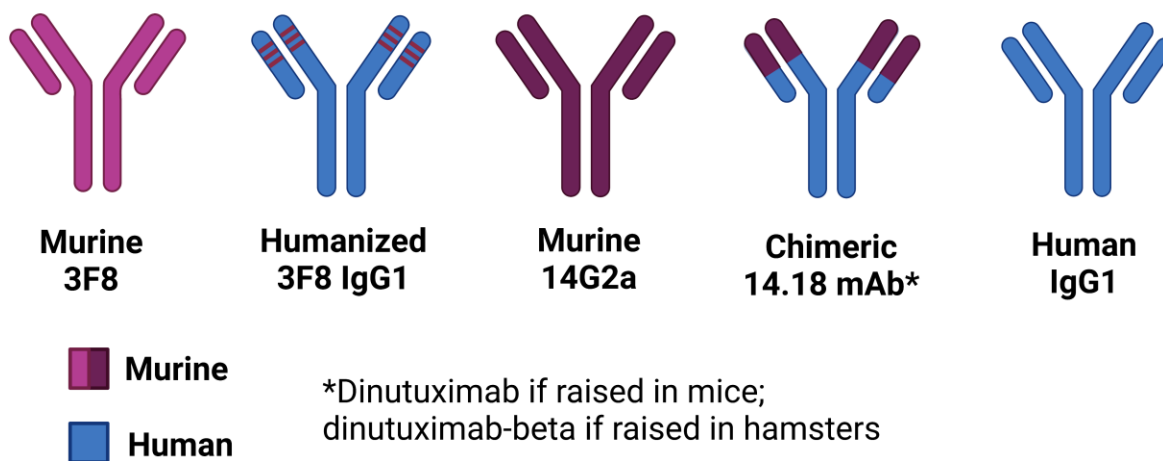


Figure 3.4. Structures of GD2-targeting monoclonal antibodies. Adapted from Mora *et al.*, 2016³⁹⁰

In 2015, the chimeric IgG1 anti-GD2 mAb, dinutuximab was the first GD2-targeting drug to be approved for clinical use.³⁹¹ This approval occurred after results of a phase III clinical trial demonstrated significant increases in event-free and overall survival when dinutuximab, GM-CSF, IL-2, and isotretinoin were used for treatment of patients with high-risk neuroblastoma.³⁹² The mechanism of action of dinutuximab is primarily complement-dependent cytotoxicity and ADCC, as well as phagocytosis of neuroblastoma cells.³⁸⁹ The normal expression of GD2 on healthy nervous tissue resulted in toxicities including neuropathic pain. However, long-term follow-up of this trial still shows that patients who received the combination of dinutuximab, GM-CSF, IL-2, and isotretinoin versus isotretinoin only had significantly increased event-free and overall survival at 5 years.³⁹³ In 2017, dinutuximab-beta (Qarziba®) was approved by the European Medicines Agency for treating patients with high-risk neuroblastoma. In 2020, naxitamab or Hu3F8 (with GM-CSF) was approved for use in patients with relapsed/refractory

high-risk neuroblastoma in bone or bone marrow ([NCT03363373](#)) and is currently being tested in a phase I trial for patients with recurrent osteosarcoma ([NCT02502786](#)).

Although GD2 has primarily been targeted in neuroblastoma, as previously mentioned, it is highly expressed in many cancers. Some brain cancers, like gliomas, express high levels of GD2. Preclinical testing of 4-1BB-based (with a 14G2A scFV) anti-GD2 CAR T cells in H3K27M-mutant diffuse midline gliomas demonstrated significant extension in survival, with complete tumor regression in some mice, and limited toxicity.³⁹⁴ A phase I clinical trial ([NCT04196413](#)) was initiated which within 2 years showed significant clinical improvement and radiographic reduction in tumor volume of patients with diffuse intrinsic pontine glioma, an extremely aggressive cancer.³⁹⁵

There are no GD2-targeting CAR T cells which have yet been approved by the Food and Drug Administration (FDA) as all currently approved CAR T cell therapies exist only for blood malignancies. A recent phase I/II clinical trial with autologous GD2-CAR T cells for treating relapsed/refractory high-risk neuroblastoma provided exciting results and will be described in section 3.3.2.³⁹⁶ However, as reported on ClinicalTrials.gov, there are at least 60 (phase I/II) clinical trials worldwide investigating novel GD2-targeting therapies in a range of solid tumors including diffuse intrinsic pontine glioma, Ewing sarcoma, melanoma, neuroblastoma, osteosarcoma, and SCLC.

3.3.2 Optimizing response to anti-GD2 immunotherapy

Although GD2 is ubiquitously expressed in neuroblastoma, GD2 expression levels vary in cell line models, and anecdotal data suggests that GD2 expression on neuroblastoma tumors may be downregulated post-chemotherapy. There have been recent efforts to increase GD2 levels on neuroblastoma cells or to optimize GD2 targeting in models that express low levels of GD2.

Antibody-drug conjugates that combine ch14.18 and the antimetabolic drugs (that inhibit tubulin polymerization) monomethyl auristatin E (MMAE) or F (MMAF), respectively were used to treat breast cancer, glioma, melanoma, neuroblastoma, and osteosarcoma cell lines with varying levels of GD2 expression *in vitro*.³⁹⁷ Since the drug-to-antibody ratio can be altered in ADCs, this represents a promising approach to targeting cells with low expression of GD2.³⁹⁷

Another strategy to improve efficacy of anti-GD2 targeting immunotherapies is to increase the expression of GD2 at the surface of neuroblastoma cells that express it at lower levels. Published studies have used epigenetic modulators such as histone deacetylase (HDAC) inhibitors, valproic acid,³⁹⁸ or vorinostat,³⁹⁹ or the EZH2 inhibitor, tazemetostat⁴⁰⁰ to increase the expression of *ST8SIA1*, the gene encoding GD3 synthase (GD3S) involved in GD2 biosynthesis; thus, increasing GD2 cell surface expression. One of these studies determined that the pan-HDAC inhibitor, vorinostat, supplemented with a sialic acid analog, significantly increased GD2 surface expression.³⁹⁹ The combination of epigenetic inhibition and anti-GD2 antibody or CAR T cell treatment was effective in reducing tumor burden in both orthotopic and disseminated neuroblastoma models in mice.^{400,401} Thus, a combination of anti-GD2 treatment and epigenetic inhibition may be effective for patients determined to have neuroblastoma tumors with reduced GD2 expression.

The combination of GD2-targeting mAb, dinutuximab, GM-CSF, and isotretinoin, while effective, still is not curative in a percentage of patients with high-risk neuroblastoma. Thus, there are redoubled efforts to determine other targets, immunotherapeutic or otherwise, that might synergize with anti-GD2 therapies. One such approach combines dinutuximab with an anti-CD47 mAb and effectively potentiates phagocytosis of neuroblastoma (as well as osteosarcoma and SCLC) cells by macrophages.⁴⁰² The mechanism of action of this combination is simultaneous blocking of an inhibitory sialic-acid-binding immunoglobulin-like lectin-7 (Siglec-7)-GD2

interaction and CD47, a checkpoint molecule expressed on tumor cells that inhibits phagocytosis by macrophages.⁴⁰² Unfortunately, the phase I clinical trial ([NCT04751383](#)) of this combination, magrolimab (anti-CD47 mAb, Hu5F9-G4) and dinutuximab for treatment of patients with relapsed/refractory neuroblastoma or relapsed osteosarcoma, was suspended for unacceptable toxicities.

Additionally, fatal neurotoxicity was induced in mice with neuroblastoma receiving a GD2-targeting CAR T cell with a 4-1BB or CD28-co-stimulatory domain.^{403,404} However, this observation was not universal with the use of GD2-targeting CAR T cells of similar design.⁴⁰⁵ To minimize the potential for on-target, off-tumor toxicity of targeting GD2, a GD2-B7-H3 (CD276) SynNotch CAR T cell was constructed that is 'AND-gated', meaning that the targets killed by these CAR-T cells must express both GD2 and B7-H3 which increases their specificity toward neuroblastoma cells only.⁴⁰⁴ GD2-targeting CAR T cells administered with cyclophosphamide and fludarabine for lymphodepletion in patients with neuroblastoma showed modest response, and the addition of PD-1 inhibition did not improve efficacy.⁴⁰⁶ This result was surprising considering the ability of PD-1 blockade to reduce activation-induced cell death of GD2-targeting CAR T cells in a phase I clinical trial for the treatment of metastatic melanoma.⁴⁰⁷

Until 2023, clinical trials of GD2-directed $\alpha\beta$ CAR T cells alone for the treatment of patients with neuroblastoma showed minimal toxicity or efficacy.^{408,409} However, in a phase I/II clinical trial testing an autologous, third-generation CAR T cell targeting GD2 (GD2-CART01), del Bufalo *et al.* demonstrated an impressive overall response rate of 63% in patients with relapsed/refractory high-risk neuroblastoma.³⁹⁶ One of 27 patients experienced severe treatment-related toxicity, cytokine release syndrome, and the inducible caspase 9 suicide gene was activated to effectively eliminate the GD2-CART01 CAR T cells.³⁹⁶ The overall survival at 3 years was 60% in patients receiving the complete dosing regimen, providing first evidence of an effective and safe GD2-

targeting CAR T cell for use as a single treatment for relapsed/refractory high-risk neuroblastoma.³⁹⁶

Apart from $\alpha\beta$ CAR T cells, V α 24-invariant natural killer T cells (NKTs) have also been generated to express a GD2-targeting CAR and IL-15 which increases the *in vivo* efficacy and persistence of CAR-NKTs in mice.⁴¹⁰ In a phase I clinical trial treating patients with relapsed or refractory neuroblastoma, GD2-specific CAR-NKTs were found to result in objective response in 25% of patients treated and persistence and anti-tumor activity of CAR-NKTs was increased by inhibition of BTG anti-proliferation factor 1 (BTG1).^{411,412} These studies all provide a rationale for determining approaches that will increase GD2 surface expression to improve the efficacy of treatments targeting this disialoganglioside in neuroblastoma.

Chapter IV: The Yes-Associated Protein (YAP) promotes resistance to anti-GD2 immunotherapy in neuroblastoma through downregulation of *ST8SIA1*.

4.1 Introduction

Clinical outcomes for children with the extracranial solid tumor neuroblastoma remain unsatisfactory. Following intensive multimodal treatment, greater than half of patients with high-risk neuroblastoma relapse with a substantially reduced chance for cure.^{1,14,15,413} To improve outcomes for these patients requires a greater understanding and therapeutic targeting of pathways regulating disease recurrence. Relapsed neuroblastoma is characterized by an increased frequency of genomic alterations that activate the RAS-MAPK pathway, such as activating mutations in *ALK*, *KRAS*, *NRAS*, *HRAS*, *PTPN11* and inactivating mutations of *NF1* and *PTPN14*.^{10,11,414} In its active state, PTPN14 inhibits the nuclear localization of the Yes-associated protein (YAP) to prevent YAP-mediated transcription.^{10-12,28,415} Accordingly, the same genome-wide association studies of relapsed neuroblastomas also identified a significant increase in YAP transcriptional activity, suggesting a potential role for YAP in recurrent neuroblastoma.¹²

YAP is a transcriptional co-regulator that primarily binds to TEAD family transcription factors.^{193,416} YAP and TEAD transcriptionally activate or repress downstream target genes, contributing to cell proliferation, self-renewal and survival in many cancers, including neuroblastoma.^{204,417} YAP is highly expressed in neuroblastoma cells that demonstrate an undifferentiated mesenchymal phenotype, which is characteristically chemotherapy resistant.^{12,132} Using paired high-risk neuroblastoma tumors derived from the same patient at diagnosis and at tumor recurrence following chemotherapy, we have previously shown increased YAP expression and transcriptional activity at relapse.¹¹⁸ Genetic inhibition of YAP delayed tumor growth and sensitized *NRAS*-mutated neuroblastoma xenografts to cytotoxic chemotherapy and MEK inhibitor treatment *in vivo*, yet failed to have the same effects *in vitro*, suggesting YAP plays

a crucial role driving therapy resistance within the solid tumor microenvironment (TME).^{118,119} RNA sequencing of neuroblastomas with and without YAP genetic knockdown revealed that YAP suppresses the BH3 pro-death gene, *HRK*, to attenuate chemotherapy and MEK inhibitor responses *in vivo*.¹¹⁸ Therefore, YAP upregulation following chemotherapy and relapse promotes therapy resistance in high-risk neuroblastoma through transcriptional repression of genes that play a role in the TME.

A common approach to treating patients with chemotherapy resistant, relapsed neuroblastoma uses immunotherapies targeting neuroblastoma-specific tumor antigens. The glycosphingolipid GD2 is expressed on the surface of neuroblastomas,^{386,418,419} and the introduction of humanized monoclonal antibodies targeting GD2 (i.e. dinutuximab) significantly improved survival for newly diagnosed patients with high-risk disease.^{392,393} Anti-GD2 antibodies have also been combined with cytotoxic chemotherapy (“chemoimmunotherapy”), which demonstrated impressive response rates for relapsed neuroblastoma and resulted in GD2 chemoimmunotherapy becoming the most widely used salvage therapy for patients with refractory or relapsed disease.^{14,420} Unfortunately, not all patients respond to GD2-targeting immunotherapies and robust biomarkers of response are so far lacking, leaving many to suffer toxicities with no clinical antitumor benefit.^{393,421,422}

Resistance to immunotherapy can be caused by lack of expression or downregulation of the cell surface target of interest.⁴²³ Indeed, GD2 can become downregulated following therapy and neuroblastoma recurrence.⁴²⁴⁻⁴²⁶ Recent studies also suggest that mesenchymal neuroblastomas resist GD2-targeted therapies via inhibition of GD2 synthesis, yet the role for YAP, a canonical mesenchymal marker, has not been explored.⁴⁰⁰ Given the increased expression and activity of YAP in relapsed neuroblastoma, and its role in mediating cytotoxic and targeted therapy resistance, we posited that YAP plays a role in GD2 immunotherapy response. Here, we

demonstrate for the first time that YAP genetic inhibition sensitizes neuroblastomas to anti-GD2 antibody *in vitro* and *in vivo*. We further show that YAP transcriptionally suppresses *ST8SIA1* that encodes GD3 synthase, the rate-limiting enzyme for GD2 synthesis, supporting that YAP inhibition can be leveraged therapeutically to enhance patient responses to immunotherapeutic approaches targeting GD2.

4.2 Materials and Methods

Cell culture

Human-derived neuroblastoma cell lines, CHLA-255, NLF, and SK-N-AS were cultured in RPMI supplemented with 10% fetal bovine serum (FBS) and 1% penicillin/streptomycin at 37°C, 5% CO₂. Cell lines were routinely STR genotyped and resulting identities were confirmed to match the COG cell line database (cccells.org). Cells were also verified to be free of *Mycoplasma* contamination using the MycoAlert contamination kit (Lonza).

Generation of stably transduced cell lines

YAP was genetically inhibited in SK-N-AS cells using short hairpin RNA (shRNA) as previously described.¹¹⁸ *TAZ* was genetically inhibited in SK-N-AS cells using three independent constructs expressing *TAZ*-targeting shRNAs (Genecopoeia LVRU6H-a (shTAZ1), LVRU6H-b (shTAZ2), and LVRU6H-c (shGD3S-2)) and a hygromycin selection marker.¹¹⁸ GFP-empty, GFP-YAP 5SA, and GFP-YAP S94A constructs were ectopically expressed in SMS-SAN. *ST8SIA1* was genetically inhibited in shYAP cells as previously published using two independent constructs expressing *ST8SIA1*-targeting shRNAs (Genecopoeia LVRU6H-b (shGD3S-1) and LVRU6H-c (shGD3S-2)) and a hygromycin selection marker.¹¹⁸ The equivalent non-targeting control vectors were transduced appropriately (Sigma SHC016 (control) and Genecopoeia CSI-neg-LVRU6H (LV control)). Cells with successful lentiviral transduction were selected with 2ug/mL puromycin (YAP constructs) and 150ug/mL hygromycin (TAZ and ST8SIA1 constructs).

Western blot analysis

Neuroblastoma cells were harvested with versene (ThermoFisher Scientific) and lysed in CHAPS buffer (10 mM HEPES, 150 mM NaCl, 2% CHAPS) supplemented with 1% PMSF, 1% Protease

Inhibitor Cocktail (Roche), and 4% sodium orthovanadate on ice for 2 hours. Debris was cleared from resulting lysates by centrifugation at 8000 rcf for 15 mins. Protein concentration was quantified by Bradford assay. 25 ug of total protein was loaded on 4-12% NuPage Bis-Tris gels (ThermoFisher Scientific) and electrophoresed at 200V for 35 mins. Separated proteins were transferred onto polyvinylidene difluoride (PVDF) membranes at 30V for 90 minutes. Primary antibodies were diluted in 5% blocking buffer (Bio-Rad) in tris-buffered saline with Tween 20 (TBST) overnight and secondary anti-rabbit or anti-mouse HRP for 2 hours as appropriate. Membranes were imaged by chemiluminescence using Pierce ECL substrate (ThermoFisher Scientific). See **Supplementary Table S1** for antibody information.

Gamma delta ($\gamma\delta$) T cell expansion

$\gamma\delta$ T cells were expanded under our 12-day protocol as previously described with $\alpha\beta$ T cell depletion on day 6 of culture from healthy donor peripheral blood mononuclear cells.³⁰⁰ The expanded $\gamma\delta$ T cell population was profiled by flow cytometry with antibodies: CD3-BV421, CD56-APC-R700, CD16-BV480, and $\alpha\beta$ -TCR-PE or $\gamma\delta$ -TCR-PE and used between days 12 and 14 in the cytotoxicity assays described below.³² See **Supplementary Table S2** for antibody information.

Cytotoxicity assays

Bioluminescence-based

GFP-luciferase-tagged neuroblastoma cell lines were plated at 34,000/well in RPMI supplemented with 10% heat-inactivated FBS in 96-well plates and allowed to adhere overnight. The following day, $\gamma\delta$ T cells were added at increasing effector-to-target (E:T) ratios (0:1, 1:1, and 5:1), with and without 5ug/mL dinutuximab. Co-cultures were incubated for 4 hours prior to the addition of luciferin (75ug/mL, PerkinElmer) for detection of viable target (NB) cells.

Luminescent signal was detected using the Promega GloMax™-Multi Detection System. The calculation of death was performed using the following formula: %specific lysis = 100 x (spontaneous death RLU – test RLU)/ (spontaneous death RLU – maximal killing RLU) where RLU is an abbreviation for relative luminescence units.

Flow cytometry-based

Neuroblastoma cells were labeled with Violet Proliferation Dye 450 (VPD450, BD Biosciences) and plated in RPMI supplemented with 10% heat-inactivated FBS at 200,000 cells/well in 24-well plates and allowed to adhere overnight. The following day, fresh $\gamma\delta$ T cells from expansion day 12 or 14 were added to neuroblastoma cells for co-culture at increasing E:T ratios ($\gamma\delta$ T cells-to-neuroblastoma cells) (0:1, 1:1 and 5:1) in the presence and absence of dinutuximab (5 ug/mL, United Therapeutics). Cells were incubated together for 4 hours and then harvested with accutase (GeminiBio). Cells were washed with PBS and resuspended in Annexin V binding buffer (Biolegend), stained with Annexin V-APC antibody (Biolegend) and analyzed immediately on the Aurora Cytok spectral flow cytometer. Prior to acquisition, BD Via-Probe cell viability solution (BD Biosciences) was added to the cell suspension. Unmixing of flow cytometry data was performed at the cytometer with further data analysis and gating performed using FlowJo v10.8.1 (FlowJo, LLC) software. See Supplementary Figure S4.1 for gating strategy.

Detection of human IFN γ by enzyme-linked immunosorbent assay (ELISA)

Human IFN γ was detected using a commercial kit (Biolegend). Supernatants were harvested from cytotoxicity assays in which SK-N-AS control, shYAP1 and shYAP2 neuroblastoma cells were co-cultured with $\gamma\delta$ T cells at E:T ratios of 0:1, 1:1, and 5:1 for 4 hours. Briefly, supernatants were centrifuged to remove cell debris. IFN γ standards were generated by reconstituting recombinant

IFN γ (Biolegend) in sterile deionized water. Concentrations of IFN γ in samples and standards were determined per manufacturer's instructions. The BioTek Synergy Mx Microplate reader was used to read absorbance at 450nm.

Flow cytometry

GD2 staining of neuroblastoma cell lines and xenografts

Cells were harvested with versene (Gibco), washed in phosphate-buffered saline (PBS), followed by resuspension in FACs buffer (PBS, 10% FBS, 0.1% sodium azide, 5mM EDTA), and then stained with the live-dead stain, fixable viability stain 780 (BD Biosciences), by incubation at room temperature protected from light. Cells were then washed and stained with Isotype-BV421/ GD2-BV421 only for *in vitro* GD2 characterization and CD45-PerCP-Cy5.5, CD56-PE, CD81-FITC, Isotype-BV421/ GD2-BV421, for *in vivo* GD2 characterization at room temperature, washed twice in FACs buffer and resuspended for data acquisition on the Cytex Aurora 5-laser spectral flow cytometer. Negative controls were fluorescence minus one (FMO) controls for NBx28r and SKNAS CDX, unstained for NBx14r, NBx27, NBx 34R (due to lack of tissue availability). All neuroblastoma patient-derived xenografts (PDXs) were passage 2 or less. Data was analyzed using FlowJo version 10.9.0. See gating strategy (*in vitro*) in Supplementary Figure S4.2. See Supplementary Table S4.3 for antibody information.

Determination of $\gamma\delta$ T cell activation state (CD107a staining)

Neuroblastoma cells (SK-N-AS control, SK-N-AS shYAP1, and shYAP2) were co-cultured with $\gamma\delta$ T cells at an E:T ratio of 1:1 as described in the flow cytometry-based cytotoxicity assay protocol above. CD107a-PE Cy7 antibody was added to each well 30 minutes after the cytotoxic assay was started. GolgiStop (BD Biosciences) was added one hour later at a final concentration of

0.7uL/mL. At the endpoint, $\gamma\delta$ T cells were harvested and stained with CD3-BV421, CD56-APC-R700, and $\gamma\delta$ TCR-PE, washed twice in FACs buffer and resuspended for data acquisition on the Cytex Aurora 5-laser spectral flow cytometer. See Supplementary Table S4.2 for antibody information. Data was analyzed using FlowJo version 10.8.1.

Extensive characterization of $\gamma\delta$ T cells pre- and post-cytotoxicity assay

Neuroblastoma cells (SK-N-AS control, shYAP1, and shYAP2) and $\gamma\delta$ T cells were co-cultured at a 1:0 or 1:1 E:T ratio for 24 hours. The $\gamma\delta$ T cells were harvested at 24 hours and profiled using our previously published extensive characterization panel.³⁰⁰ See Supplementary Table S4 for antibody information.

Reverse transcription quantitative real-time PCR (RT-qPCR)

RNA was extracted from neuroblastoma cell lines using the TRIzol (Ambion)-chloroform (Millipore Sigma) extraction method and quantified using a NanoDrop 2000 (Thermo Scientific). cDNA was prepared from 2ug RNA by using the high-capacity cDNA reverse transcription kit (Applied Biosystems) per manufacturer's protocol. For real-time qPCR, SYBR green reagent (Applied Biosystems) was used with the primers listed in Supplementary Table S5. Gene expression was normalized to *GAPDH* and *HPRT* using the CFX96 Touch Real-Time PCR Detection System software (Bio-Rad).

Mouse xenograft *in vivo* studies

All animal studies were conducted in accordance with policies set forth by the Emory University Institutional Animal Care and Use Committee (IACUC). Our protocol was approved by the Emory

IACUC (PROTO201700089). Euthanasia was performed by asphyxiation with CO₂ and cervical dislocation. 4 x 10⁶ SK-N-AS cells were combined at a 1:1 ratio (by volume) with Matrigel (Corning) and injected subcutaneously into the flank of 4 – 6-week-old female and male NOD-*scid* IL2Rgamma^{null} (NSG) mice (The Jackson Laboratory). Tumor volume was calculated using the formula: length x width x height x $\pi/6$. When tumors grew to a volume of 100-200mm³, mice were randomized to the treatment groups. Mice receiving the full regimen were treated on days 1, 4, 7 and 10 with 75mg/kg cyclophosphamide (McKesson) intraperitoneally; on days 2, 8, and 14 with 100ug dinutuximab intravenously; on days 3, 6, 9, 12, 15, and 18 with 2.5 x 10⁶ $\gamma\delta$ T cells (expanded from healthy human blood as described above) intratumorally. Mice were sacrificed when tumor burden reached IACUC-prescribed limit based on tumor volume (1500mm³) and physical burden. Tumors were harvested and mechanically dissociated to extract RNA and protein to perform RT-qPCR, western blots, and flow cytometry as described above.

Statistical analyses

GraphPad Prism v9.4.1 was used to perform all statistical analyses. For pairwise comparisons throughout, unpaired t-tests with Welch's correction were calculated. Kaplan-Meier survival plots were generated for *in vivo* investigations, and log rank test performed to determine statistical significance.

4.3 Results

Neuroblastoma cell lines that express high YAP and low GD2 are resistant to dinutuximab and gamma delta ($\gamma\delta$) T cell treatment *in vitro*. Given the increased expression and activity of YAP in relapsed neuroblastoma and its influence on chemotherapy response, we sought to determine if YAP might also play a role in GD2 immunotherapy response. We first evaluated YAP and GD2 expression in three neuroblastoma cell lines: SK-N-AS, NLF, and CHLA-255. YAP protein expression was high in SK-N-AS (MYCN non-amplified) and NLF (MYCN amplified) while undetectable in CHLA-255 (MYCN amplified) (**Figure 4.1A**). GD2 cell surface expression was conversely low in neuroblastoma cells with high YAP expression, SK-N-AS and NLF, and high in CHLA-255 that expresses no YAP (**Figure 4.1B**). Gamma delta ($\gamma\delta$) T cells are an innate effector immune cell subset that can regulate antibody-dependent cell-mediated cytotoxicity (ADCC). $\gamma\delta$ T cells have been shown by our group to synergize with dinutuximab against neuroblastoma models both *in vitro* and *in vivo*.^{299,300} We therefore used *ex vivo* expanded $\gamma\delta$ T cells as the immune effectors in combination with dinutuximab in these investigations. Agnostic of MYCN amplification state, GD2^{low}/YAP^{high} cell lines, SK-N-AS and NLF were resistant to $\gamma\delta$ T cell-induced specific lysis with and without dinutuximab treatment (**Figure 4.1C**). Contrastingly, $\gamma\delta$ T cells alone induced specific lysis of GD2^{high}/YAP^{low} cell line CHLA-255, with $\gamma\delta$ T cell-mediated specific lysis significantly enhanced by the addition of dinutuximab at both 1:1 and 5:1 effector: target (E:T) ratios (**Figure 4.1C**).

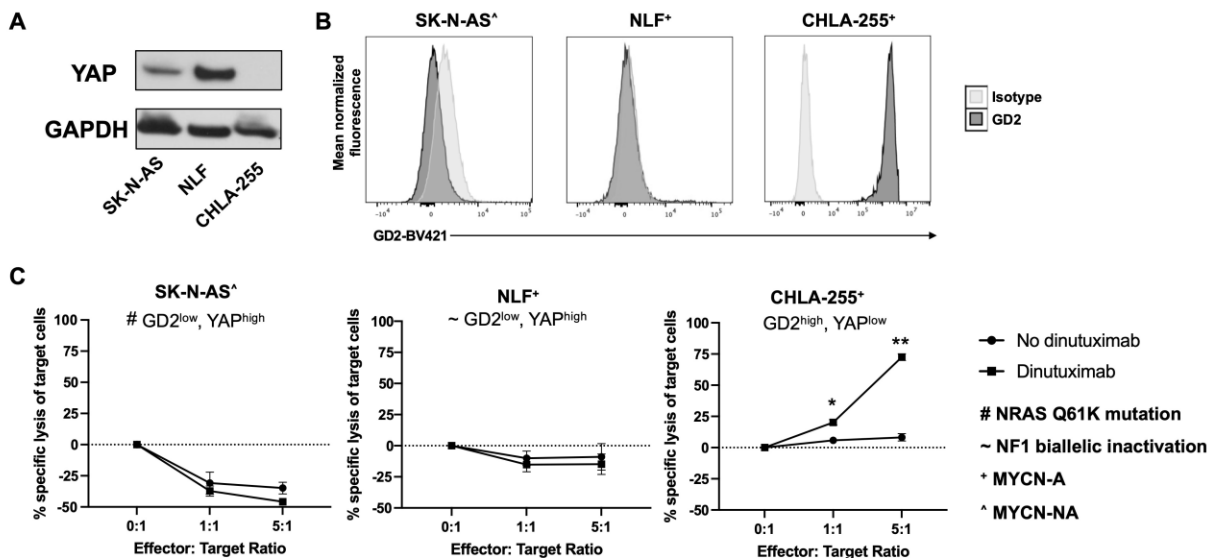


Figure 4.1. YAP expression is high in neuroblastoma cell lines that are resistant to anti-GD2/ $\gamma\delta$ T cell immunotherapy. **A**, Western blot of YAP expression in the neuroblastoma cell lines, SK-N-AS, NLF, and CHLA-255. GAPDH is the loading control. **B**, Mean normalized fluorescence of GD2 cell surface expression by flow cytometry in SK-N-AS, NLF, and CHLA-255. **C**, Percentage specific lysis after 4-hour cytotoxicity assays between $\gamma\delta$ T cells (effector) and the neuroblastoma cell lines (target), CHLA-255, NLF and SK-N-AS at effector: target (E:T) ratios of 0:1, 1:1, and 5:1 with or without the addition of the anti-GD2 monoclonal antibody, dinutuximab. For CHLA-255, 1:1, * $p=0.0235$, 5:1, ** $p=0.0072$. All other differences are not statistically significant.

YAP inhibition sensitizes neuroblastomas to dinutuximab and $\gamma\delta$ T cells *in vitro* and *in vivo* through upregulation of GD2 cell surface expression. Based on the inverse correlation of YAP and GD2 expression in neuroblastomas and differential dinutuximab responses, we evaluated the role for YAP in dinutuximab response through genetic knockdown. Using GD2^{low} and dinutuximab-resistant SK-N-AS that harbors an activating *NRAS Q61K* mutation, we generated stable YAP knockdown models using short hairpin (sh)RNA. Western blot analysis confirmed genetic inhibition of YAP in SK-N-AS cells selected to stably express YAP-silencing shRNA (shYAP1, shYAP2) compared to a non-targeting, scrambled control (**Figure 4.2A**). Increased cytotoxicity of $\gamma\delta$ T cells alone was observed in SK-N-AS shYAP1 and shYAP2

cells at an E:T ratio of 5:1 compared to SK-N-AS control (**Figure 4.2B**). The addition of dinutuximab in the coculture further augmented cytotoxicity of YAP-inhibited SK-N-AS by the $\gamma\delta$ T cells (**Figure 4.2B**).

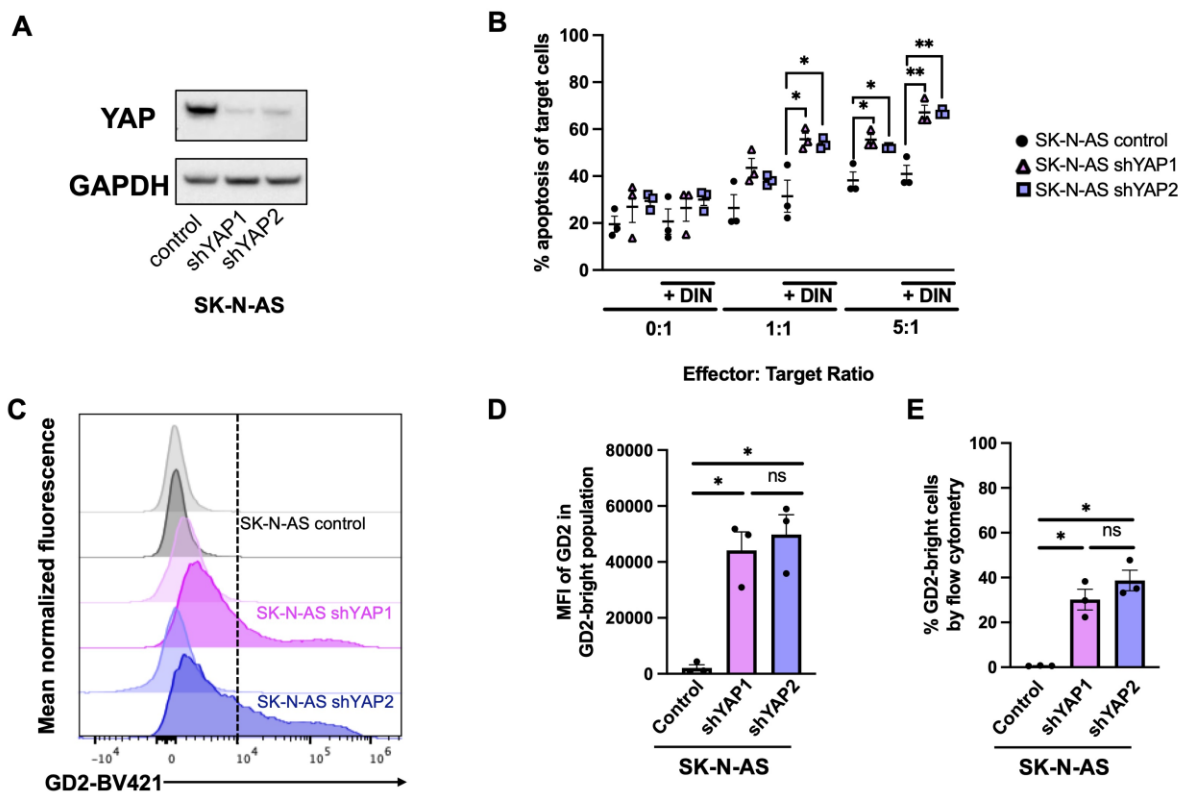


Figure 4.2. Genetic inhibition of YAP increases in vitro response to anti-GD2/ $\gamma\delta$ T cell immunotherapy with corresponding upregulation of GD2 surface expression in SK-N-AS. **A**, Western blot of YAP expression in control- (SK-N-AS control) and shYAP-transduced cells (SK-N-AS shYAP1 and shYAP2). GAPDH is the loading control. **B**, Percentage apoptosis of neuroblastoma target cells, SK-N-AS control, shYAP1 and shYAP2 when co-cultured for 4 hours with $\gamma\delta$ T cells, with (+ DIN) and without dinutuximab, 1:1 +DIN: control vs shYAP1, * $p=0.0292$, control vs shYAP2, * $p=0.0327$; 5:1: control vs shYAP1, * $p=0.0146$, control vs shYAP2, * $p=0.0185$; 5:1 +DIN: control vs shYAP1, ** $p=0.0054$, control vs shYAP2, ** $p=0.0022$; Data represent mean \pm standard error of $n = 3$ independent experiments with 2 technical replicates per condition, student's T-test with Welch's correction. All other comparisons were not significant. **C**, Representative graph showing mean normalized fluorescence of GD2 cell surface expression by flow cytometry in SK-N-AS control, shYAP1 and shYAP2 cell lines. **D**, Quantification of median fluorescence intensity (MFI) of GD2 in SK-N-AS control, shYAP1 and shYAP2 cell lines. SK-N-AS control vs shYAP1: ** $p=0.0045$; SK-N-AS control vs shYAP2: *** $p<0.0001$; SK-N-AS shYAP1 vs shYAP2: *** $p<0.0001$. Data represent mean \pm standard error of $n = 3$ independent experiments.

To determine the mechanism of increased sensitivity of YAP-inhibited SK-N-AS to $\gamma\delta$ T cells both alone and in combination with dinutuximab, we first evaluated for changes in the intrinsic killing mechanisms of $\gamma\delta$ T cells imparted by YAP knockdown in the tumor.³²⁷ We performed flow cytometric analysis of CD107a, a cell surface marker of early degranulation used as a surrogate for $\gamma\delta$ T cell activation.⁴²⁷⁻⁴²⁹ No detectable differences in early degranulation were observed between $\gamma\delta$ T cells co-cultured with SK-N-AS control or SK-N-AS^{shYAP1} cells +/- dinutuximab (**Supplementary Figure S4.3**). Immunophenotyping of expanded $\gamma\delta$ T cells before and after the 24-hour co-culture with SK-N-AS control, SK-N-AS shYAP1, or SK-N-AS shYAP2 cells showed no differences or changes in $\gamma\delta$ T cell surface expression of common markers of activation (DNAM1, NKG2D), inhibition (KIR2DL1), or exhaustion (PD1, TIM3, CTLA4, TIGIT) (**Supplementary Figure S4.4**).³⁰⁰ $\gamma\delta$ T lymphocytes harbor innate receptors that recognize and bind to stress ligands on the tumor cell surface, leading to T cell activation. In addition, they express FASL that binds to death receptors expressed on tumor cells, leading to perforin and granzyme release.^{296,305} To elucidate whether the mechanism of increased death of SK-N-AS shYAP cells is due to changes in tumor cell surface markers or death receptors, we assessed the expression of NKG2D receptor ligands (MICA, MICB, and ULBP1/2/5/6), as well as death receptors (TRAIL-R1/2, CD95/FAS) and DNAM1 ligands (CD112/Nectin-2 and CD155/PVR). These markers did not change with YAP knockdown in SK-N-AS (**Supplementary Figure S4.5**).

In response to major histocompatibility complex (MHC)-independent activation by tumor cells, $\gamma\delta$ T cells can produce IFN γ .⁴³⁰ IFN γ can induce apoptosis in tumor cells.⁴³¹ We therefore examined IFN γ production when $\gamma\delta$ T cells were co-cultured with SK-N-AS shYAP or control cell lines with or without dinutuximab. In the absence of dinutuximab, we observed no difference in IFN γ concentrations when $\gamma\delta$ T cells were co-cultured with SK-N-AS control, shYAP1 and shYAP2 cells (**Supplementary Figure S4.6A**). However, in the presence of dinutuximab, a statistically

significant increase in IFN γ release was observed in the shYAP1 and shYAP2 co-cultures compared to control (**Supplementary Figure S4.6B**), corresponding with the increased cytotoxicity observed in the shYAP cells exposed to dinutuximab and $\gamma\delta$ T cells at 1:1 and 5:1 (**Figure 4.2B**).

The presence of antigen or changes in antigen density at the cell surface are essential determinants of response to therapies that depend on ADCC.⁴² Given that intrinsic killing properties of $\gamma\delta$ T cells are not significantly changed by differences in tumor YAP expression, we focused our attention on GD2 surface expression and its potential contribution to augment dinutuximab/ $\gamma\delta$ T cell combination effects. Wild type SK-N-AS expresses low levels of GD2 on the cell surface (**Figure 4.1B**). The median fluorescent intensity (MFI) of the GD2-bright population (defined by GD2 MFI of $>10^4$ based on the brightest point in the isotype staining - dotted line, Figure 2C) significantly increased for SK-N-AS shYAP1 (mean MFI = 44136) and SK-N-AS shYAP2 (mean MFI = 39032) following YAP knockdown compared to the SK-N-AS control (mean MFI = 2115) (**Figures 4.2C and 4.2D**). Additionally, the percentage of the GD2-bright cells as defined above was similar for SK-N-AS shYAP1 (mean = 30.2%) and SK-N-AS shYAP2 (mean = 38.7%) compared to the SK-NAS control (mean = 0.63%) (**Figure 4.2E**).

The GD2^{high} cell line, SMS-SAN, expresses no YAP (**Supplementary Figure S4.7A**). We generated SMS-SAN YAP5SA, a cell line with constitutively active YAP, which has increased YAP and CYR61 expression but reduced, GD2 expression (**Supplementary Figure S4.7B**). In contrast, SMS-SAN YAPS94A, a cell line with defective TEAD binding, expresses increased levels of phospho-YAP (S127), cytoplasmic YAP, and no CYR61, a downstream target of YAP (**Supplementary Figure S4.7A**). SMS-SAN YAP S94A like SMS-SAN control has high GD2 expression (**Supplementary Figure S4.7B**).

The paralog of YAP, TAZ, has been found to have non-overlapping roles with YAP in many cancers. We determined whether genetic inhibition of TAZ also elicited a change in GD2 surface expression in SK-N-AS neuroblastoma cells which it did not (**Supplementary Figure S4.8**). Thus, we focused on a role for YAP in regulation of GD2 cell surface expression in SK-N-AS cells.

To determine whether complete ablation of YAP through genetic knockout (KO) would result in a more robust increase in cell surface expression of GD2, we generated SK-N-AS YAP KO cells (SK-N-AS YAP KO1, and SK-N-AS YAP KO2) (**Supplementary Figure S4.9A**). There was no change in GD2 cell surface expression in SK-N-AS cells in which YAP is completely ablated (**Supplementary Figure S4.9B**). Thus, we hypothesized that TAZ, in the context of complete YAP ablation, (**Supplementary Figure S4.9C**) may bind TEAD, compensating for the role of YAP in mediating repression of GD2 surface expression. Indeed, coimmunoprecipitation of SK-N-AS shYAP1 and shYAP2 compared to SK-N-AS control show no difference in binding of TAZ to TEAD2; while there is robust binding of TAZ to TEAD2 in SK-N-AS YAP KO1 and KO2 compared to KO control. (**Supplementary Figure S4.9D**)

Given that YAP regulates chemotherapy response within the neuroblastoma TME and response to dinutuximab and $\gamma\delta$ T cells *in vitro*, we ascertained whether YAP inhibition also influences tumor response to dinutuximab and $\gamma\delta$ T cells *in vivo*.¹¹⁸ We have previously shown that dinutuximab and $\gamma\delta$ T cells are more effective against tumors *in vivo* with the addition of a cytotoxic agent, in keeping with clinical trials showing dinutuximab in combination with chemotherapy is more effective in patients with relapsed neuroblastoma compared to dinutuximab alone.^{14,118,432} We treated NSG mice harboring established SK-N-AS control or shYAP subcutaneous tumors with dinutuximab, $\gamma\delta$ T cells, and cyclophosphamide and monitored tumors for growth (Treatment schema, **Supplementary Figure S4.10A**). SK-N-AS shYAP tumors had a significant prolongation of tumor regression and survival following treatment with

dinutuximab, $\gamma\delta$ T cells, and cyclophosphamide compared to mice with SK-N-AS control tumors ($p=0.0024$) (**Supplementary Figure S4.10B**). We confirmed that YAP knockdown and lower expression of its canonical target, *CYR61*, were maintained in the SK-N-AS xenograft tumors at experimental endpoint after tumors recurred (**Supplementary Figure S4.10C and S4.10D**).

YAP inhibition increases cell surface expression of GD2 through upregulation of *ST8SIA1*. YAP can transcriptionally repress genes involved in therapy response.^{118,204} Next generation sequencing of paired diagnostic and relapsed high-risk neuroblastomas showed a significant decrease in expression of genes normally suppressed by YAP in relapsed tumors.¹² We therefore examined genes in the biosynthetic pathway of GD2 (**Figure 4.3A**), using RNA sequencing data from SK-N-AS control versus SK-N-AS shYAP1 cells.¹¹⁸ *ST8SIA1*, that encodes for the critical rate-limiting enzyme GD3 synthase (GD3S) in the GD2 biosynthesis pathway, was found to be significantly increased ($\log_{2}FC = 2.62$; $p = 5.87 \times 10^{-3}$) in SK-N-AS shYAP1 versus SK-N-AS control (**Figure 4.3B**). We validated this finding in both SK-N-AS shYAP1 and SK-N-AS shYAP2 models by RT-qPCR (**Figure 4.3C**). Reduced expression of *YAP* and its canonical target *CYR61* were confirmed in shYAP1 and shYAP2 cells compared to control and corresponded to significantly increased expression of *ST8SIA1* (>100-fold, $p < 0.01$) (**Figure 4.3C**). In the same model, other genes involved in the biosynthesis of GD2 (*B4GALT5/6*, *ST3GAL5*, *ST8SIA5*, *B4GALNT1*, *B3GALT4*, *ST3GAL2*) were either marginally changed or unchanged (**Supplementary Figure S4.11**). Notably, the gene encoding GD2 synthase (GD2S), *B4GALNT1*, was unchanged. Others have shown that forced expression of the master transcription factor *PRRX1* causes adrenergic-to-mesenchymal transition, leading to epigenetic suppression of genes like *ST8SIA1* in neuroblastoma.¹³³ Interestingly, the expression of *PRRX1* significantly increased with YAP knockdown for both SK-N-AS shYAP1 and shYAP2 compared to control, yet *ST8SIA1* expression and GD2 surface expression were not impacted (**Figure 4.3C**).

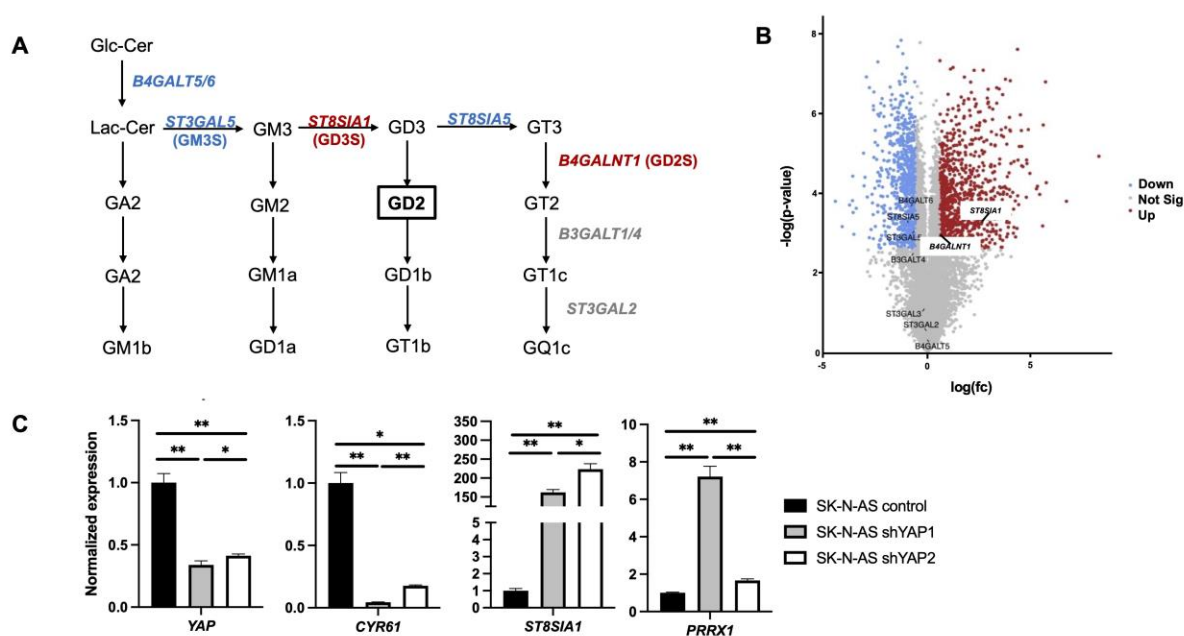


Figure 4.3. YAP inhibition mediates significantly increased gene expression of the GD2 biosynthetic enzyme, *ST8SIA1*. **A**, Schematic of ganglioside biosynthesis showing genes encoding enzymes in the biosynthetic pathway of GD2. Blue denotes genes downregulated, Red denotes genes upregulated, and Gray denotes genes unchanged in RNA sequencing data: SK-N-AS shYAP1 vs control. **B**, Volcano plot of $-\log(p\text{-value})$ vs $\log(\text{fold change}(fc))$ for GD2 biosynthetic genes from A. Blue denotes genes downregulated, Red denotes genes upregulated, and Gray denotes genes not significantly changed. **C**, Normalized gene expression as determined by RT-qPCR of YAP: SK-N-AS control vs shYAP1: $**p=0.0011$, SK-N-AS control vs shYAP2: $**p=0.0040$, SK-N-AS shYAP1 vs shYAP2: $*p=0.0467$; YAP canonical target, CYR61: SK-N-AS control vs shYAP1: $**p=0.0078$, SK-N-AS control vs shYAP2: $*p=0.0102$, SK-N-AS shYAP1 vs shYAP2: $**p=0.0010$; *ST8SIA1*: SK-N-AS control vs shYAP1: $**p=0.0021$; SK-N-AS control vs shYAP2: $**p=0.0043$; SK-N-AS shYAP1 vs shYAP2: $*p=0.0349$; and *PRRX1*: SK-N-AS control vs shYAP1: $**p=0.0081$; SK-N-AS control vs shYAP2: $**p=0.0085$; SK-N-AS shYAP1 vs shYAP2: $**p=0.0091$. Data represent mean \pm standard error of $n = 3$ independent experiments.

To confirm that GD2 cell surface changes were the result of YAP suppression of *ST8SIA1* (**Supplementary Figure S4.12**), we genetically inhibited *ST8SIA1* by shRNA in the SK-N-AS shYAP2 model. YAP knockdown was maintained in the control- and sh*ST8SIA1*- lentiviral transduced SK-N-AS shYAP2 cells (**Figure 4.4A**) and successful knockdown of *ST8SIA1* was achieved using two separate sh*ST8SIA1* constructs (**Figure 4.4B** and **Supplementary Figure**

S4.12). Genetic inhibition of *ST8SIA1* in the SK-N-AS shYAP2 cells led to significantly decreased median fluorescence intensity (MFI) of GD2 cell surface expression in SK-N-AS shYAP/shST8SIA1-1 and the SK-N-AS shYAP/shST8SIA1-2 compared to SK-N-AS shYAP/control, completely reversing the phenotype of increased GD2 surface expression upon YAP knockdown (**Figure 4.4C and D**). The percentage of GD2-positive cells in SK-N-AS shYAP shST8SIA1-1 and SK-N-AS shYAP shST8SIA1-2 was also >50-fold less than SK-N-AS shYAP control (**Figure 4.4E**). Furthermore, knockdown of *ST8SIA1* in SK-N-AS shYAP cells reduced their in vitro sensitivity to $\gamma\delta$ T cells in the presence of dinutuximab compared to SK-N-AS shYAP/LV control, with no difference in neuroblastoma killing by $\gamma\delta$ T cells in the absence of GD2-targeting antibody (**Figure 4.4F**).

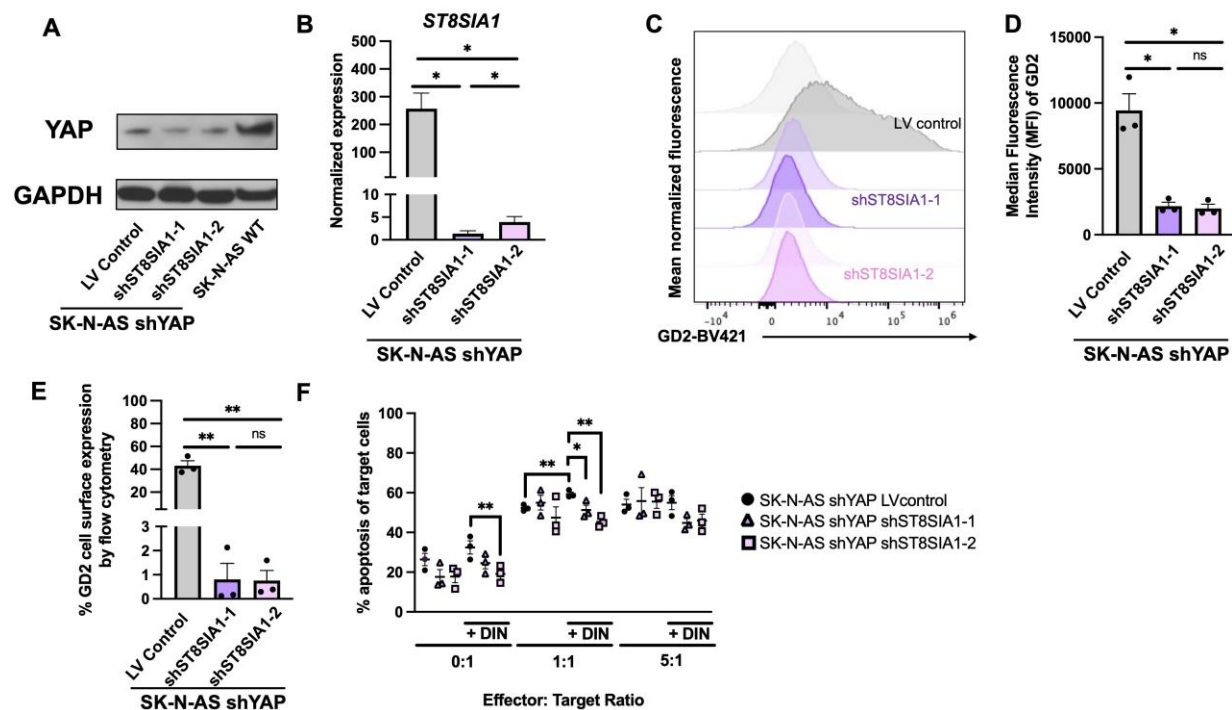


Figure 4.4. GD3S (*ST8SIA1*) inhibition reverses the phenotypes of increased GD2 surface expression and sensitivity to anti-GD2/ $\gamma\delta$ T cell immunotherapy when YAP is inhibited in SK-N-AS cells. **A**, Western blot of YAP expression in SK-N-AS shYAP LV control, shYAP shST8SIA1-1, shYAP shST8SIA1-2, and SK-N-AS WT cells. GAPDH is the loading control. **B**, Normalized gene expression as determined by RT-qPCR of *ST8SIA1* in dually transduced cells, SK-N-AS shYAP LV Control, SK-N-AS shYAP shST8SIA1-1, and SK-N-AS shYAP

shST8SIA-2, SK-N-AS shYAP LV Control vs shYAP shST8SIA1-1: *p=0.0155, SK-N-AS shYAP LV Control vs shYAP shST8SIA-2: *p=0.0157, SK-N-AS shYAP shST8SIA1-1 vs shYAP shST8SIA-2: *p=0.0460. **C**, Representative graph showing mean normalized fluorescence of GD2 cell surface expression by flow cytometry in SK-N-AS shYAP LV Control, SK-N-AS shYAP shST8SIA1-1, and SK-N-AS shYAP shST8SIA-2 cell lines. Lighter colors indicate isotype controls and darker colors indicate GD2-BV421 staining. **D**, Quantification of median fluorescence intensity (MFI) of GD2 in SK-N-AS shYAP LV Control, SK-N-AS shYAP shST8SIA1-1, and SK-N-AS shYAP shST8SIA-2 cell lines: SK-N-AS shYAP LV Control vs shYAP shST8SIA1-1: *p = 0.0242, SK-N-AS shYAP LV Control vs shYAP shST8SIA-2: *p = 0.0221. Data represent mean \pm standard error of n = 3 independent experiments. **E**, Percentage of GD2 cell surface expression by flow cytometry in SK-N-AS shYAP LV Control, SK-N-AS shYAP shST8SIA1-1, SK-N-AS shYAP shST8SIA-2 cell lines; SK-N-AS shYAP LV Control vs shYAP LV shST8SIA1-1: **p = 0.0088, SK-N-AS shYAP LV Control vs shYAP shST8SIA-2: **p = 0.0095. Data represent mean \pm standard error of n = 3 independent experiments. **F**, Percentage apoptosis of neuroblastoma target cells, SK-N-AS shYAP LV control, shYAP shST8SIA1-1, and shYAP shST8SIA1-2 when co-cultured for 4 hours with $\gamma\delta$ T cells, with (+ DIN) and without dinutuximab, 0:1 +DIN: shYAP LV control vs shYAP shST8SIA1-2, **p=0.0056; 1:1: shYAP LV control without DIN vs +DIN: **p=0.0076; 1:1 +DIN: shYAP LV control vs shYAP shST8SIA1-1, *p=0.0392; shYAP LV control vs shYAP shST8SIA1-2, **p=0.0018; Data represent mean \pm standard error of n = 3 independent experiments with 2 technical replicates per condition, student's T-test with Welch's correction. All other comparisons were not significant.

YAP and *ST8SIA1* or GD2 cell surface expression are inversely correlated in neuroblastoma primary tumors and patient derived xenografts. We queried publicly available gene expression datasets of primary neuroblastoma tumors to validate the clinical relevance of the regulation of GD2 by YAP through *ST8SIA1*. An inverse relationship between *YAP* and *ST8SIA1* expression was demonstrated in two separate datasets with non-overlapping cohorts: in the TARGET (Asgharzadeh) dataset, which consists of 249 samples assessed by exon array, $R=-0.233$, $p=2.05 \times 10^{-4}$ (**Figure 4.5A**), and for the Kocak dataset, which consists of 648 samples assessed by microarray, $R=-0.132$, $p=7.89 \times 10^{-4}$ (**Figure 4.5B**). Additionally, Kaplan-Meier survival analysis shows that the overall survival probability is reduced when *ST8SIA1* expression is lower (**Figure 4.5C and 4.5D**).

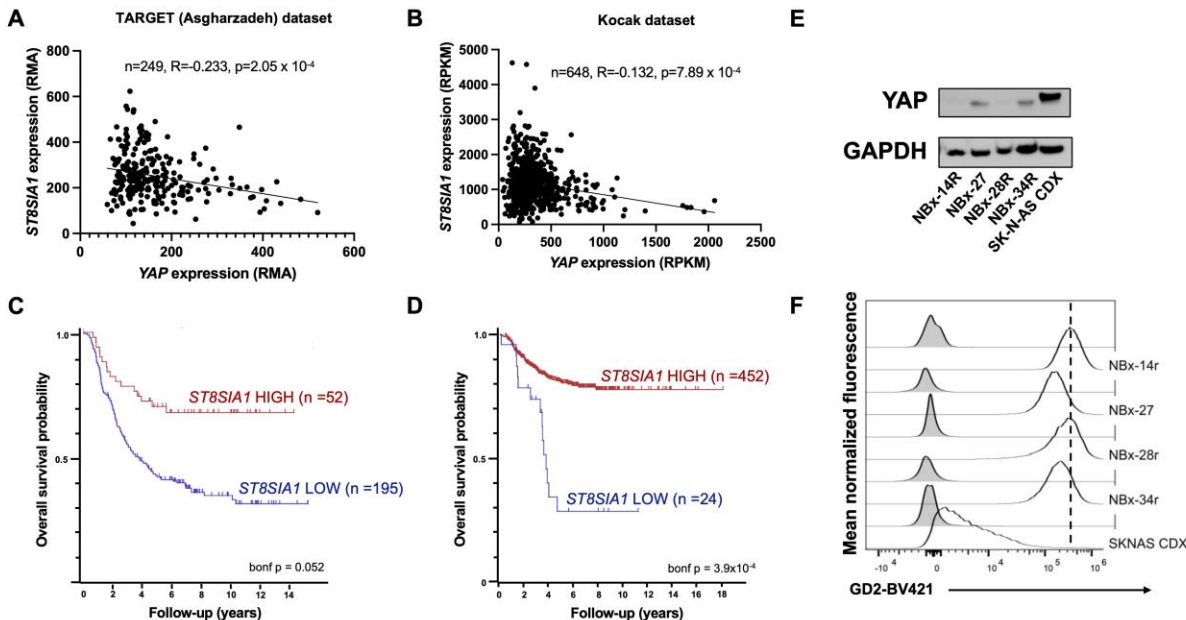


Figure 4.5. YAP and *ST8SIA1* expression are negatively correlated in primary neuroblastoma tumors, low *ST8SIA1* expression is associated with worse overall survival and YAP and GD2 are inversely correlated in neuroblastoma patient derived xenografts (PDXs). YAP and *ST8SIA1* expression in primary neuroblastoma tumors from patients: **A**, TARGET (Asghardazeh) dataset: $n=249$, $R=-0.233$, $p=2.05 \times 10^{-4}$. **B**, Kocak dataset: $n=648$, $R=-0.132$, $p=7.89 \times 10^{-4}$. Low *ST8SIA1* expression in primary neuroblastoma tumors from patients is associated with worse overall survival: **C**, TARGET (Asghardazeh) dataset: $n=247$, Bonferroni-corrected (bonf.) $p=0.052$. **D**, Kocak dataset: $n=476$, $R=-0.137$, bonf. $p=3.9 \times 10^{-4}$. <https://r2.amc.nl>. **E**, Western blot of YAP expression in neuroblastoma patient-derived xenografts (PDXs), NBx-14R, NBx-27, NBx-28R, NBx-34R and the SK-N-AS neuroblastoma cell line-derived xenograft (CDX). GAPDH is the loading control. **F**, Mean normalized fluorescence of GD2 cell surface expression by flow cytometry in neuroblastoma patient-derived xenografts (PDXs), NBx-14R, NBx-27, NBx-28R, NBx-34R and the SK-N-AS neuroblastoma cell line-derived xenograft (CDX). Grey denotes isotype control staining and white denotes GD2-BV421 staining.

Since GD2 is a glycosphingolipid and thus, not genetically encoded, we sought to determine whether YAP protein expression and GD2 surface expression also inversely correlated by performing immunoblot and flow cytometry, respectively, in low-passage neuroblastoma patient derived xenografts (PDXs). YAP expression was lower in NBx14R and NBx28R than in NBx27 and

NBx34R (**Figure 4.5E**) and correspondingly, the MFI of GD2 on the surface of NBx14R and NBx28R was higher than that of NBx27 and NBx34R (**Figure 4.5F**).

4.4 Discussion

High-risk neuroblastomas that recur are notoriously chemotherapy resistant, leading to improvements in survival focused on immunotherapy approaches. Indeed, anti-GD2 antibodies in combination with chemotherapy have resulted in unprecedented response rates in relapsed patients.³⁹² However, challenges to GD2 targeted immunotherapies remain, such as an incomplete understanding of biomarkers predicting response and mechanisms of resistance.^{400,425} High-risk neuroblastoma tumors that relapse are enriched with mesenchymal cells as well as RAS pathway mutations,^{11,132,133} leading many to investigate how these properties may influence immunotherapy resistance to identify new therapeutic targets.

YAP is a canonical mesenchymal gene that encodes for the YAP protein known to cooperate with hyperactivated RAS.¹⁷ Indeed, the *YAP* expressing neuroblastoma cell lines we investigated are RAS pathway mutated (SK-N-AS, NLF) and harbor the mesenchymal gene signature.^{132,133,433} Our findings demonstrate that *YAP* genetic inhibition paradoxically leads to upregulated expression of *PRRX1*, one of the master transcription factors that can drive the mesenchymal phenotype.¹³³ Previously, it was shown that genetic induction of mesenchymal neuroblastoma via overexpression of *PRRX1* induces similar transcriptional downregulation of *ST8SIA1* with resultant decrease of cell surface GD2.⁴⁰⁰ *PRRX1* converts an adrenergic neuroblastoma cell to a mesenchymal neuroblastoma cell (adrenergic to mesenchymal transition) with a decrease in adrenergic-differentiating genes like *PHOX2B*, *GATA2*, *DLK1* and an increase in mesenchymal stem-like genes such as *SOX2*, *SNAI2* and *YAP*.¹³³ We now show that *YAP* is sufficient to suppress the same glycosphingolipid biosynthesis pathway regardless of *PRRX1* gene expression, suggesting that GD2 synthesis may be more directly regulated by *YAP* downstream of its mesenchymal driving forces such as *PRRX1* and other master mesenchymal transcription factors. Further studies are warranted to validate the full functional roles for *YAP* within the mesenchymal neuroblastoma phenotype.

Despite the success of dinutuximab and other anti-GD2 antibodies, not all patients respond, and preclinical data suggests that it is likely due to lack of GD2 on the tumor cell surface. Detection of GD2 in primary neuroblastoma tissue is limited since GD2 is a glycosphingolipid and its presence is therefore not detectable by immunohistochemistry on paraffin embedded tissue.³⁸⁶ Recent studies have therefore sought to determine and provide surrogate biomarkers for GD2 expression in an effort to triage patients most likely to benefit from GD2 immunotherapy.⁴⁰⁰ We found that neuroblastomas with low GD2 have high YAP gene and protein expression. Furthermore, this inverse correlation has functional relevance as YAP suppresses GD2 expression through inhibition of the GD3 synthase (GD3S) gene *ST8SIA1*. By suppressing GD3S and thus GD2 synthesis, YAP indeed serves as a mediator and potential biomarker of anti-GD2 antibody resistance. We validated this relationship through genetic knockdown studies showing YAP inhibition restores response to dinutuximab and $\gamma\delta$ T cells both *in vitro* and *in vivo*. Furthermore, we observed an inverse correlation between YAP and GD2 in low-passage high risk and relapsed neuroblastoma PDXs. Based on these data, we hypothesize that high YAP expression in neuroblastoma tumors may predict GD2 immunotherapy resistance clinically. Immunohistochemical staining of YAP in primary neuroblastoma tumors is feasible and should be characterized prospectively to statistically correlate results to patient outcomes following anti-GD2 therapy.

A slight increase in neuroblastoma cell death was observed following coculture with just $\gamma\delta$ T cells alone in the SK-N-AS shYAP cells compared to control. We therefore investigated whether increased tumor cell death was due to paracrine effects of the YAP-inhibited neuroblastoma cells towards the $\gamma\delta$ T cells. When SK-N-AS shYAP cells were co-cultured with $\gamma\delta$ T cells, we observed no difference in $\gamma\delta$ T cell markers of exhaustion, activation, or apoptosis, nor an increase in tumor-resident stress antigens or FAS/TRAIL receptors. Although there was an increase in IFN γ release when SK-N-AS shYAP cells were treated with the combination of $\gamma\delta$ T cells and dinutuximab *in*

in vitro, this increased IFN γ release was not consistently observed in the absence of dinutuximab. This suggests that differences in cytotoxicity were not due to $\gamma\delta$ T cell-intrinsic changes, increased release of cytotoxic mediators, or by increased T cell recognition ligands on the tumor cells. Further investigation is warranted to understand the effect of tumor YAP inhibition on increased $\gamma\delta$ T cell activity.

We have shown that the use of IL-2 and zoledronate to expand $\gamma\delta$ T cells from peripheral blood results in varying percentages of NK cells in the final cell therapy product.³⁰⁰ Both NK cells and $\gamma\delta$ T cells in the expanded product have high CD16 and equivalent anti-tumor potency when combined with dinutuximab. Thus, while we used $\gamma\delta$ T cell-dominant expansions through all experiments, a fraction of NK cells was also present, supporting that tumor YAP expression most likely affects ADCC immune cell antitumor activity similarly.

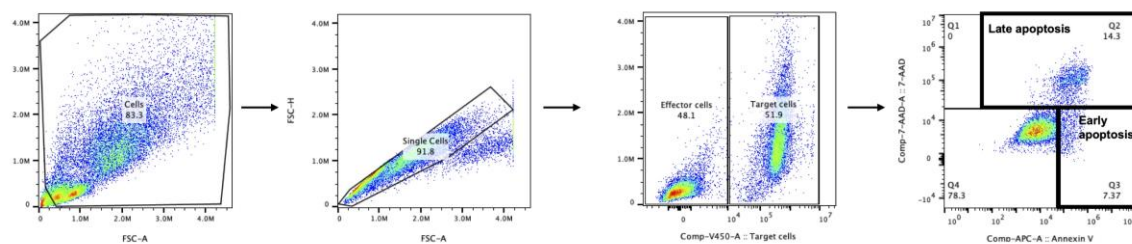
Importantly, we found the addition of anti-GD2 antibody further augmented $\gamma\delta$ T cell mediated cytotoxicity against neuroblastomas with YAP inhibition, that could be reverted upon *ST8SIA1* knockdown in the YAP inhibited neuroblastoma, supporting GD3 synthase as a mediary of GD2 expression by YAP. Resistance of RAS mutated, YAP expressing neuroblastoma to $\gamma\delta$ T cell/dinutuximab mediated cytotoxicity *in vitro* was restored by reducing GD2 surface expression through genetic inhibition of the GD3S gene, *ST8SIA1*. YAP expression by immune cells themselves has been shown to promote immunosuppression and suppress immunotherapy activity.²⁴⁶ For example, high YAP expression in regulatory T cells of hepatocellular carcinoma patients was found to facilitate an immunosuppressive TME and was an indicator of poor prognosis.²⁴³ Since YAP has a well-established role in the TME, its role in the TME-enacted resistance to anti-GD2 immunotherapy warrants evaluation by using immunocompetent murine models. Indeed, therapeutic targeting of YAP may be beneficial by not only making tumor cells

more vulnerable through upregulation of the immunotherapy target, but also through inhibition of immune cells contributing to the immune hostile TME.

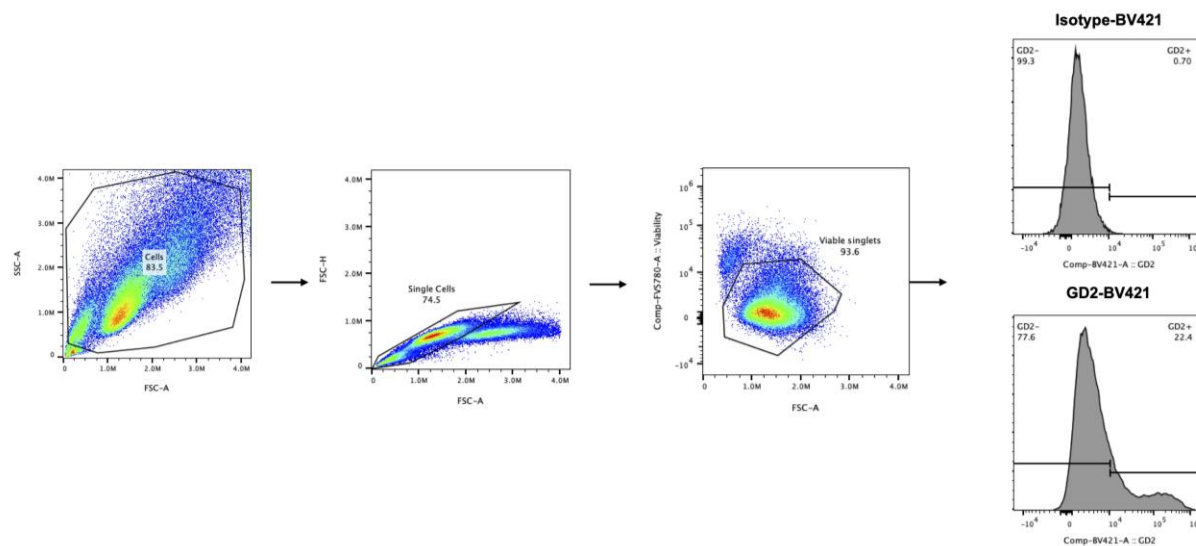
Others have identified that mesenchymal transcription factors epigenetically suppress *ST8SIA1* expression, leading clinical efforts to evaluate the combination of GD2 antibodies with epigenetic modifying agents such as EZH2 inhibitors (tazemetostat).⁴⁰⁰ Based on our data, one could potentially take a more direct approach by therapeutically inhibiting YAP to avoid the broad effects of epigenetic inhibiting agents. Currently, inhibitors of the YAP/TEAD interaction have shown preclinical promise in adult cancers with one agent in clinical application for adult mesothelioma,²⁷³ and investigations are ongoing to evaluate such inhibitors in neuroblastoma.

Overall, our findings define a novel role for YAP in GD2 immunotherapy resistance in neuroblastoma. Therefore, our study highlights the potential of YAP as a biomarker for resistance to GD2-targeting therapies as well as indicates the direct translational relevance of combining pharmacological YAP inhibition with current standard-of-care regimens. Specifically, incorporating YAP inhibitors with GD2 targeted immunotherapies, such as GD2-directed chimeric antigen receptor (CAR) T cells or novel anti-GD2 antibody combinations ($\gamma\delta$ T cells with dinutuximab and chemotherapy; [NCT05400603](#)) shows promise to improve outcomes for patients with high-risk and relapsed neuroblastoma.³⁹⁶

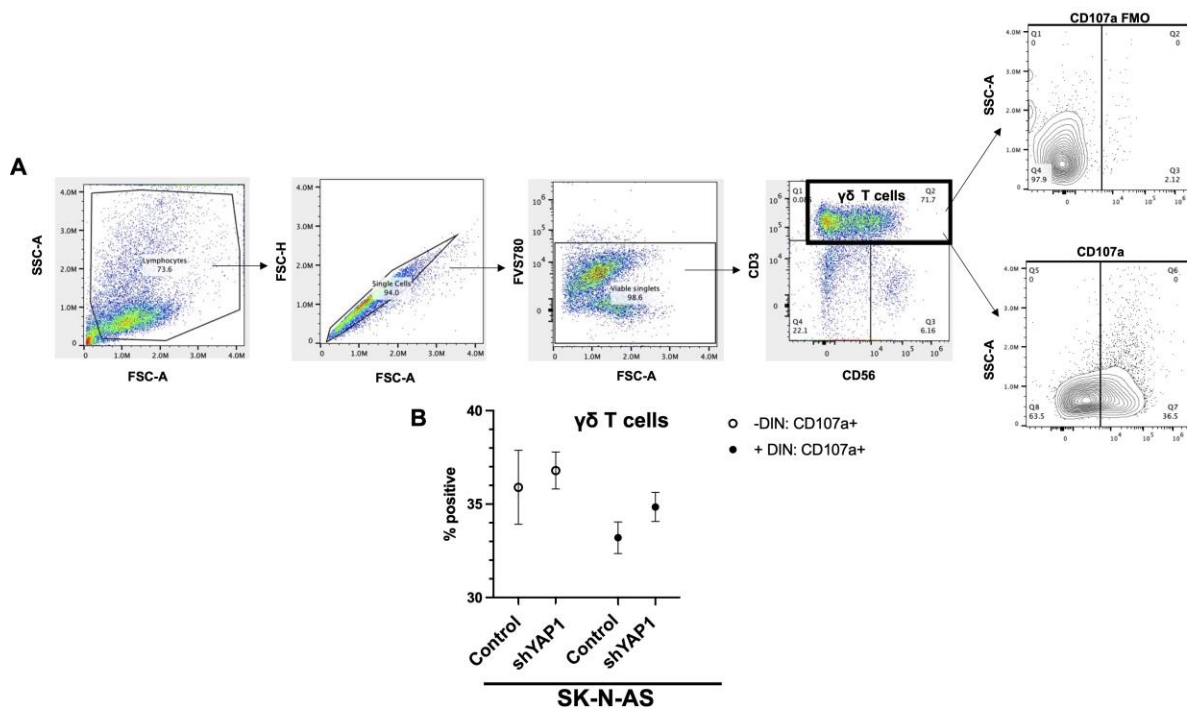
4.5 Supplementary figures and tables



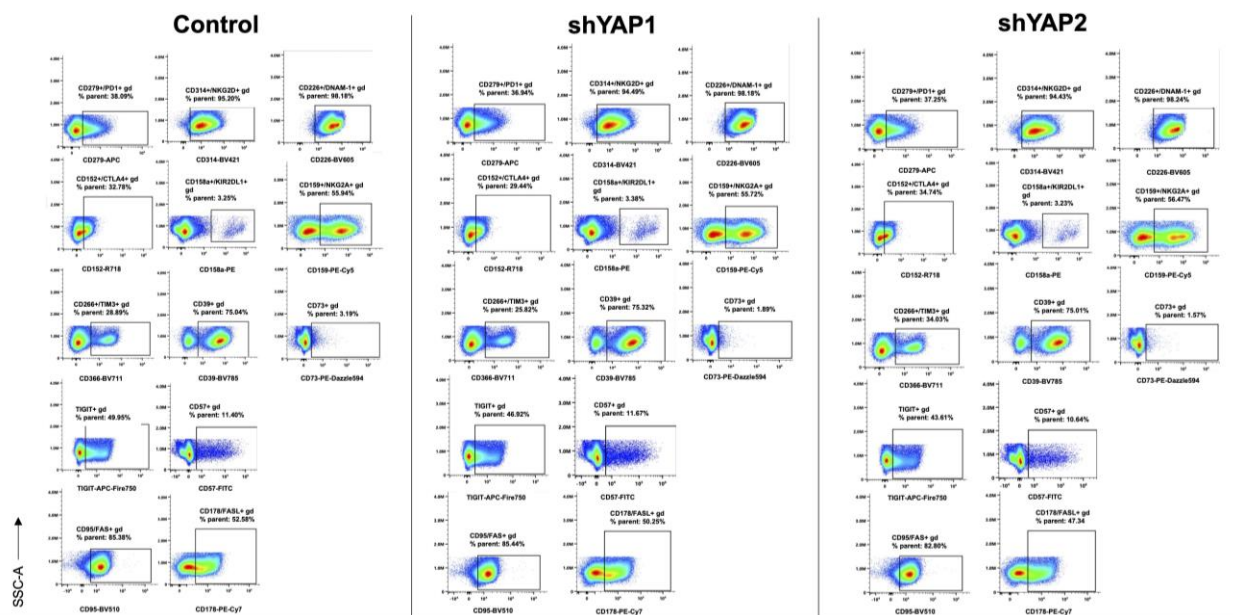
Supplementary Figure S4.1. Representative gating strategy for apoptotic cells in neuroblastoma cytotoxicity assays (at 1:1 effector:target ratio)



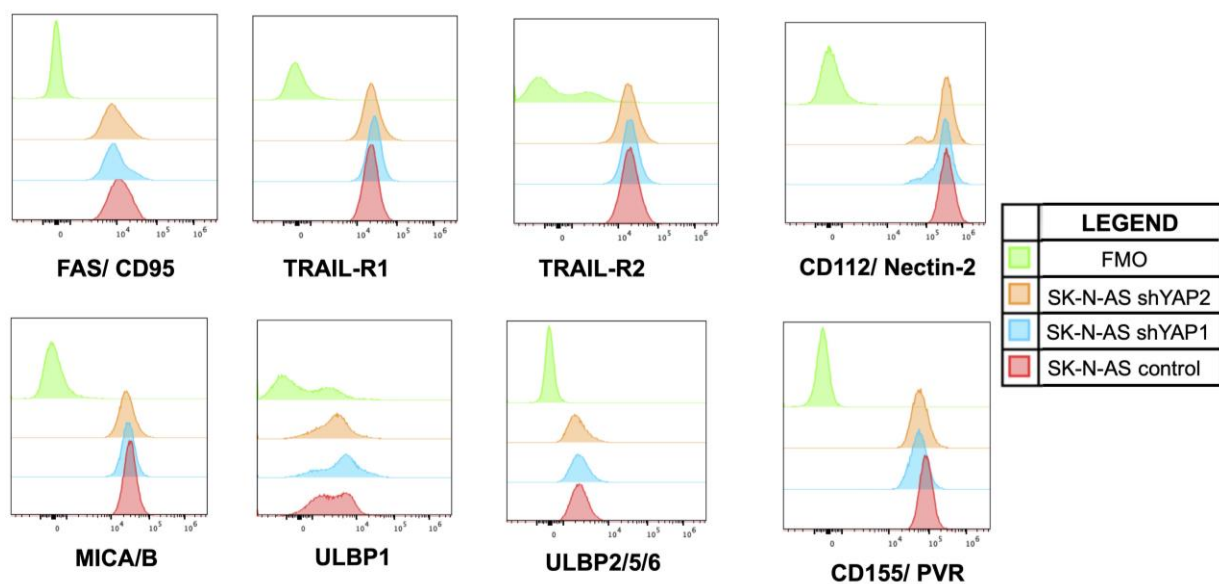
Supplementary Figure S4.2. Representative gating strategy for GD2 cell surface expression in neuroblastoma cell lines by flow cytometry.



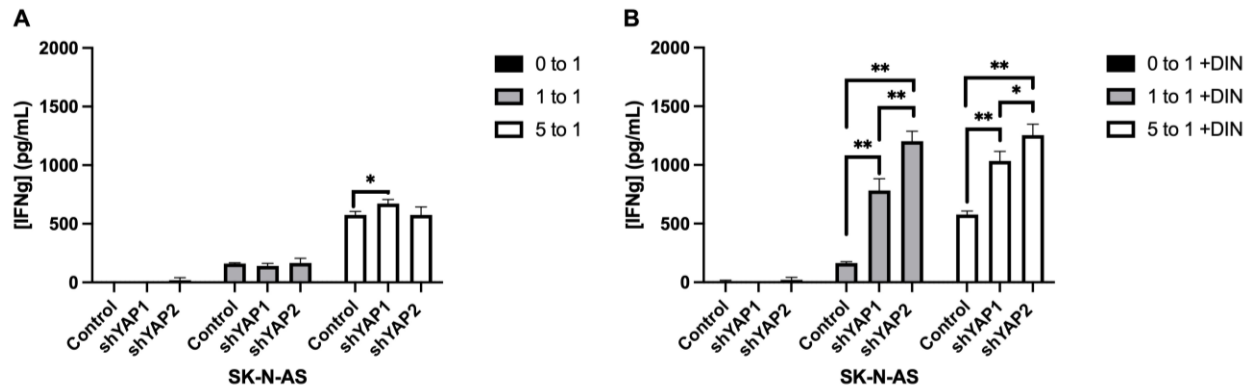
Supplementary Figure S4.3. Early degranulation (CD107a) is unchanged in $\gamma\delta$ T cells post-co-culture with SK-N-AS control and shYAP1 cells with or without dinutuximab treatment. **A**, Representative gating strategy to determine CD107a⁺ $\gamma\delta$ T cells showing CD107a fluorescence minus one (FMO) control and CD107a staining. **B**, Percentage CD107a⁺ $\gamma\delta$ T cells in 24-hour co-culture with SK-N-AS control or SK-N-AS shYAP1 neuroblastoma cells with or without the addition of dinutuximab (DIN).



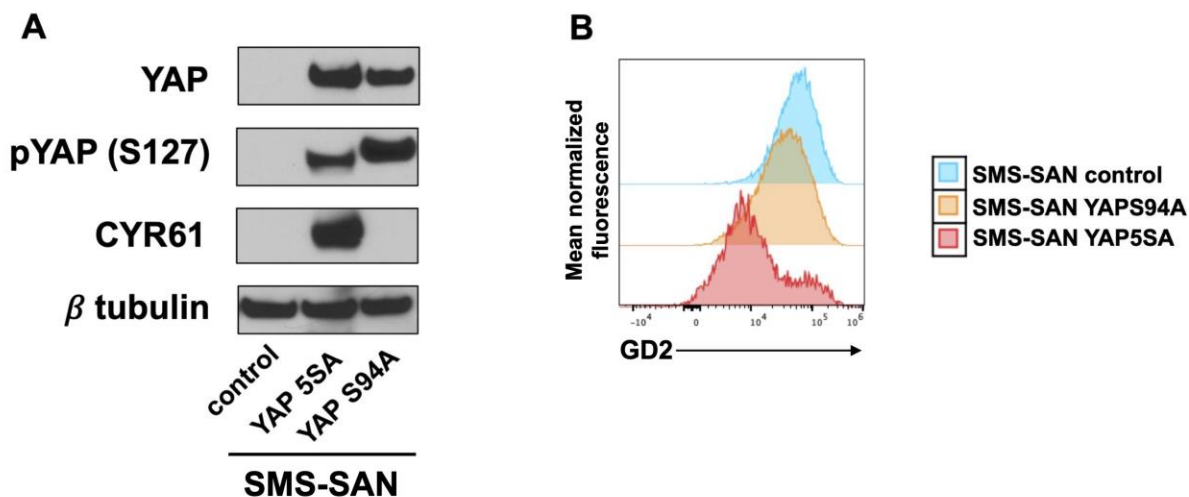
Supplementary Figure S4.4. Immunophenotyping of $\gamma\delta$ T cells co-cultured with SK-N-AS control, shYAP1 and shYAP2 cells for 24 hours. Representative flow cytometry panels of $\gamma\delta$ T cell markers of exhaustion (PD1, TIM3, CTLA4, TIGIT), inhibition (KIR2DL1, NKG2A), activation (DNAM1, NKG2D), terminal differentiation (CD39, CD57, CD73), and apoptosis (FAS, FASL) in $\gamma\delta$ T cells co-cultured with SK-N-AS control, shYAP1 and shYAP2 cells.



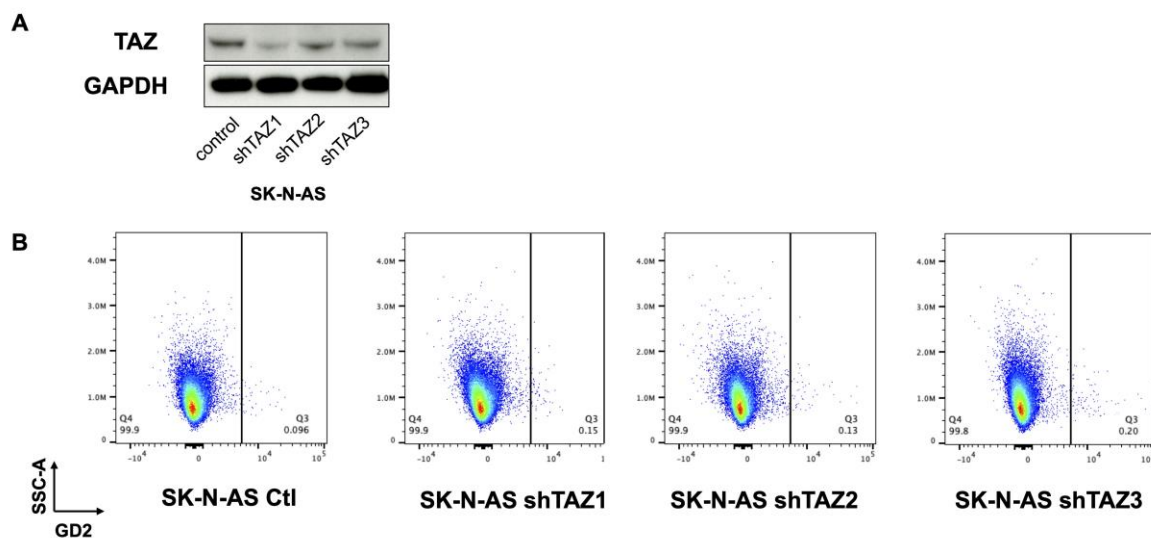
Supplementary Figure S4.5. YAP does not affect expression of tumor stress antigens, DNAM-1 ligands, and death receptors on SK-N-AS cells. Representative flow cytometry plots of stress antigens (MICA/B, ULBP1/2/5/6), DNAM-1 ligands (CD112/Nectin-2, CD155/PVR) and death receptors (FAS/CD95, TRAIL-R1, TRAIL-R2) on the surface of SK-N-AS control, shYAP1 and shYAP2 cells and their respective fluorescence minus one (FMO) controls.



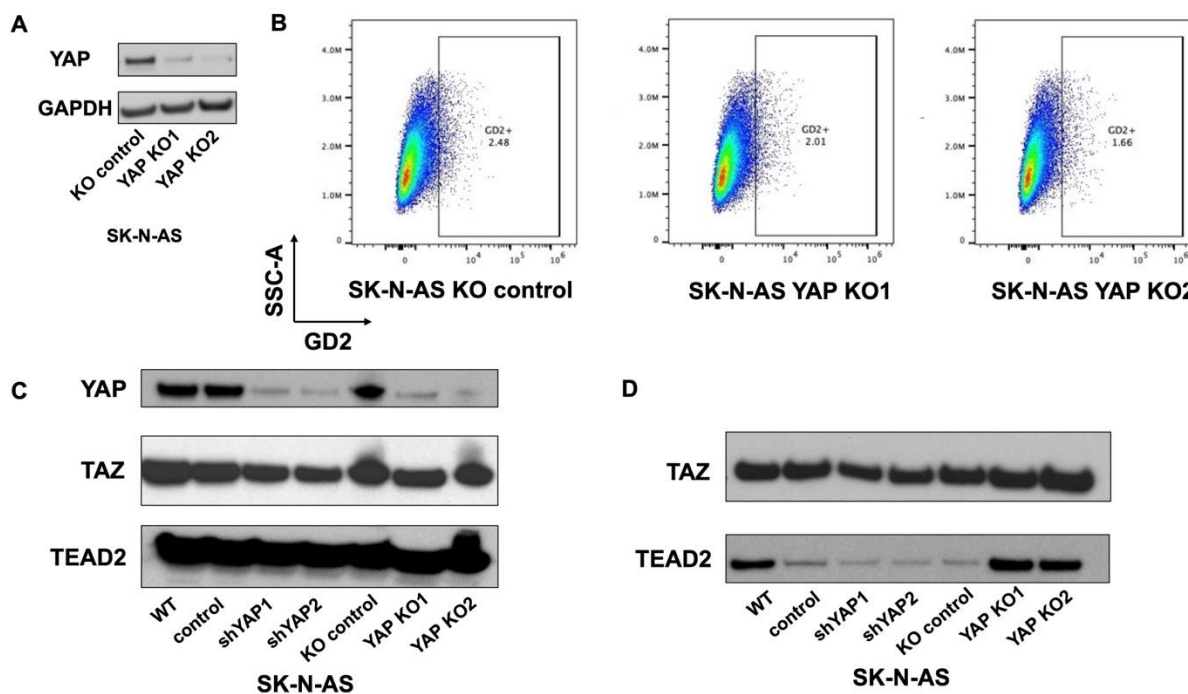
Supplementary Figure S4.6. IFN̳ release by ̳̳ T cells is increased when co-cultured with SK-N-AS shYAP cells in the presence of dinutuximab. **A**, IFN̳ concentrations (pg/mL) of supernatants collected from co-cultures of ̳̳ T cells with SK-N-AS control, shYAP1, and shYAP2 cells without dinutuximab at E:T ratios of 0:1, 1:1, 5:1. At 5:1, SK-N-AS control vs shYAP1: * $p=0.0219$. **B**, IFN̳ concentrations (pg/mL) of supernatants collected from co-cultures of ̳̳ T cells with SK-N-AS control, shYAP1, and shYAP2 cells with dinutuximab at E:T ratios of 0:1, 1:1, 5:1. At 1:1, SK-N-AS control vs shYAP1: ** $p=0.0080$; SK-N-AS shYAP1 vs shYAP2: ** $p=0.0057$, SK-N-AS control vs shYAP2: ** $p=0.0019$. At 5:1, SK-N-AS control vs shYAP1: ** $p=0.0054$; SK-N-AS shYAP1 vs shYAP2: * $p=0.0377$, and SK-N-AS control vs shYAP2: ** $p=0.0032$.



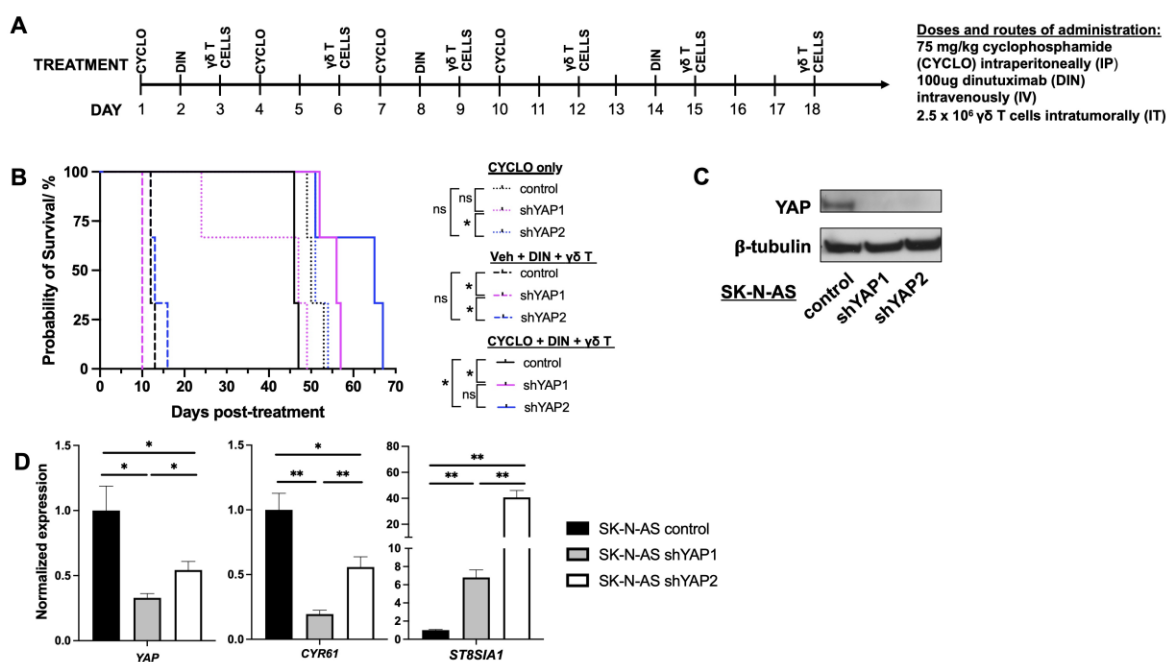
Supplementary Figure S4.7. Ectopic expression of YAP 5SA and YAP S94A in SMS-SAN cells reduces GD2 cell surface expression. **A**, Western blot of YAP, phospho-YAP (S127), and CYR61, a canonical YAP target, expression in SMS-SAN control, YAP5SA, and YAP S94A cell lines. β -tubulin is a loading control. **B**, Representative flow cytometry plot of GD2 MFI in SMS-SAN control, YAP5SA, and YAP S94A cell lines.



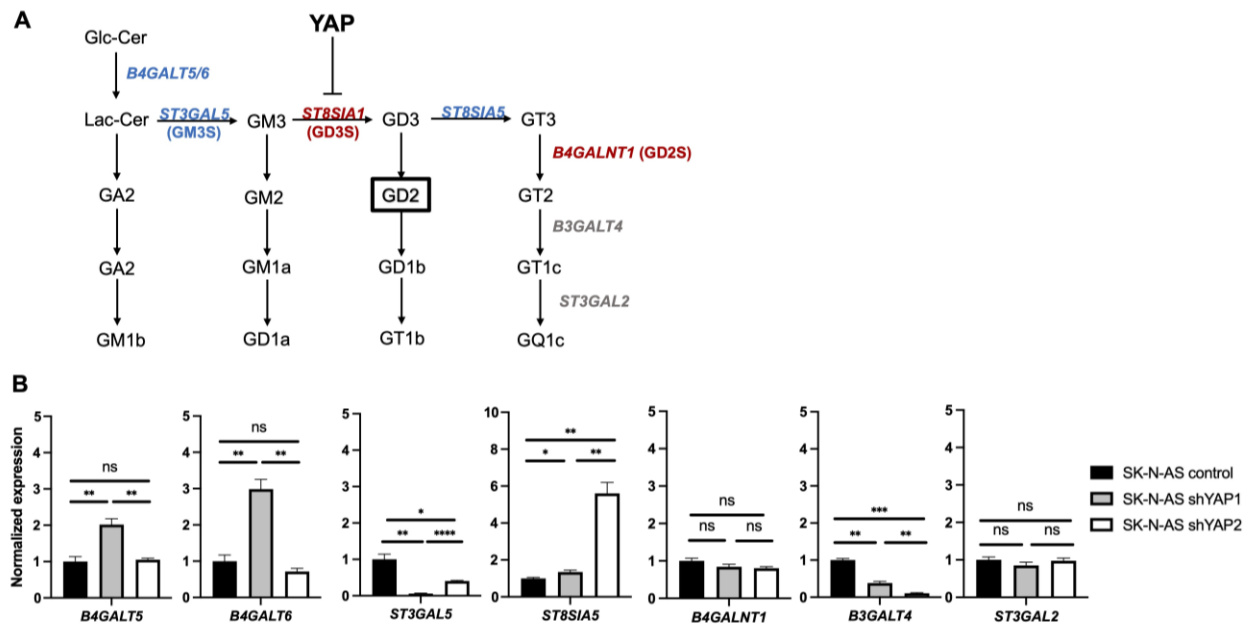
Supplementary Figure S4.8. Genetic inhibition of TAZ in SK-N-AS neuroblastoma cells does not cause increased cell surface expression of GD2. **A**, Western blot of TAZ expression in control- (SK-N-AS control) and shTAZ-transduced cells (SK-N-AS shTAZ1, shTAZ2 and shTAZ3). GAPDH is the loading control. **B**, GD2 cell surface expression by flow cytometry in SK-N-AS control, SK-N-AS shTAZ1, SK-N-AS shTAZ2, and SK-N-AS shTAZ3.



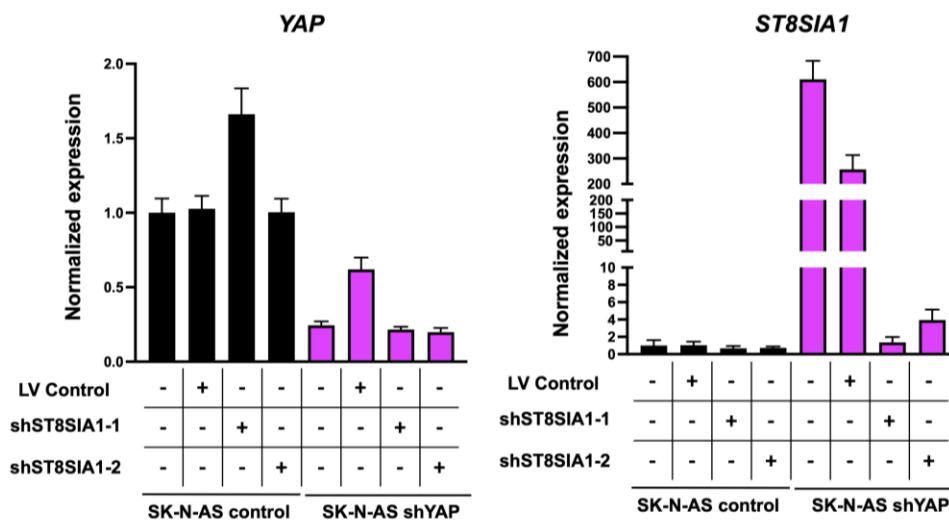
Supplementary Figure S4.9. Genetic ablation of YAP in SK-N-AS neuroblastoma cells does not cause increased cell surface expression of GD2 but results in compensatory TAZ binding to TEAD2. **A**, Western blot of YAP expression in control- (SK-N-AS knockout (KO) control) and YAP KO-transduced cells (SK-N-AS YAP KO1 and YAP KO2). GAPDH is the loading control. **B**, GD2 cell surface expression by flow cytometry in SK-N-AS KO control, YAP KO1, and YAP KO2. **C**, Western blots of YAP, TAZ and TEAD2 in SK-N-AS wildtype (WT), control, YAP knockdowns (KD): shYAP1 and shYAP2 cells, and YAP knockouts: SK-N-AS KO control, YAP KO1, and YAP KO2. **D**, Western blots of TAZ and TEAD2 from TAZ co-immunoprecipitations in SK-N-AS wildtype (WT), control, YAP knockdowns (KD): shYAP1 and shYAP2 cells, and YAP knockouts: SK-N-AS KO control, YAP KO1, and YAP KO2.



Supplementary Figure S4.10. Inhibition of YAP in SK-N-AS neuroblastoma cells prolongs survival of mice treated with cyclophosphamide (CYCLO)/ dinutuximab (DIN)/ $\gamma\delta$ T cell ($\gamma\delta$ T) chemoimmunotherapy. **A**, Schema of in vivo chemoimmunotherapeutic regimen with dosage, timing, and route of administration of cyclophosphamide (CYCLO), dinutuximab (DIN), and $\gamma\delta$ T cells ($\gamma\delta$ T); **B**, Survival of mice receiving CYCLO only; vehicle (Veh), DIN, and $\gamma\delta$ T; or CYCLO, DIN, and $\gamma\delta$ T. For mice receiving CYCLO only: SK-N-AS control vs shYAP1: $p=0.0629$, ns, SK-N-AS control vs shYAP2: $p=0.7009$, ns, SK-N-AS shYAP1 vs shYAP2: $*p=0.0246$; Veh, DIN and $\gamma\delta$ T: SK-N-AS control vs shYAP1: $*p=0.0455$, SK-N-AS control vs shYAP2: $p=0.3094$, ns, SK-N-AS shYAP1 vs shYAP2 $*p=0.0455$; CYCLO, DIN and $\gamma\delta$ T: SK-N-AS control vs shYAP1: $*p = 0.0224$, SK-N-AS control vs shYAP2 $*p=0.0224$, SK-N-AS shYAP1 vs shYAP2: $p=0.2116$; $n=3$ mice/group. **C**, YAP knockdown is maintained to the end of the in vivo experiment as shown by western blot of tumors harvested from mice at the experimental endpoint. **D**, Normalized gene expression as determined by RT-qPCR of YAP, CYR61 and ST8SIA1 in SK-N-AS control, shYAP1 and shYAP2 xenograft tumors (size = $\sim 1000\text{mm}^3$) harvested from untreated mice, YAP: SK-N-AS control vs shYAP1: $*p=0.0223$; SK-N-AS control vs shYAP2: $*p=0.0395$; SK-N-AS shYAP1 and shYAP2: $*p=0.0164$; CYR61: SK-N-AS control vs shYAP1: $**p=0.0061$; SK-N-AS control vs shYAP2: $*p=0.0112$; SK-N-AS shYAP1 and shYAP2: $**p=0.0088$; ST8SIA1: SK-N-AS control vs shYAP1: $**p=0.0064$; SK-N-AS control vs shYAP2: $**p=0.0058$; SK-N-AS shYAP1 and shYAP2: $**p=0.0069$.



Supplementary Figure S4.11. Gene expression of enzymes in the biosynthetic pathway of GD2. **A**, GD2 biosynthetic pathway including the postulated role of YAP in *ST8SIA1* suppression. **B**, Expression of genes in the biosynthetic pathway other than *ST8SIA1* which is the most significantly upregulated.



Supplementary Figure S4.12. Gene expression of YAP and ST8SIA1 in dually transduced control or YAP/*ST8SIA1* knockdown models.

Supplementary Data Tables

Supplementary Table S4.1. Antibodies used for western blot and co-immunoprecipitation.

Antigen	Species	Company/Product Number	RRID
Anti-Mouse IgG HRP	Goat	Abcam/ab205719	AB_2755049
Anti-Rabbit IgG HRP	Goat	R & D Systems	AB_357235
β -tubulin	Mouse	Sigma Aldrich/T8328	AB_1844090
CYR61	Rabbit	Cell Signaling Technologies/39382	AB_2799154
GAPDH	Rabbit	Cell Signaling Technologies/ 2118	AB_561053
pYAP (S127)	Rabbit	Cell Signaling Technologies/4911	AB_2218913
TAZ (Co-IP)	Mouse	Cell Signaling Technologies/71192	AB_2799797
TAZ (WB)	Rabbit	Cell Signaling Technologies/4883	AB_1904158
TEAD2	Rabbit	Biorbyt/orb382464	AB_2941665
YAP	Rabbit	Cell Signaling Technologies/4912	AB_2218911

Supplementary Table S4.2. Antibodies used to profile $\gamma\delta$ T cells for use in cytotoxic assays.

Antigen (Clone)	Marker	Company/Product Number	RRID
Viability (FVS780)	---	Invitrogen/65086518	
CD3 (UCHT1)	BV421	BD Biosciences/562426	AB_11152082
CD16 (3G8)	BV480	BD Biosciences/566108	AB_2739510
CD56 (NCAM16.2)	APC-R700	BD Biosciences/565139	AB_2744429
$\alpha\beta$ -TCR (IP26)	PE	BD Biosciences/564728	AB_2738921
$\gamma\delta$ -TCR (11F2)	PE	BD Biosciences/347907	AB_400359
CD107a (H4A3)	PE-Cy7	BD Biosciences/561348	AB_10644018

Supplementary Table S4.3. Antibodies used for determination of *in vitro* or *in vivo* GD2 surface expression of neuroblastoma cells.

Antigen (Clone)	Marker	Company/Product Number	RRID
Viability (FVS780)	---	Invitrogen/65086518	
CD45 (2D1)	PerCp-Cy5.5	BD Biosciences/340953	AB_400194
CD56 (NCAM16.2)	PE	BD Biosciences/340363	AB_400017
CD81 (JS-81)	FITC	BD Biosciences/561956	AB_10896976
GD2 (14G2a)	BV421	BD Biosciences/565991	AB_2739442
IgG2A Isotype, k	BV421	BD Biosciences/562439	AB_11151914

Supplementary Table S4.4. Antibodies used for in-depth characterization of expanded $\gamma\delta$ T cells pre- and post-cytotoxicity assay.

Antigen (Clone)	Marker	Company/Product Number	RRID
Viability (ZombieNiR)	---	BioLegend/423105	
CD3 (SK7)	SparkBlue550	BioLegend/344851	AB_2819984
CD16 (3G8)	BV650	BD Biosciences/302041	AB_11125578
CD39 (A1)	BV785	BioLegend/328239	AB_2814190
CD45 (HI30)	BUV395	BD Biosciences/563791	AB_2869519
CD56 (5.1H11)	BV750	BioLegend/362555	AB_2734396
CD57 (HNK-1)	FITC	BD Biosciences/561906	AB_395986
CD73 (AD2)	PE-Dazzle594	BioLegend/344019	AB_2565300
CD95/FAS (DX2)	BV510	BioLegend/305639	AB_2629737
CD152/CTLA-4 (BNI3)	R718	BD Biosciences/567226	Not Identified
CD158a/KIR2DL1 (HP-DM1)	PE	BioLegend/374903	AB_2832735
CD159a/NKG2A (S19004C)	PE-Cy5	BioLegend/375111	AB_2888864
CD178/FAS-L (NOK-1)	PE-Cy7	BioLegend/306417	AB_2814147
CD226/DNAM-1 (11A8)	BV605	BioLegend/338323	AB_2721542
CD279/PD-1 (A17188B)	APC	BioLegend/621609	AB_2832829
CD314/NKG2D (1D11)	BV421	BioLegend/320821	AB_2566510
CD366/TIM-3 (F38-2E2)	BV711	BioLegend/345023	AB_2564045
$\gamma\delta$ -TCR (B1)	PerCP-Cy5.5	BioLegend/331223	AB_2563012
TIGIT (A15153G)	APC-Fire750	BioLegend/372707	AB_2632754

Supplementary Table S4.5. Primer sequences

Gene	Forward primer (5'>3')	Reverse primer (5'>3')
<i>B3GALT4</i>	ACG CTA TTC TTG CTG GGA GA	ACC AGT TCA GGG ACG TTG AC
<i>B4GALT5</i>	TCC TCG CTG CTG TAC TTC G	AAT GCC TTG GGC TTG CAT CA
<i>B4GALT6</i>	TAT GTC ATC GAA CAG ACC GGC ACA	AGG CTC TGT CTT TCA TGG CCT CTT
<i>B4GALNT1</i>	GCT ACC AGA CCA ACA CAG CA	TGG TGG CAA TCG TGA CTA GA
<i>CYR61</i>	CTT GTT GGC GTC TTC GTC G	AGC CTG GTC AAG TGG AGA AG
<i>GAPDH</i>	GAG TCA ACG GAT TTG GTC GT	GAC AAG CTT CCC GTT CTC AG
<i>HPRT</i>	ATG CTG AGG ATT TGG AAA GGG TGT TTA TT	TGA AGT ATT CAT TAT AGT CAA GGG CAT AT
<i>ST3GAL2</i>	AAC CAC CCA CCA TTT CAT GT	TGA TGC TCT GTC CAC CTG TC
<i>ST3GAL5</i>	CCC TGA ACC AGT TCG ATG TT	CAT TGC TTG AAG CCA GTT GA
<i>ST8SIA1</i>	AGC GTT CAG GAA ACA AAT GG	TGC CTG TGG GAA GAG AGA GT
<i>ST8SIA5</i>	CCT TTG CCT TGG TGA CCT	CAT GGA CAG CAC CTT CAC T
<i>YAP</i>	CCC GAC AGG CCA GTA CTG AT	CAG AGA AGC TGG AGA GGA ATG AG

Chapter V: Conclusions and Future Directions

5.1 Summary of findings and implications of this study

The survival of patients with high-risk neuroblastoma is ~50% even though they receive aggressive multimodal treatment including chemoimmunotherapy with GD2-targeting agents. Unfortunately, despite advancements in treatment, patients who relapse have <5% chance of cure. Relapsed neuroblastoma is characterized by enrichment of mesenchymal neuroblastoma cells that express high levels of YAP and hyperactivation of RAS/MAPK signaling.¹⁰⁻¹² Thus, given these statistics, and the current standard-of-care including dinutuximab, a GD2-targeting mAb, there is a dire need to understand biomarkers of GD2 response, the mechanisms of resistance to anti-GD2 treatment, and alternative approaches for patient non-responders. Given the high expression and increased transcriptional activity of YAP in relapsed neuroblastoma tumors, we hypothesized that, YAP regulates GD2, a target of the post-induction phase of treatment. Since one of the major mechanisms of action of dinutuximab is ADCC, we sought to determine how YAP regulates GD2 expression in neuroblastoma and the role of YAP in modulation of ADCC in neuroblastoma.

Treatment with dinutuximab is dependent on native immunity for efficacy since dinutuximab opsonizes target neuroblastoma cells that are then phagocytosed or lysed as a result of CDC or ADCC elicited by a patient's macrophages, neutrophils, NK cells, and/or $\gamma\delta$ T cells. Given that patients with high-risk neuroblastoma who have already received chemotherapy and other myeloablative treatments are immunocompromised, one approach is to use allogeneic donation of MHC-independent $\gamma\delta$ T cells in combination with dinutuximab and other chemotherapeutic drugs. This is the premise of a phase I clinical trial initiated by the Goldsmith lab ([NCT05400603](https://clinicaltrials.gov/ct2/show/study/NCT05400603)). Thus, our work seeks to determine mechanisms of resistance to this anti-GD2/ $\gamma\delta$ T cell immunotherapy and potential synergies with this treatment approach.

To this end, YAP and GD2 expression were assessed and determined to be inversely correlated in a panel of neuroblastoma cell lines; perhaps suggestive of YAP suppression of GD2 cell surface expression. To further understand this relationship, a highly therapy-resistant, MYCN-NA, RAS-mutant neuroblastoma cell line with high YAP expression, SK-N-AS, was selected as this can be considered to exemplify a relapsed neuroblastoma model. Inhibition of YAP sensitized SK-N-AS neuroblastoma cells to anti-GD2/ $\gamma\delta$ T cell immunotherapy as well as $\gamma\delta$ T cell immunotherapy alone. The mechanism of resistance to anti-GD2 (dinutuximab)/ $\gamma\delta$ T cell immunotherapy is, at least in part, because YAP suppresses GD2 surface expression by repressing *ST8SIA1*, a gene encoding GD3 synthase, the rate-limiting enzyme in GD2 biosynthesis. To determine the clinical relevance of the YAP/ GD2 relationship, we assessed gene expression of *YAP* and *ST8SIA1* in primary neuroblastoma tumor datasets, and there was an inverse relationship. We also confirmed that YAP and GD2 are inversely correlated in neuroblastoma PDXs.

Since GD2 is a glycosphingolipid, assessing its expression in cryopreserved or formalin-fixed neuroblastoma tumors is not possible. The protein expression of YAP can be measured by immunohistochemistry and potentially be a proxy for GD2 expression in neuroblastoma. Thus, determining YAP expression in primary pre-treatment high-risk neuroblastoma tumors may be a useful biomarker of patient response to anti-GD2 treatment, predicting resistance prior to deciding on a therapeutic course. Additionally, pharmacological YAP inhibition may synergize with current standard-of-care for patients with relapsed/refractory high-risk neuroblastoma.

5.2 Limitations of this work and future directions

5.2.1 Mechanism of YAP-GD2 regulation in neuroblastoma

The question of whether the inverse correlation of YAP and GD2 expression is generalizable in high-risk neuroblastoma remains to be answered. The YAP/*ST8SIA1*(GD3S)/GD2 relationship is likely dependent on, or interacts with, other genetic alterations in neuroblastoma. Increasing

GD3S/GD2 expression in neuroblastoma through epigenetic inhibition has been previously investigated.³⁹⁸⁻⁴⁰⁰ However, to date, there are few published data that link YAP expression to GD3S or GD2, directly. A physical interaction between GD3 and the Src family kinase, Yes, in GEMs enhances downstream kinase signaling and consequently, invasion and proliferation in models of melanoma⁴³⁴ and glioma.⁴³⁵ Thus, one future direction would be to determine whether GD3 and YAP also directly interact in neuroblastoma cell lines.

The exact mechanism through which YAP is regulating expression of *ST8SIA1* has not been determined in this work. We sought to elucidate whether the repression of *ST8SIA1* is TEAD-dependent as this understanding is crucial for determining the most effective pharmacological inhibitor of YAP that would replicate the findings of increased GD2 expression upon genetic inhibition of YAP. However, neither transient knockdown of the entire TEAD family nor stable knockdown or knockout of individual TEAD family members affected *ST8SIA1* or GD2 surface expression (data not shown). The only published mechanism of gene repression by YAP that may be TEAD-independent involves the binding of YAP to YY1 and EZH2, and the addition of H3K27me3 marks at TEAD-adjacent YY1 motifs in promoters of target genes (**Figure 2.3**).²⁰³ It will be important through ChIP-PCR, re-expression of YAP mutant constructs defective in TEAD binding (YAP S94A), and promoter reporter studies to determine the mechanism of repression involved in the YAP-*ST8SIA1*-GD2 axis in neuroblastoma.

In general, increased expression of GD3S is understood to drive proliferation and metastasis in a number of cancers including breast cancer,³⁸³ glioma,⁴³⁶ lung cancer,⁴³⁷ and melanoma.⁴³⁸ The consequence of higher GD3S expression is increased intracellular and extracellular GD3 and GD2 gangliosides and in some models, resistance to immunotherapy and chemotherapy.⁴³⁹ In this study, we did not assess the protein expression or enzymatic activity of GD3S, nor did we assess the expression of GD3 ganglioside. Future experiments may determine whether GD3, an

intermediate in GD2 biosynthesis, is involved in mediating increased sensitivity of YAP-inhibited neuroblastoma cells to $\gamma\delta$ T cell killing in the absence of dinutuximab. Overexpression of GD3S in a neuroblastoma cell line, SHSY5Y, paradoxically, led to reduced growth rate.⁴⁴⁰ Other previously published studies demonstrated that intracellular accumulation of GD3 occurs rapidly after engagement of CD95 on tumor cells, inducing apoptosis.⁴⁴¹ Thus, it will be important to examine the roles of GD3S/GD3 in sensitivity of neuroblastoma cells to combination $\gamma\delta$ T cell/dinutuximab immunotherapy.

5.2.2 The role of TAZ in regulation of GD2 in neuroblastoma

As discussed in chapter 2, the paralog of YAP, TAZ has distinct structure and functions from YAP. In our study, we determined that stable knockdown of TAZ did not recapitulate the phenotype of increased *ST8SIA1*/GD2 expression in neuroblastoma (**Supplementary Figure S4.7**). Neither partial genetic inhibition by knockdown nor complete ablation by knockout of YAP resulted in increased expression of TAZ (**Supplementary Figure S4.8C**); however, ablation of YAP does lead to compensatory binding of TAZ to TEAD2, perhaps resulting in contextual regulation of *ST8SIA1*/GD2 expression (**Supplementary Figure S4.8D**). In the future, it will be important to determine whether this compensatory binding of TAZ to TEAD2 has the functional consequence of *ST8SIA1* suppression through promoter reporter assays. If TEAD is not involved in the regulation of this process, it is still possible that TAZ may perform its compensatory function through another means. Thus, further mechanistic insight into the requirement for various domains of the TAZ protein in the regulation of this process can be obtained by ablating TAZ and re-expressing constructs that are defective in TEAD binding (TAZ S89A), lack the TAZ WW domain (TAZ- Δ WW) or PDZ-binding motif (TAZ- Δ PDZ).

5.2.3 Role of YAP inhibition in sensitization to $\gamma\delta$ T cell cytotoxicity

In addition to increasing GD2 cell surface expression and sensitivity to dinutuximab/ $\gamma\delta$ T cell combination immunotherapy, we observed increased killing of neuroblastoma cells by $\gamma\delta$ T cells in the absence of dinutuximab (**Figure 4.2B**). Thus, we investigated tumor cell-intrinsic and $\gamma\delta$ T cell-intrinsic factors in which YAP might be mechanistically involved. There were no changes in death receptor, NK cell ligand, and stress antigen expression on the surface of neuroblastoma cells upon genetic inhibition of YAP (**Supplementary Figure S4.5**). Extensive characterization of $\gamma\delta$ T cells was not indicative of any changes in their activation state after co-culture with control versus YAP knockdown cells (**Supplementary Figure S4.4**). As discussed in section 2.2.2, increased YAP in cancer cells mediates the expression and release of various cytokines or chemokines. We examined the supernatants of SK-N-AS shYAP cells with or without $\gamma\delta$ T cells and determined that there were no differences in a range of cytokines that might affect $\gamma\delta$ T cell chemotaxis or cytolytic function (data not shown). However, further exploration with a more sensitive and extensive cytokine array (such as a multiplex protein immunoassay) may be informative.

The role of YAP in mechanotransduction potentially increases susceptibility of YAP-inhibited neuroblastoma cells to $\gamma\delta$ T cells. YAP is required for focal adhesion formation and assembly, as well as maintenance of integrity of the cytoskeleton.⁴⁴² Cytotoxicity by $\gamma\delta$ T cells is dependent on effective immunological synapse formation between tumor cells and $\gamma\delta$ T cells.⁴⁴³ Therefore, inhibition of YAP in neuroblastoma cells may potentiate the ability of $\gamma\delta$ T cells to attach to tumor cells, effectively deploying cytolytic mediators. To evaluate whether alterations in the cytoskeletal structure of YAP-inhibited neuroblastoma cells are responsible for their increased sensitivity to $\gamma\delta$ T cell killing, neuroblastoma- $\gamma\delta$ T cell interactions may be assessed using confocal microscopy or imaging flow cytometry.

In a KRAS-mutant immunocompetent murine model of lung cancer, increased IFN γ in the tumor microenvironment caused YAP phase separation and assembly of transcriptional machinery that increased expression of YAP target genes which induced resistance to anti-PD1 immunotherapy.²⁴⁰ Since YAP is known to exert pleiotropic effects in the TME, in the future, it will be important to determine the relevance of the YAP-GD2 axis in immunocompetent models.

5.3 Overall Conclusions

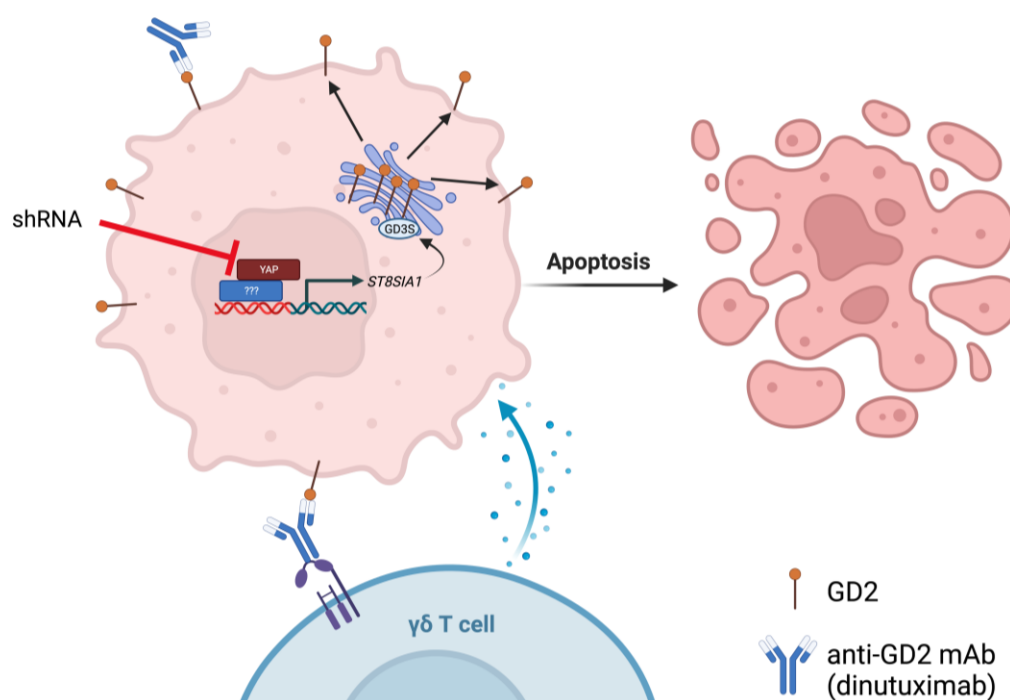


Figure 5.1. Model showing the role of YAP in response to $\gamma\delta$ T cell/dinutuximab immunotherapy in neuroblastoma.

There is an established role for YAP in resistance to chemotherapy and targeted MEK inhibition in neuroblastoma.^{118,119} YAP expression and downstream transcriptional activity are increased in relapsed neuroblastomas.¹² Due to the inclusion of GD2-targeting immunotherapy in treatment regimens for relapsed neuroblastoma, we sought to investigate a role for YAP in regulation of GD2. There are no current biomarkers of GD2 response and little or no understanding of the

mechanisms of resistance to anti-GD2 immunotherapy. Thus, we propose that, given the inverse correlation between YAP and GD2 expression, immunohistochemistry for YAP may be a novel biomarker or response to GD2-targeting therapies. Additionally, pharmacological YAP inhibition may synergize with GD2-targeting immunotherapy combinations. Zoledronate may synergize with dinutuximab/ $\gamma\delta$ T cell combination immunotherapy. Zoledronate inhibits mevalonate biosynthesis, reducing nuclear YAP localization and function and activates $\gamma\delta$ T cells as mentioned in sections 2.1.2 and 3.1.3, respectively. Thus, inclusion of pharmacological YAP inhibition and zoledronate may increase the efficacy of dinutuximab/ $\gamma\delta$ T cell combination immunotherapy. This dissertation establishes a role for YAP in determining response to anti-GD2 immunotherapy in neuroblastoma.

References

1. Matthay KK, Maris JM, Schleiermacher G, et al. Neuroblastoma. *Nat Rev Dis Primers*. Nov 10 2016;2:16078. doi:10.1038/nrdp.2016.78
2. Brodeur GM, Seeger RC, Barrett A, et al. International criteria for diagnosis, staging, and response to treatment in patients with neuroblastoma. *J Clin Oncol*. Dec 1988;6(12):1874-81. doi:10.1200/JCO.1988.6.12.1874
3. Brodeur GM, Pritchard J, Berthold F, et al. Revisions of the international criteria for neuroblastoma diagnosis, staging, and response to treatment. *J Clin Oncol*. Aug 1993;11(8):1466-77. doi:10.1200/JCO.1993.11.8.1466
4. Cohn SL, Pearson AD, London WB, et al. The International Neuroblastoma Risk Group (INRG) classification system: an INRG Task Force report. *J Clin Oncol*. Jan 10 2009;27(2):289-97. doi:10.1200/JCO.2008.16.6785
5. Monclair T, Brodeur GM, Ambros PF, et al. The International Neuroblastoma Risk Group (INRG) staging system: an INRG Task Force report. *J Clin Oncol*. Jan 10 2009;27(2):298-303. doi:10.1200/JCO.2008.16.6876
6. Irwin MS, Naranjo A, Zhang FF, et al. Revised Neuroblastoma Risk Classification System: A Report From the Children's Oncology Group. *J Clin Oncol*. Oct 10 2021;39(29):3229-3241. doi:10.1200/JCO.21.00278
7. Pinto NR, Applebaum MA, Volchenboum SL, et al. Advances in Risk Classification and Treatment Strategies for Neuroblastoma. *J Clin Oncol*. Sep 2015;33(27):3008-17. doi:10.1200/JCO.2014.59.4648
8. Park JR, Scott JR, Stewart CF, et al. Pilot induction regimen incorporating pharmacokinetically guided topotecan for treatment of newly diagnosed high-risk neuroblastoma: a Children's Oncology Group study. *J Clin Oncol*. Nov 20 2011;29(33):4351-7. doi:10.1200/JCO.2010.34.3293
9. Park JR, Kreissman SG, London WB, et al. Effect of Tandem Autologous Stem Cell Transplant vs Single Transplant on Event-Free Survival in Patients With High-Risk Neuroblastoma: A Randomized Clinical Trial. *JAMA*. Aug 27 2019;322(8):746-755. doi:10.1001/jama.2019.11642
10. Padovan-Merhar OM, Raman P, Ostrovnaya I, et al. Enrichment of Targetable Mutations in the Relapsed Neuroblastoma Genome. *PLoS Genet*. Dec 2016;12(12):e1006501. doi:10.1371/journal.pgen.1006501
11. Eleveld TF, Oldridge DA, Bernard V, et al. Relapsed neuroblastomas show frequent RAS-MAPK pathway mutations. *Nat Genet*. 08 2015;47(8):864-71. doi:10.1038/ng.3333
12. Schramm A, Köster J, Assenov Y, et al. Mutational dynamics between primary and relapse neuroblastomas. *Nat Genet*. Aug 2015;47(8):872-7. doi:10.1038/ng.3349
13. Manas A, Aaltonen K, Andersson N, et al. Clinically relevant treatment of PDX models reveals patterns of neuroblastoma chemoresistance. *Sci Adv*. Oct 28 2022;8(43):eabq4617. doi:10.1126/sciadv.abq4617
14. Mody R, Yu AL, Naranjo A, et al. Irinotecan, Temozolomide, and Dinutuximab With GM-CSF in Children With Refractory or Relapsed Neuroblastoma: A Report From the Children's Oncology Group. *J Clin Oncol*. 07 01 2020;38(19):2160-2169. doi:10.1200/JCO.20.00203
15. Lerman BJ, Li Y, Carlowicz C, et al. Progression-Free Survival and Patterns of Response in Patients With Relapsed High-Risk Neuroblastoma Treated With Irinotecan/Temozolomide/Dinutuximab/Granulocyte-Macrophage Colony-Stimulating Factor. *J Clin Oncol*. Jan 20 2023;41(3):508-516. doi:10.1200/JCO.22.01273
16. Gröbner SN, Worst BC, Weischenfeldt J, et al. The landscape of genomic alterations across childhood cancers. *Nature*. Mar 15 2018;555(7696):321-327. doi:10.1038/nature25480
17. Schwab M, Alitalo K, Klempnauer KH, et al. Amplified DNA with limited homology to myc cellular oncogene is shared by human neuroblastoma cell lines and a neuroblastoma tumour. *Nature*. 1983 Sep 15-21 1983;305(5931):245-8. doi:10.1038/305245a0
18. Schwab M, Ellison J, Busch M, Rosenau W, Varmus HE, Bishop JM. Enhanced expression of the human gene N-myc consequent to amplification of DNA may contribute to malignant progression of neuroblastoma. *Proc Natl Acad Sci U S A*. Aug 1984;81(15):4940-4. doi:10.1073/pnas.81.15.4940
19. Kohl NE, Kanda N, Schreck RR, et al. Transposition and amplification of oncogene-related sequences in human neuroblastomas. *Cell*. Dec 1983;35(2 Pt 1):359-67. doi:10.1016/0092-8674(83)90169-1

20. Peifer M, Hertwig F, Roels F, et al. Telomerase activation by genomic rearrangements in high-risk neuroblastoma. *Nature*. Oct 29 2015;526(7575):700-4. doi:10.1038/nature14980
21. Valentijn LJ, Koster J, Zwijnenburg DA, et al. TERT rearrangements are frequent in neuroblastoma and identify aggressive tumors. *Nat Genet*. Dec 2015;47(12):1411-4. doi:10.1038/ng.3438
22. Schleiermacher G, Janoueix-Lerosey I, Ribeiro A, et al. Accumulation of segmental alterations determines progression in neuroblastoma. *J Clin Oncol*. Jul 01 2010;28(19):3122-30. doi:10.1200/JCO.2009.26.7955
23. Pugh TJ, Morozova O, Attiyeh EF, et al. The genetic landscape of high-risk neuroblastoma. *Nat Genet*. Mar 2013;45(3):279-84. doi:10.1038/ng.2529
24. Janoueix-Lerosey I, Lequin D, Brugières L, et al. Somatic and germline activating mutations of the ALK kinase receptor in neuroblastoma. *Nature*. Oct 16 2008;455(7215):967-70. doi:10.1038/nature07398
25. Mossé YP, Laudenslager M, Longo L, et al. Identification of ALK as a major familial neuroblastoma predisposition gene. *Nature*. Oct 16 2008;455(7215):930-5. doi:10.1038/nature07261
26. Chen Y, Takita J, Choi YL, et al. Oncogenic mutations of ALK kinase in neuroblastoma. *Nature*. Oct 16 2008;455(7215):971-4. doi:10.1038/nature07399
27. George RE, Sanda T, Hanna M, et al. Activating mutations in ALK provide a therapeutic target in neuroblastoma. *Nature*. Oct 16 2008;455(7215):975-8. doi:10.1038/nature07397
28. Schleiermacher G, Javanmardi N, Bernard V, et al. Emergence of new ALK mutations at relapse of neuroblastoma. *J Clin Oncol*. Sep 01 2014;32(25):2727-34. doi:10.1200/JCO.2013.54.0674
29. Eleveld TF, Schild L, Koster J, et al. RAS-MAPK Pathway-Driven Tumor Progression Is Associated with Loss of CIC and Other Genomic Aberrations in Neuroblastoma. *Cancer Res*. Nov 2018;78(21):6297-6307. doi:10.1158/0008-5472.CAN-18-1045
30. Blackwell TK, Kretzner L, Blackwood EM, Eisenman RN, Weintraub H. Sequence-specific DNA binding by the c-Myc protein. *Science*. Nov 23 1990;250(4984):1149-51. doi:10.1126/science.2251503
31. Solomon DL, Amati B, Land H. Distinct DNA binding preferences for the c-Myc/Max and Max/Max dimers. *Nucleic Acids Res*. Nov 25 1993;21(23):5372-6. doi:10.1093/nar/21.23.5372
32. Nau MM, Brooks BJ, Battey J, et al. L-myc, a new myc-related gene amplified and expressed in human small cell lung cancer. *Nature*. Nov 7-13 1985;318(6041):69-73. doi:10.1038/318069a0
33. Seoane J, Le HV, Massagué J. Myc suppression of the p21(Cip1) Cdk inhibitor influences the outcome of the p53 response to DNA damage. *Nature*. Oct 17 2002;419(6908):729-34. doi:10.1038/nature01119
34. Peukert K, Staller P, Schneider A, Carmichael G, Hänel F, Eilers M. An alternative pathway for gene regulation by Myc. *EMBO J*. Sep 15 1997;16(18):5672-86. doi:10.1093/emboj/16.18.5672
35. Vo BT, Wolf E, Kawauchi D, et al. The Interaction of Myc with Miz1 Defines Medulloblastoma Subgroup Identity. *Cancer Cell*. Jan 11 2016;29(1):5-16. doi:10.1016/j.ccell.2015.12.003
36. Akter J, Takatori A, Hossain MS, et al. Expression of NLRR3 orphan receptor gene is negatively regulated by MYCN and Miz-1, and its downregulation is associated with unfavorable outcome in neuroblastoma. *Clin Cancer Res*. Nov 01 2011;17(21):6681-92. doi:10.1158/1078-0432.CCR-11-0313
37. Dardenne E, Beltran H, Benelli M, et al. N-Myc Induces an EZH2-Mediated Transcriptional Program Driving Neuroendocrine Prostate Cancer. *Cancer Cell*. Oct 10 2016;30(4):563-577. doi:10.1016/j.ccell.2016.09.005
38. Kohl NE, Gee CE, Alt FW. Activated expression of the N-myc gene in human neuroblastomas and related tumors. *Science*. Dec 14 1984;226(4680):1335-7. doi:10.1126/science.6505694
39. Brodeur GM, Seeger RC, Schwab M, Varmus HE, Bishop JM. Amplification of N-myc in untreated human neuroblastomas correlates with advanced disease stage. *Science*. Jun 08 1984;224(4653):1121-4. doi:10.1126/science.6719137
40. Seeger RC, Brodeur GM, Sather H, et al. Association of multiple copies of the N-myc oncogene with rapid progression of neuroblastomas. *N Engl J Med*. Oct 31 1985;313(18):1111-6. doi:10.1056/NEJM198510313131802
41. Zimmerman MW, Liu Y, He S, et al. MYC Drives a Subset of High-Risk Pediatric Neuroblastomas and Is Activated through Mechanisms Including Enhancer Hijacking and Focal Enhancer Amplification. *Cancer Discov*. Mar 2018;8(3):320-335. doi:10.1158/2159-8290.CD-17-0993
42. Olsen RR, Otero JH, García-López J, et al. MYCN induces neuroblastoma in primary neural crest cells. *Oncogene*. Aug 31 2017;36(35):5075-5082. doi:10.1038/onc.2017.128
43. Dang CV. MYC on the path to cancer. *Cell*. Mar 2012;149(1):22-35. doi:10.1016/j.cell.2012.03.003
44. Mac SM, D'Cunha CA, Farnham PJ. Direct recruitment of N-myc to target gene promoters. *Mol Carcinog*. Oct 2000;29(2):76-86.

45. Metelitsa LS, Gillies SD, Super M, Shimada H, Reynolds CP, Seeger RC. Antidisialoganglioside/granulocyte macrophage-colony-stimulating factor fusion protein facilitates neutrophil antibody-dependent cellular cytotoxicity and depends on FcγRII (CD32) and Mac-1 (CD11b/CD18) for enhanced effector cell adhesion and azurophil granule exocytosis. *Blood*. Jun 01 2002;99(11):4166-73. doi:10.1182/blood.v99.11.4166
46. Chan HS, Gallie BL, DeBoer G, et al. MYCN protein expression as a predictor of neuroblastoma prognosis. *Clin Cancer Res*. Oct 1997;3(10):1699-706.
47. Lamant L, Pulford K, Bischof D, et al. Expression of the ALK tyrosine kinase gene in neuroblastoma. *Am J Pathol*. May 2000;156(5):1711-21. doi:10.1016/S0002-9440(10)65042-0
48. Iwahara T, Fujimoto J, Wen D, et al. Molecular characterization of ALK, a receptor tyrosine kinase expressed specifically in the nervous system. *Oncogene*. Jan 30 1997;14(4):439-49. doi:10.1038/sj.onc.1200849
49. Morris SW, Naeve C, Mathew P, et al. ALK, the chromosome 2 gene locus altered by the t(2;5) in non-Hodgkin's lymphoma, encodes a novel neural receptor tyrosine kinase that is highly related to leukocyte tyrosine kinase (LTK). *Oncogene*. May 08 1997;14(18):2175-88. doi:10.1038/sj.onc.1201062
50. Reshetnyak AV, Mohanty J, Tome F, et al. Identification of a biologically active fragment of ALK and LTK-Ligand 2 (augmentor-alpha). *Proc Natl Acad Sci U S A*. Aug 14 2018;115(33):8340-8345. doi:10.1073/pnas.1807881115
51. Guan J, Umopathy G, Yamazaki Y, et al. FAM150A and FAM150B are activating ligands for anaplastic lymphoma kinase. *Elife*. Sep 29 2015;4:e09811. doi:10.7554/eLife.09811
52. Reshetnyak AV, Murray PB, Shi X, et al. Augmentor alpha and beta (FAM150) are ligands of the receptor tyrosine kinases ALK and LTK: Hierarchy and specificity of ligand-receptor interactions. *Proc Natl Acad Sci U S A*. Dec 29 2015;112(52):15862-7. doi:10.1073/pnas.1520099112
53. Morris SW, Kirstein MN, Valentine MB, et al. Fusion of a kinase gene, ALK, to a nucleolar protein gene, NPM, in non-Hodgkin's lymphoma. *Science*. Mar 04 1994;263(5151):1281-4. doi:10.1126/science.8122112
54. Shiota M, Fujimoto J, Semba T, Satoh H, Yamamoto T, Mori S. Hyperphosphorylation of a novel 80 kDa protein-tyrosine kinase similar to Ltk in a human Ki-1 lymphoma cell line, AMS3. *Oncogene*. Jun 1994;9(6):1567-74.
55. Soda M, Choi YL, Enomoto M, et al. Identification of the transforming EML4-ALK fusion gene in non-small-cell lung cancer. *Nature*. Aug 02 2007;448(7153):561-6. doi:10.1038/nature05945
56. Fransson S, Hansson M, Ruuth K, et al. Intragenic anaplastic lymphoma kinase (ALK) rearrangements: translocations as a novel mechanism of ALK activation in neuroblastoma tumors. *Genes Chromosomes Cancer*. Feb 2015;54(2):99-109. doi:10.1002/gcc.22223
57. Cazes A, Louis-Brennetot C, Mazot P, et al. Characterization of rearrangements involving the ALK gene reveals a novel truncated form associated with tumor aggressiveness in neuroblastoma. *Cancer Res*. Jan 01 2013;73(1):195-204. doi:10.1158/0008-5472.CAN-12-1242
58. Bresler SC, Weiser DA, Huwe PJ, et al. ALK mutations confer differential oncogenic activation and sensitivity to ALK inhibition therapy in neuroblastoma. *Cancer Cell*. Nov 10 2014;26(5):682-94. doi:10.1016/j.ccell.2014.09.019
59. Holla VR, Elamin YY, Bailey AM, et al. ALK: a tyrosine kinase target for cancer therapy. *Cold Spring Harb Mol Case Stud*. Jan 2017;3(1):a001115. doi:10.1101/mcs.a001115
60. Borenas M, Umopathy G, Lai WY, et al. ALK ligand ALKAL2 potentiates MYCN-driven neuroblastoma in the absence of ALK mutation. *EMBO J*. Feb 1 2021;40(3):e105784. doi:10.15252/embj.2020105784
61. Mosse YP, Laudenslager M, Khazi D, et al. Germline PHOX2B mutation in hereditary neuroblastoma. *Am J Hum Genet*. Oct 2004;75(4):727-30. doi:10.1086/424530
62. Leape LL, Lowman JT, Loveland GC. Multifocal nondisseminated neuroblastoma. Report of two cases in siblings. *J Pediatr*. Jan 1978;92(1):75-7. doi:10.1016/s0022-3476(78)80075-4
63. Spagnuolo A, Maione P, Gridelli C. Evolution in the treatment landscape of non-small cell lung cancer with ALK gene alterations: from the first- to third-generation of ALK inhibitors. *Expert Opin Emerg Drugs*. Sep 2018;23(3):231-241. doi:10.1080/14728214.2018.1527902
64. Trigg RM, Turner SD. ALK in Neuroblastoma: Biological and Therapeutic Implications. *Cancers (Basel)*. Apr 2018;10(4)doi:10.3390/cancers10040113
65. Mossé YP, Lim MS, Voss SD, et al. Safety and activity of crizotinib for paediatric patients with refractory solid tumours or anaplastic large-cell lymphoma: a Children's Oncology Group phase 1 consortium study. *Lancet Oncol*. May 2013;14(6):472-80. doi:10.1016/S1470-2045(13)70095-0

66. Berlak M, Tucker E, Dorel M, et al. Mutations in ALK signaling pathways conferring resistance to ALK inhibitor treatment lead to collateral vulnerabilities in neuroblastoma cells. *Mol Cancer*. Jun 10 2022;21(1):126. doi:10.1186/s12943-022-01583-z
67. Berko ER, Witek GM, Matkar S, et al. Circulating tumor DNA reveals mechanisms of lorlatinib resistance in patients with relapsed/refractory ALK-driven neuroblastoma. *Nat Commun*. May 5 2023;14(1):2601. doi:10.1038/s41467-023-38195-0
68. Goldsmith KC, Park JR, Kayser K, et al. Lorlatinib with or without chemotherapy in ALK-driven refractory/relapsed neuroblastoma: phase 1 trial results. *Nat Med*. Apr 03 2023;doi:10.1038/s41591-023-02297-5
69. Counter CM, Hirte HW, Bacchetti S, Harley CB. Telomerase activity in human ovarian carcinoma. *Proc Natl Acad Sci U S A*. Apr 12 1994;91(8):2900-4. doi:10.1073/pnas.91.8.2900
70. Bryan TM, Englezou A, Gupta J, Bacchetti S, Reddel RR. Telomere elongation in immortal human cells without detectable telomerase activity. *EMBO J*. Sep 1 1995;14(17):4240-8. doi:10.1002/j.1460-2075.1995.tb00098.x
71. Koneru B, Lopez G, Farooqi A, et al. Telomere Maintenance Mechanisms Define Clinical Outcome in High-Risk Neuroblastoma. *Cancer Res*. Jun 15 2020;80(12):2663-2675. doi:10.1158/0008-5472.CAN-19-3068
72. Nakamura TM, Morin GB, Chapman KB, et al. Telomerase catalytic subunit homologs from fission yeast and human. *Science*. Aug 15 1997;277(5328):955-9. doi:10.1126/science.277.5328.955
73. Hanahan D, Weinberg RA. Hallmarks of cancer: the next generation. *Cell*. Mar 2011;144(5):646-74. doi:10.1016/j.cell.2011.02.013
74. Hanahan D, Weinberg RA. The hallmarks of cancer. *Cell*. Jan 07 2000;100(1):57-70. doi:10.1016/S0092-8674(00)81683-9
75. Hanahan D. Hallmarks of Cancer: New Dimensions. *Cancer Discov*. Jan 2022;12(1):31-46. doi:10.1158/2159-8290.CD-21-1059
76. Colebatch AJ, Dobrovic A, Cooper WA. TERT gene: its function and dysregulation in cancer. *J Clin Pathol*. Apr 2019;72(4):281-284. doi:10.1136/jclinpath-2018-205653
77. Roderwieser A, Sand F, Walter E, et al. Telomerase Is a Prognostic Marker of Poor Outcome and a Therapeutic Target in Neuroblastoma. *JCO Precis Oncol*. Dec 2019;3:1-20. doi:10.1200/PO.19.00072
78. Fransson S, Martinez-Monleon A, Johansson M, et al. Whole-genome sequencing of recurrent neuroblastoma reveals somatic mutations that affect key players in cancer progression and telomere maintenance. *Sci Rep*. 12 31 2020;10(1):22432. doi:10.1038/s41598-020-78370-7
79. Chen J, Nelson C, Wong M, et al. Targeted Therapy of TERT-Rearranged Neuroblastoma with BET Bromodomain Inhibitor and Proteasome Inhibitor Combination Therapy. *Clin Cancer Res*. Mar 01 2021;27(5):1438-1451. doi:10.1158/1078-0432.CCR-20-3044
80. Huang M, Zeki J, Sumarsono N, et al. Epigenetic Targeting of TERT-Associated Gene Expression Signature in Human Neuroblastoma with TERT Overexpression. *Cancer Res*. Mar 01 2020;80(5):1024-1035. doi:10.1158/0008-5472.CAN-19-2560
81. Moreno V, Vieito M, Sepulveda JM, et al. BET inhibitor trotabresib in heavily pretreated patients with solid tumors and diffuse large B-cell lymphomas. *Nat Commun*. Mar 13 2023;14(1):1359. doi:10.1038/s41467-023-36976-1
82. Ackermann S, Cartolano M, Hero B, et al. A mechanistic classification of clinical phenotypes in neuroblastoma. *Science*. Dec 07 2018;362(6419):1165-1170. doi:10.1126/science.aat6768
83. Hartlieb SA, Sieverling L, Nadler-Holly M, et al. Alternative lengthening of telomeres in childhood neuroblastoma from genome to proteome. *Nat Commun*. Feb 24 2021;12(1):1269. doi:10.1038/s41467-021-21247-8
84. Picketts DJ, Higgs DR, Bachoo S, Blake DJ, Quarrell OW, Gibbons RJ. ATRX encodes a novel member of the SNF2 family of proteins: mutations point to a common mechanism underlying the ATR-X syndrome. *Hum Mol Genet*. Dec 1996;5(12):1899-907. doi:10.1093/hmg/5.12.1899
85. Brady SW, Liu Y, Ma X, et al. Pan-neuroblastoma analysis reveals age- and signature-associated driver alterations. *Nat Commun*. Oct 14 2020;11(1):5183. doi:10.1038/s41467-020-18987-4
86. Zeineldin M, Federico S, Chen X, et al. MYCN amplification and ATRX mutations are incompatible in neuroblastoma. *Nat Commun*. Feb 14 2020;11(1):913. doi:10.1038/s41467-020-14682-6
87. Paolini L, Hussain S, Galardy PJ. Chromosome instability in neuroblastoma: A pathway to aggressive disease. *Front Oncol*. 2022;12:988972. doi:10.3389/fonc.2022.988972

88. Molenaar JJ, Koster J, Zwijnenburg DA, et al. Sequencing of neuroblastoma identifies chromothripsis and defects in neuritogenesis genes. *Nature*. Feb 22 2012;483(7391):589-93. doi:10.1038/nature10910
89. Chicard M, Boyault S, Colmet Daage L, et al. Genomic Copy Number Profiling Using Circulating Free Tumor DNA Highlights Heterogeneity in Neuroblastoma. *Clin Cancer Res*. Nov 15 2016;22(22):5564-5573. doi:10.1158/1078-0432.CCR-16-0500
90. Maris JM, White PS, Beltinger CP, et al. Significance of chromosome 1p loss of heterozygosity in neuroblastoma. *Cancer Res*. Oct 15 1995;55(20):4664-9.
91. Savelyeva L, Corvi R, Schwab M. Translocation involving 1p and 17q is a recurrent genetic alteration of human neuroblastoma cells. *Am J Hum Genet*. Aug 1994;55(2):334-40.
92. Van Roy N, Laureys G, Cheng NC, et al. 1;17 translocations and other chromosome 17 rearrangements in human primary neuroblastoma tumors and cell lines. *Genes Chromosomes Cancer*. Jun 1994;10(2):103-14. doi:10.1002/gcc.2870100205
93. Ejeskär K, Aburatani H, Abrahamsson J, Kogner P, Martinsson T. Loss of heterozygosity of 3p markers in neuroblastoma tumours implicate a tumour-suppressor locus distal to the FHIT gene. *Br J Cancer*. Jun 1998;77(11):1787-91. doi:10.1038/bjc.1998.297
94. Caron H, van Sluis P, Buschman R, et al. Allelic loss of the short arm of chromosome 4 in neuroblastoma suggests a novel tumour suppressor gene locus. *Hum Genet*. Jun 1996;97(6):834-7. doi:10.1007/BF02346199
95. Marshall B, Isidro G, Martins AG, Boavida MG. Loss of heterozygosity at chromosome 9p21 in primary neuroblastomas: evidence for two deleted regions. *Cancer Genet Cytogenet*. Jul 15 1997;96(2):134-9. doi:10.1016/S0165-4608(96)00300-7
96. Giordani L, Iolascon A, Servedio V, Mazzocco K, Longo L, Tonini GP. Two regions of deletion in 9p22- p24 in neuroblastoma are frequently observed in favorable tumors. *Cancer Genet Cytogenet*. May 2002;135(1):42-7. doi:10.1016/S0165-4608(01)00640-9
97. Mora J, Gerald WL, Qin J, Cheung NK. Evolving significance of prognostic markers associated with treatment improvement in patients with stage 4 neuroblastoma. *Cancer*. May 15 2002;94(10):2756-65. doi:10.1002/cncr.10548
98. Srivatsan ES, Murali V, Seeger RC. Loss of heterozygosity for alleles on chromosomes 11q and 14q in neuroblastoma. *Prog Clin Biol Res*. 1991;366:91-8.
99. Attiyeh EF, London WB, Mossé YP, et al. Chromosome 1p and 11q deletions and outcome in neuroblastoma. *N Engl J Med*. Nov 24 2005;353(21):2243-53. doi:10.1056/NEJMoa052399
100. Suzuki T, Yokota J, Mugishima H, et al. Frequent loss of heterozygosity on chromosome 14q in neuroblastoma. *Cancer Res*. Mar 01 1989;49(5):1095-8.
101. Caron H. Allelic loss of chromosome 1 and additional chromosome 17 material are both unfavourable prognostic markers in neuroblastoma. *Med Pediatr Oncol*. Apr 1995;24(4):215-21. doi:10.1002/mpo.2950240402
102. Bown N, Cotterill S, Lastowska M, et al. Gain of chromosome arm 17q and adverse outcome in patients with neuroblastoma. *N Engl J Med*. Jun 24 1999;340(25):1954-61. doi:10.1056/NEJM199906243402504
103. Brodeur GM. Clinical significance of genetic rearrangements in human neuroblastomas. *Clin Chem*. Jul 1989;35(7 Suppl):B38-42.
104. Schleiermacher G, Bourdeaut F, Combaret V, et al. Stepwise occurrence of a complex unbalanced translocation in neuroblastoma leading to insertion of a telomere sequence and late chromosome 17q gain. *Oncogene*. May 05 2005;24(20):3377-84. doi:10.1038/sj.onc.1208486
105. Taparowsky E, Shimizu K, Goldfarb M, Wigler M. Structure and activation of the human N-ras gene. *Cell*. Sep 1983;34(2):581-6. doi:10.1016/0092-8674(83)90390-2
106. Shimizu K, Goldfarb M, Suard Y, et al. Three human transforming genes are related to the viral ras oncogenes. *Proc Natl Acad Sci U S A*. Apr 1983;80(8):2112-6. doi:10.1073/pnas.80.8.2112
107. Hall A, Marshall CJ, Spurr NK, Weiss RA. Identification of transforming gene in two human sarcoma cell lines as a new member of the ras gene family located on chromosome 1. *Nature*. Jun 2-8 1983;303(5916):396-400. doi:10.1038/303396a0
108. Murray MJ, Cunningham JM, Parada LF, Dautry F, Lebowitz P, Weinberg RA. The HL-60 transforming sequence: a ras oncogene coexisting with altered myc genes in hematopoietic tumors. *Cell*. Jul 1983;33(3):749-57. doi:10.1016/0092-8674(83)90017-x

109. Shimizu K, Goldfarb M, Perucho M, Wigler M. Isolation and preliminary characterization of the transforming gene of a human neuroblastoma cell line. *Proc Natl Acad Sci U S A*. Jan 1983;80(2):383-7. doi:10.1073/pnas.80.2.383
110. Boguski MS, McCormick F. Proteins regulating Ras and its relatives. *Nature*. Dec 16 1993;366(6456):643-54. doi:10.1038/366643a0
111. Eisfeld AK, Schwind S, Hoag KW, et al. NRAS isoforms differentially affect downstream pathways, cell growth, and cell transformation. *Proc Natl Acad Sci U S A*. Mar 18 2014;111(11):4179-84. doi:10.1073/pnas.1401727111
112. Sweetser DA, Kapur RP, Froelick GJ, Kafer KE, Palmiter RD. Oncogenesis and altered differentiation induced by activated Ras in neuroblasts of transgenic mice. *Oncogene*. Dec 4 1997;15(23):2783-94. doi:10.1038/sj.onc.1201452
113. The I, Murthy AE, Hannigan GE, et al. Neurofibromatosis type 1 gene mutations in neuroblastoma. *Nat Genet*. Jan 1993;3(1):62-6. doi:10.1038/ng0193-62
114. Holzel M, Huang S, Koster J, et al. NF1 is a tumor suppressor in neuroblastoma that determines retinoic acid response and disease outcome. *Cell*. Jul 23 2010;142(2):218-29. doi:10.1016/j.cell.2010.06.004
115. Cai J, Jacob S, Kurupi R, et al. High-risk neuroblastoma with NF1 loss of function is targetable using SHP2 inhibition. *Cell Rep*. Jul 26 2022;40(4):111095. doi:10.1016/j.celrep.2022.111095
116. Valencia-Sama I, Ladumor Y, Kee L, et al. NRAS Status Determines Sensitivity to SHP2 Inhibitor Combination Therapies Targeting the RAS-MAPK Pathway in Neuroblastoma. *Cancer Res*. 08 15 2020;80(16):3413-3423. doi:10.1158/0008-5472.CAN-19-3822
117. Bentires-Alj M, Paez JG, David FS, et al. Activating mutations of the noonan syndrome-associated SHP2/PTPN11 gene in human solid tumors and adult acute myelogenous leukemia. *Cancer Res*. Dec 15 2004;64(24):8816-20. doi:10.1158/0008-5472.CAN-04-1923
118. Shim J, Lee JY, Jonus HC, et al. YAP-Mediated Repression of HRK Regulates Tumor Growth, Therapy Response, and Survival Under Tumor Environmental Stress in Neuroblastoma. *Cancer Res*. 11 2020;80(21):4741-4753. doi:10.1158/0008-5472.CAN-20-0025
119. Coggins GE, Farrel A, Rathi KS, et al. YAP1 Mediates Resistance to MEK1/2 Inhibition in Neuroblastomas with Hyperactivated RAS Signaling. *Cancer Res*. 12 15 2019;79(24):6204-6214. doi:10.1158/0008-5472.CAN-19-1415
120. Slemmons KK, Crose LE, Rudzinski E, Bentley RC, Linardic CM. Role of the YAP Oncoprotein in Priming Ras-Driven Rhabdomyosarcoma. *PLoS One*. 2015;10(10):e0140781. doi:10.1371/journal.pone.0140781
121. Kapoor A, Yao W, Ying H, et al. Yap1 activation enables bypass of oncogenic Kras addiction in pancreatic cancer. *Cell*. Jul 03 2014;158(1):185-197. doi:10.1016/j.cell.2014.06.003
122. Cooper MJ, Hutchins GM, Cohen PS, Helman LJ, Mennie RJ, Israel MA. Human neuroblastoma tumor cell lines correspond to the arrested differentiation of chromaffin adrenal medullary neuroblasts. *Cell Growth Differ*. Apr 1990;1(4):149-59.
123. De Preter K, Vandesompele J, Heimann P, et al. Human fetal neuroblast and neuroblastoma transcriptome analysis confirms neuroblast origin and highlights neuroblastoma candidate genes. *Genome Biol*. 2006;7(9):R84. doi:10.1186/gb-2006-7-9-r84
124. Soldatov R, Kaucka M, Kastriti ME, et al. Spatiotemporal structure of cell fate decisions in murine neural crest. *Science*. Jun 07 2019;364(6444)doi:10.1126/science.aas9536
125. Hanemaaijer ES, Margaritis T, Sanders K, et al. Single-cell atlas of developing murine adrenal gland reveals relation of Schwann cell precursor signature to neuroblastoma phenotype. *Proc Natl Acad Sci U S A*. Feb 02 2021;118(5)doi:10.1073/pnas.2022350118
126. Dong R, Yang R, Zhan Y, et al. Single-Cell Characterization of Malignant Phenotypes and Developmental Trajectories of Adrenal Neuroblastoma. *Cancer Cell*. Nov 09 2020;38(5):716-733.e6. doi:10.1016/j.ccell.2020.08.014
127. Bedoya-Reina OC, Li W, Arceo M, et al. Single-nuclei transcriptomes from human adrenal gland reveal distinct cellular identities of low and high-risk neuroblastoma tumors. *Nat Commun*. Sep 07 2021;12(1):5309. doi:10.1038/s41467-021-24870-7
128. Kameneva P, Artemov AV, Kastriti ME, et al. Single-cell transcriptomics of human embryos identifies multiple sympathoblast lineages with potential implications for neuroblastoma origin. *Nat Genet*. May 2021;53(5):694-706. doi:10.1038/s41588-021-00818-x
129. Kildisiute G, Kholosy WM, Young MD, et al. Tumor to normal single-cell mRNA comparisons reveal a pan-neuroblastoma cancer cell. *Sci Adv*. 02 2021;7(6)doi:10.1126/sciadv.abd3311

130. Shendry NAM, Zimmerman MW, Abraham BJ, Durbin AD. Intrinsic transcriptional heterogeneity in neuroblastoma guides mechanistic and therapeutic insights. *Cell Rep Med*. May 17 2022;3(5):100632. doi:10.1016/j.xcrm.2022.100632
131. Ross RA, Spengler BA, Biedler JL. Coordinate morphological and biochemical interconversion of human neuroblastoma cells. *J Natl Cancer Inst*. Oct 1983;71(4):741-7.
132. Boeva V, Louis-Brennetot C, Peltier A, et al. Heterogeneity of neuroblastoma cell identity defined by transcriptional circuitries. *Nat Genet*. Sep 2017;49(9):1408-1413. doi:10.1038/ng.3921
133. van Groningen T, Koster J, Valentijn LJ, et al. Neuroblastoma is composed of two super-enhancer-associated differentiation states. *Nat Genet*. Aug 2017;49(8):1261-1266. doi:10.1038/ng.3899
134. Yuan X, Seneviratne JA, Du S, et al. Single-cell profiling of peripheral neuroblastic tumors identifies an aggressive transitional state that bridges an adrenergic-mesenchymal trajectory. *Cell Rep*. Oct 04 2022;41(1):111455. doi:10.1016/j.celrep.2022.111455
135. Hnisz D, Abraham BJ, Lee TI, et al. Super-enhancers in the control of cell identity and disease. *Cell*. Nov 07 2013;155(4):934-47. doi:10.1016/j.cell.2013.09.053
136. Whyte WA, Orlando DA, Hnisz D, et al. Master transcription factors and mediator establish super-enhancers at key cell identity genes. *Cell*. Apr 11 2013;153(2):307-19. doi:10.1016/j.cell.2013.03.035
137. Lovén J, Hoke HA, Lin CY, et al. Selective inhibition of tumor oncogenes by disruption of super-enhancers. *Cell*. Apr 2013;153(2):320-34. doi:10.1016/j.cell.2013.03.036
138. Van Limpt VA, Chan AJ, Van Sluis PG, Caron HN, Van Noesel CJ, Versteeg R. High delta-like 1 expression in a subset of neuroblastoma cell lines corresponds to a differentiated chromaffin cell type. *Int J Cancer*. May 20 2003;105(1):61-9. doi:10.1002/ijc.11047
139. Gartlgruber M, Sharma AK, Quintero A, et al. Super enhancers define regulatory subtypes and cell identity in neuroblastoma. *Nat Cancer*. Jan 2021;2(1):114-128. doi:10.1038/s43018-020-00145-w
140. Durbin AD, Zimmerman MW, Dharia NV, et al. Selective gene dependencies in MYCN-amplified neuroblastoma include the core transcriptional regulatory circuitry. *Nat Genet*. Sep 2018;50(9):1240-1246. doi:10.1038/s41588-018-0191-z
141. Yarmarkovich M, Marshall QF, Warrington JM, et al. Cross-HLA targeting of intracellular oncoproteins with peptide-centric CARs. *Nature*. Nov 2021;599(7885):477-484. doi:10.1038/s41586-021-04061-6
142. Sengupta S, Das S, Crespo AC, et al. Mesenchymal and adrenergic cell lineage states in neuroblastoma possess distinct immunogenic phenotypes. *Nat Cancer*. Oct 2022;3(10):1228-1246. doi:10.1038/s43018-022-00427-5
143. Wolpaw AJ, Grossmann LD, Dessau JL, et al. Epigenetic state determines inflammatory sensing in neuroblastoma. *Proc Natl Acad Sci U S A*. 02 08 2022;119(6)doi:10.1073/pnas.2102358119
144. Sudol M. Yes-associated protein (YAP65) is a proline-rich phosphoprotein that binds to the SH3 domain of the Yes proto-oncogene product. *Oncogene*. Aug 1994;9(8):2145-52.
145. Sudol M, Bork P, Einbond A, et al. Characterization of the mammalian YAP (Yes-associated protein) gene and its role in defining a novel protein module, the WW domain. *J Biol Chem*. Jun 16 1995;270(24):14733-41. doi:10.1074/jbc.270.24.14733
146. Sudol M. YAP1 oncogene and its eight isoforms. *Oncogene*. Aug 15 2013;32(33):3922. doi:10.1038/onc.2012.520
147. Piccolo S, Dupont S, Cordenonsi M. The biology of YAP/TAZ: hippo signaling and beyond. *Physiol Rev*. Oct 2014;94(4):1287-312. doi:10.1152/physrev.00005.2014
148. Zhao B, Li L, Lei Q, Guan KL. The Hippo-YAP pathway in organ size control and tumorigenesis: an updated version. *Genes Dev*. May 2010;24(9):862-74. doi:10.1101/gad.1909210
149. Finch-Edmondson ML, Strauss RP, Clayton JS, Yeoh GC, Callus BA. Splice variant insertions in the C-terminus impairs YAP's transactivation domain. *Biochem Biophys Res Commun*. Jul 2016;6:24-31. doi:10.1016/j.bbrep.2016.02.015
150. Kanai F, Marignani PA, Sarbassova D, et al. TAZ: a novel transcriptional co-activator regulated by interactions with 14-3-3 and PDZ domain proteins. *EMBO J*. Dec 15 2000;19(24):6778-91. doi:10.1093/emboj/19.24.6778
151. Kaan HYK, Chan SW, Tan SKJ, et al. Crystal structure of TAZ-TEAD complex reveals a distinct interaction mode from that of YAP-TEAD complex. *Sci Rep*. May 17 2017;7(1):2035. doi:10.1038/s41598-017-02219-9
152. Zhan T, Rindtorff N, Boutros M. Wnt signaling in cancer. *Oncogene*. Mar 2017;36(11):1461-1473. doi:10.1038/onc.2016.304

153. Azzolin L, Zanconato F, Bresolin S, et al. Role of TAZ as mediator of Wnt signaling. *Cell*. Dec 21 2012;151(7):1443-56. doi:10.1016/j.cell.2012.11.027
154. Konsavage WM, Jr., Kyler SL, Rennoll SA, Jin G, Yochum GS. Wnt/beta-catenin signaling regulates Yes-associated protein (YAP) gene expression in colorectal carcinoma cells. *J Biol Chem*. Apr 6 2012;287(15):11730-9. doi:10.1074/jbc.M111.327767
155. Imajo M, Miyatake K, Iimura A, Miyamoto A, Nishida E. A molecular mechanism that links Hippo signalling to the inhibition of Wnt/beta-catenin signalling. *EMBO J*. Mar 7 2012;31(5):1109-22. doi:10.1038/emboj.2011.487
156. Chaudhary PK, Kim S. An Insight into GPCR and G-Proteins as Cancer Drivers. *Cells*. Nov 24 2021;10(12)doi:10.3390/cells10123288
157. Yu FX, Zhao B, Panupinthu N, et al. Regulation of the Hippo-YAP pathway by G-protein-coupled receptor signaling. *Cell*. Aug 17 2012;150(4):780-91. doi:10.1016/j.cell.2012.06.037
158. Yu FX, Luo J, Mo JS, et al. Mutant Gq/11 promote uveal melanoma tumorigenesis by activating YAP. *Cancer Cell*. Jun 16 2014;25(6):822-30. doi:10.1016/j.ccr.2014.04.017
159. Feng X, Degese MS, Iglesias-Bartolome R, et al. Hippo-independent activation of YAP by the GNAQ uveal melanoma oncogene through a trio-regulated rho GTPase signaling circuitry. *Cancer Cell*. Jun 16 2014;25(6):831-45. doi:10.1016/j.ccr.2014.04.016
160. Zhao B, Li L, Lu Q, et al. Angiomotin is a novel Hippo pathway component that inhibits YAP oncoprotein. *Genes Dev*. Jan 1 2011;25(1):51-63. doi:10.1101/gad.2000111
161. Dupont S, Morsut L, Aragona M, et al. Role of YAP/TAZ in mechanotransduction. *Nature*. Jun 8 2011;474(7350):179-83. doi:10.1038/nature10137
162. Scott KE, Fraley SI, Rangamani P. A spatial model of YAP/TAZ signaling reveals how stiffness, dimensionality, and shape contribute to emergent outcomes. *Proc Natl Acad Sci U S A*. May 18 2021;118(20)doi:10.1073/pnas.2021571118
163. Aragona M, Panciera T, Manfrin A, et al. A mechanical checkpoint controls multicellular growth through YAP/TAZ regulation by actin-processing factors. *Cell*. Aug 29 2013;154(5):1047-1059. doi:10.1016/j.cell.2013.07.042
164. Driscoll TP, Cosgrove BD, Heo SJ, Shurden ZE, Mauck RL. Cytoskeletal to Nuclear Strain Transfer Regulates YAP Signaling in Mesenchymal Stem Cells. *Biophys J*. Jun 16 2015;108(12):2783-93. doi:10.1016/j.bpj.2015.05.010
165. Elosegui-Artola A, Andreu I, Beedle AEM, et al. Force Triggers YAP Nuclear Entry by Regulating Transport across Nuclear Pores. *Cell*. Nov 30 2017;171(6):1397-1410 e14. doi:10.1016/j.cell.2017.10.008
166. Chang L, Azzolin L, Di Biagio D, et al. The SWI/SNF complex is a mechanoregulated inhibitor of YAP and TAZ. *Nature*. Nov 2018;563(7730):265-269. doi:10.1038/s41586-018-0658-1
167. McClatchey AI, Yap AS. Contact inhibition (of proliferation) redux. *Curr Opin Cell Biol*. Oct 2012;24(5):685-94. doi:10.1016/j.ccb.2012.06.009
168. Shalhout SZ, Yang PY, Grzelak EM, et al. YAP-dependent proliferation by a small molecule targeting annexin A2. *Nat Chem Biol*. Jul 2021;17(7):767-775. doi:10.1038/s41589-021-00755-0
169. Mugahid D, Kalocsay M, Liu X, Gruver JS, Peshkin L, Kirschner MW. YAP regulates cell size and growth dynamics via non-cell autonomous mediators. *Elife*. Jan 9 2020;9doi:10.7554/eLife.53404
170. Koo JH, Guan KL. Interplay between YAP/TAZ and Metabolism. *Cell Metab*. Aug 7 2018;28(2):196-206. doi:10.1016/j.cmet.2018.07.010
171. Wang W, Xiao ZD, Li X, et al. AMPK modulates Hippo pathway activity to regulate energy homeostasis. *Nat Cell Biol*. Apr 2015;17(4):490-9. doi:10.1038/ncb3113
172. Mo JS, Meng Z, Kim YC, et al. Cellular energy stress induces AMPK-mediated regulation of YAP and the Hippo pathway. *Nat Cell Biol*. Apr 2015;17(4):500-10. doi:10.1038/ncb3111
173. DeRan M, Yang J, Shen CH, et al. Energy stress regulates hippo-YAP signaling involving AMPK-mediated regulation of angiomotin-like 1 protein. *Cell Rep*. Oct 23 2014;9(2):495-503. doi:10.1016/j.celrep.2014.09.036
174. Wu H, Wei L, Fan F, et al. Integration of Hippo signalling and the unfolded protein response to restrain liver overgrowth and tumorigenesis. *Nat Commun*. Feb 19 2015;6:6239. doi:10.1038/ncomms7239
175. Luo M, Meng Z, Moroiishi T, et al. Heat stress activates YAP/TAZ to induce the heat shock transcriptome. *Nat Cell Biol*. Dec 2020;22(12):1447-1459. doi:10.1038/s41556-020-00602-9
176. Ma B, Chen Y, Chen L, et al. Hypoxia regulates Hippo signalling through the SIAH2 ubiquitin E3 ligase. *Nat Cell Biol*. Jan 2015;17(1):95-103. doi:10.1038/ncb3073
177. Ma B, Cheng H, Gao R, et al. Zyxin-Siah2-Lats2 axis mediates cooperation between Hippo and TGF-beta signalling pathways. *Nat Commun*. Mar 31 2016;7:11123. doi:10.1038/ncomms11123

178. Hong AW, Meng Z, Yuan HX, et al. Osmotic stress-induced phosphorylation by NLK at Ser128 activates YAP. *EMBO Rep.* Jan 2017;18(1):72-86. doi:10.15252/embr.201642681
179. Moon S, Kim W, Kim S, et al. Phosphorylation by NLK inhibits YAP-14-3-3-interactions and induces its nuclear localization. *EMBO Rep.* Jan 2017;18(1):61-71. doi:10.15252/embr.201642683
180. Shao D, Zhai P, Del Re DP, et al. A functional interaction between Hippo-YAP signalling and FoxO1 mediates the oxidative stress response. *Nat Commun.* 2014;5:3315. doi:10.1038/ncomms4315
181. Jin J, Zhang L, Li X, et al. Oxidative stress-CBP axis modulates MOB1 acetylation and activates the Hippo signaling pathway. *Nucleic Acids Res.* Apr 22 2022;50(7):3817-3834. doi:10.1093/nar/gkac189
182. Yang CS, Stampouloglou E, Kingston NM, Zhang L, Monti S, Varelas X. Glutamine-utilizing transaminases are a metabolic vulnerability of TAZ/YAP-activated cancer cells. *EMBO Rep.* Jun 2018;19(6)doi:10.15252/embr.201643577
183. Peng C, Zhu Y, Zhang W, et al. Regulation of the Hippo-YAP Pathway by Glucose Sensor O-GlcNAcylation. *Mol Cell.* Nov 2 2017;68(3):591-604 e5. doi:10.1016/j.molcel.2017.10.010
184. Yuan L, Mao Y, Luo W, et al. Palmitic acid dysregulates the Hippo-YAP pathway and inhibits angiogenesis by inducing mitochondrial damage and activating the cytosolic DNA sensor cGAS-STING-IRF3 signaling mechanism. *J Biol Chem.* Sep 8 2017;292(36):15002-15015. doi:10.1074/jbc.M117.804005
185. Noto A, De Vitis C, Pisanu ME, et al. Stearoyl-CoA-desaturase 1 regulates lung cancer stemness via stabilization and nuclear localization of YAP/TAZ. *Oncogene.* Aug 10 2017;36(32):4573-4584. doi:10.1038/onc.2017.75
186. Chan P, Han X, Zheng B, et al. Autopalmitoylation of TEAD proteins regulates transcriptional output of the Hippo pathway. *Nat Chem Biol.* Apr 2016;12(4):282-9. doi:10.1038/nchembio.2036
187. Sorrentino G, Ruggeri N, Specchia V, et al. Metabolic control of YAP and TAZ by the mevalonate pathway. *Nat Cell Biol.* Apr 2014;16(4):357-66. doi:10.1038/ncb2936
188. Komuro A, Nagai M, Navin NE, Sudol M. WW domain-containing protein YAP associates with ErbB-4 and acts as a co-transcriptional activator for the carboxyl-terminal fragment of ErbB-4 that translocates to the nucleus. *J Biol Chem.* Aug 29 2003;278(35):33334-41. doi:10.1074/jbc.M305597200
189. Zagurovskaya M, Shareef MM, Das A, et al. EGR-1 forms a complex with YAP-1 and upregulates Bax expression in irradiated prostate carcinoma cells. *Oncogene.* Feb 26 2009;28(8):1121-31. doi:10.1038/onc.2008.461
190. Strano S, Munarriz E, Rossi M, et al. Physical interaction with Yes-associated protein enhances p73 transcriptional activity. *J Biol Chem.* May 4 2001;276(18):15164-73. doi:10.1074/jbc.M010484200
191. Qiao Y, Lin SJ, Chen Y, et al. RUNX3 is a novel negative regulator of oncogenic TEAD-YAP complex in gastric cancer. *Oncogene.* May 19 2016;35(20):2664-74. doi:10.1038/onc.2015.338
192. Ferrigno O, Lallemand F, Verrecchia F, et al. Yes-associated protein (YAP65) interacts with Smad7 and potentiates its inhibitory activity against TGF-beta/Smad signaling. *Oncogene.* Jul 25 2002;21(32):4879-84. doi:10.1038/sj.onc.1205623
193. Vassilev A, Kaneko KJ, Shu H, Zhao Y, DePamphilis ML. TEAD/TEF transcription factors utilize the activation domain of YAP65, a Src/Yes-associated protein localized in the cytoplasm. *Genes Dev.* May 15 2001;15(10):1229-41. doi:10.1101/gad.888601
194. Zhao B, Ye X, Yu J, et al. TEAD mediates YAP-dependent gene induction and growth control. *Genes Dev.* Jul 15 2008;22(14):1962-71. doi:10.1101/gad.1664408
195. Stein C, Bardet AF, Roma G, et al. YAP1 Exerts Its Transcriptional Control via TEAD-Mediated Activation of Enhancers. *PLoS Genet.* Aug 2015;11(8):e1005465. doi:10.1371/journal.pgen.1005465
196. Zanconato F, Forcato M, Battilana G, et al. Genome-wide association between YAP/TAZ/TEAD and AP-1 at enhancers drives oncogenic growth. *Nat Cell Biol.* Sep 2015;17(9):1218-27. doi:10.1038/ncb3216
197. Plouffe SW, Lin KC, Moore JL, 3rd, et al. The Hippo pathway effector proteins YAP and TAZ have both distinct and overlapping functions in the cell. *J Biol Chem.* Jul 13 2018;293(28):11230-11240. doi:10.1074/jbc.RA118.002715
198. Skibinski A, Breindel JL, Prat A, et al. The Hippo transducer TAZ interacts with the SWI/SNF complex to regulate breast epithelial lineage commitment. *Cell Rep.* Mar 27 2014;6(6):1059-1072. doi:10.1016/j.celrep.2014.02.038
199. Galli GG, Carrara M, Yuan WC, et al. YAP Drives Growth by Controlling Transcriptional Pause Release from Dynamic Enhancers. *Mol Cell.* Oct 15 2015;60(2):328-37. doi:10.1016/j.molcel.2015.09.001
200. Zanconato F, Battilana G, Forcato M, et al. Transcriptional addiction in cancer cells is mediated by YAP/TAZ through BRD4. *Nat Med.* Oct 2018;24(10):1599-1610. doi:10.1038/s41591-018-0158-8

201. Oh H, Slattery M, Ma L, White KP, Mann RS, Irvine KD. Yorkie promotes transcription by recruiting a histone methyltransferase complex. *Cell Rep.* Jul 24 2014;8(2):449-59. doi:10.1016/j.celrep.2014.06.017
202. Cho YS, Li S, Wang X, et al. CDK7 regulates organ size and tumor growth by safeguarding the Hippo pathway effector Yki/Yap/Taz in the nucleus. *Genes Dev.* Jan 1 2020;34(1-2):53-71. doi:10.1101/gad.333146.119
203. Hoxha S, Shepard A, Troutman S, et al. YAP-Mediated Recruitment of YY1 and EZH2 Represses Transcription of Key Cell-Cycle Regulators. *Cancer Res.* Jun 15 2020;80(12):2512-2522. doi:10.1158/0008-5472.CAN-19-2415
204. Kim M, Kim T, Johnson RL, Lim DS. Transcriptional co-repressor function of the hippo pathway transducers YAP and TAZ. *Cell Rep.* Apr 14 2015;11(2):270-82. doi:10.1016/j.celrep.2015.03.015
205. Piccolo S, Panciera T, Contessotto P, Cordenonsi M. YAP/TAZ as master regulators in cancer: modulation, function and therapeutic approaches. *Nat Cancer.* Jan 2023;4(1):9-26. doi:10.1038/s43018-022-00473-z
206. He L, Yuan L, Yu W, et al. A Regulation Loop between YAP and NR4A1 Balances Cell Proliferation and Apoptosis. *Cell Rep.* Oct 20 2020;33(3):108284. doi:10.1016/j.celrep.2020.108284
207. Beyer TA, Weiss A, Khomchuk Y, et al. Switch enhancers interpret TGF-beta and Hippo signaling to control cell fate in human embryonic stem cells. *Cell Rep.* Dec 26 2013;5(6):1611-24. doi:10.1016/j.celrep.2013.11.021
208. Cai D, Feliciano D, Dong P, et al. Phase separation of YAP reorganizes genome topology for long-term YAP target gene expression. *Nat Cell Biol.* Dec 2019;21(12):1578-1589. doi:10.1038/s41556-019-0433-z
209. Szulzewsky F, Holland EC, Vasioukhin V. YAP1 and its fusion proteins in cancer initiation, progression and therapeutic resistance. *Dev Biol.* Jul 2021;475:205-221. doi:10.1016/j.ydbio.2020.12.018
210. Huang J, Wu S, Barrera J, Matthews K, Pan D. The Hippo signaling pathway coordinately regulates cell proliferation and apoptosis by inactivating Yorkie, the Drosophila Homolog of YAP. *Cell.* Aug 12 2005;122(3):421-34. doi:10.1016/j.cell.2005.06.007
211. Dong J, Feldmann G, Huang J, et al. Elucidation of a universal size-control mechanism in Drosophila and mammals. *Cell.* Sep 21 2007;130(6):1120-33. doi:10.1016/j.cell.2007.07.019
212. Zhao B, Wei X, Li W, et al. Inactivation of YAP oncoprotein by the Hippo pathway is involved in cell contact inhibition and tissue growth control. *Genes Dev.* Nov 1 2007;21(21):2747-61. doi:10.1101/gad.1602907
213. Camargo FD, Gokhale S, Johnnidis JB, et al. YAP1 increases organ size and expands undifferentiated progenitor cells. *Curr Biol.* Dec 4 2007;17(23):2054-60. doi:10.1016/j.cub.2007.10.039
214. Chan SW, Lim CJ, Guo K, et al. A role for TAZ in migration, invasion, and tumorigenesis of breast cancer cells. *Cancer Res.* Apr 15 2008;68(8):2592-8. doi:10.1158/0008-5472.CAN-07-2696
215. Overholtzer M, Zhang J, Smolen GA, et al. Transforming properties of YAP, a candidate oncogene on the chromosome 11q22 amplicon. *Proc Natl Acad Sci U S A.* Aug 15 2006;103(33):12405-10. doi:10.1073/pnas.0605579103
216. Mizuno T, Murakami H, Fujii M, et al. YAP induces malignant mesothelioma cell proliferation by upregulating transcription of cell cycle-promoting genes. *Oncogene.* Dec 6 2012;31(49):5117-22. doi:10.1038/onc.2012.5
217. Tschaharganeh DF, Chen X, Latzko P, et al. Yes-associated protein up-regulates Jagged-1 and activates the Notch pathway in human hepatocellular carcinoma. *Gastroenterology.* Jun 2013;144(7):1530-1542 e12. doi:10.1053/j.gastro.2013.02.009
218. Basu S, Totty NF, Irwin MS, Sudol M, Downward J. Akt phosphorylates the Yes-associated protein, YAP, to induce interaction with 14-3-3 and attenuation of p73-mediated apoptosis. *Mol Cell.* Jan 2003;11(1):11-23. doi:10.1016/s1097-2765(02)00776-1
219. Strano S, Monti O, Pediconi N, et al. The transcriptional coactivator Yes-associated protein drives p73 gene-target specificity in response to DNA Damage. *Mol Cell.* May 13 2005;18(4):447-59. doi:10.1016/j.molcel.2005.04.008
220. Levy D, Adamovich Y, Reuven N, Shaul Y. Yap1 phosphorylation by c-Abl is a critical step in selective activation of proapoptotic genes in response to DNA damage. *Mol Cell.* Feb 15 2008;29(3):350-61. doi:10.1016/j.molcel.2007.12.022
221. Jin L, Chen Y, Cheng D, et al. YAP inhibits autophagy and promotes progression of colorectal cancer via upregulating Bcl-2 expression. *Cell Death Dis.* May 7 2021;12(5):457. doi:10.1038/s41419-021-03722-8

222. Genevet A, Tapon N. The Hippo pathway and apico-basal cell polarity. *Biochem J*. Jun 1 2011;436(2):213-24. doi:10.1042/BJ20110217
223. Liu X, Li H, Rajurkar M, et al. Tead and AP1 Coordinate Transcription and Motility. *Cell Rep*. Feb 9 2016;14(5):1169-1180. doi:10.1016/j.celrep.2015.12.104
224. Lamar JM, Stern P, Liu H, Schindler JW, Jiang ZG, Hynes RO. The Hippo pathway target, YAP, promotes metastasis through its TEAD-interaction domain. *Proc Natl Acad Sci U S A*. Sep 11 2012;109(37):E2441-50. doi:10.1073/pnas.1212021109
225. Shao DD, Xue W, Krall EB, et al. KRAS and YAP1 converge to regulate EMT and tumor survival. *Cell*. Jul 3 2014;158(1):171-84. doi:10.1016/j.cell.2014.06.004
226. Kim MH, Kim J, Hong H, et al. Actin remodeling confers BRAF inhibitor resistance to melanoma cells through YAP/TAZ activation. *EMBO J*. Mar 1 2016;35(5):462-78. doi:10.15252/embj.201592081
227. Lin L, Sabnis AJ, Chan E, et al. The Hippo effector YAP promotes resistance to RAF- and MEK-targeted cancer therapies. *Nat Genet*. Mar 2015;47(3):250-6. doi:10.1038/ng.3218
228. Hugo W, Shi H, Sun L, et al. Non-genomic and Immune Evolution of Melanoma Acquiring MAPKi Resistance. *Cell*. Sep 10 2015;162(6):1271-85. doi:10.1016/j.cell.2015.07.061
229. Yeung B, Khanal P, Mehta V, Trinkle-Mulcahy L, Yang X. Identification of Cdk1-LATS-Pin1 as a Novel Signaling Axis in Anti-tubulin Drug Response of Cancer Cells. *Mol Cancer Res*. Jun 2018;16(6):1035-1045. doi:10.1158/1541-7786.MCR-17-0684
230. Mohamed Z, Hassan MK, Okasha S, et al. miR-363 confers taxane resistance in ovarian cancer by targeting the Hippo pathway member, LATS2. *Oncotarget*. Jul 10 2018;9(53):30053-30065. doi:10.18632/oncotarget.25698
231. Wang MY, Chen PS, Prakash E, et al. Connective tissue growth factor confers drug resistance in breast cancer through concomitant up-regulation of Bcl-xL and cIAP1. *Cancer Res*. Apr 15 2009;69(8):3482-91. doi:10.1158/0008-5472.CAN-08-2524
232. Tsai HC, Huang CY, Su HL, Tang CH. CTGF increases drug resistance to paclitaxel by upregulating survivin expression in human osteosarcoma cells. *Biochim Biophys Acta*. May 2014;1843(5):846-54. doi:10.1016/j.bbamcr.2014.01.007
233. Menendez JA, Vellon L, Mehmi I, Teng PK, Griggs DW, Lupu R. A novel CYR61-triggered 'CYR61-alpha-vbeta3 integrin loop' regulates breast cancer cell survival and chemosensitivity through activation of ERK1/ERK2 MAPK signaling pathway. *Oncogene*. Jan 27 2005;24(5):761-79. doi:10.1038/sj.onc.1208238
234. Lin MT, Chang CC, Chen ST, et al. Cyr61 expression confers resistance to apoptosis in breast cancer MCF-7 cells by a mechanism of NF-kappaB-dependent XIAP up-regulation. *J Biol Chem*. Jun 4 2004;279(23):24015-23. doi:10.1074/jbc.M402305200
235. Miao J, Hsu PC, Yang YL, et al. YAP regulates PD-L1 expression in human NSCLC cells. *Oncotarget*. Dec 29 2017;8(70):114576-114587. doi:10.18632/oncotarget.23051
236. Lee BS, Park DI, Lee DH, et al. Hippo effector YAP directly regulates the expression of PD-L1 transcripts in EGFR-TKI-resistant lung adenocarcinoma. *Biochem Biophys Res Commun*. Sep 16 2017;491(2):493-499. doi:10.1016/j.bbrc.2017.07.007
237. Janse van Rensburg HJ, Azad T, Ling M, et al. The Hippo Pathway Component TAZ Promotes Immune Evasion in Human Cancer through PD-L1. *Cancer Res*. Mar 15 2018;78(6):1457-1470. doi:10.1158/0008-5472.CAN-17-3139
238. Hsu PC, Miao J, Wang YC, et al. Inhibition of yes-associated protein down-regulates PD-L1 (CD274) expression in human malignant pleural mesothelioma. *J Cell Mol Med*. Jun 2018;22(6):3139-3148. doi:10.1111/jcmm.13593
239. Kim MH, Kim CG, Kim SK, et al. YAP-Induced PD-L1 Expression Drives Immune Evasion in BRAFi-Resistant Melanoma. *Cancer Immunol Res*. Mar 2018;6(3):255-266. doi:10.1158/2326-6066.CIR-17-0320
240. Yu M, Peng Z, Qin M, et al. Interferon-gamma induces tumor resistance to anti-PD-1 immunotherapy by promoting YAP phase separation. *Mol Cell*. Mar 18 2021;81(6):1216-1230 e9. doi:10.1016/j.molcel.2021.01.010
241. Gentles AJ, Newman AM, Liu CL, et al. The prognostic landscape of genes and infiltrating immune cells across human cancers. *Nat Med*. Aug 2015;21(8):938-945. doi:10.1038/nm.3909
242. Ni X, Tao J, Barbi J, et al. YAP Is Essential for Treg-Mediated Suppression of Antitumor Immunity. *Cancer Discov*. Aug 2018;8(8):1026-1043. doi:10.1158/2159-8290.CD-17-1124
243. Fan Y, Gao Y, Rao J, Wang K, Zhang F, Zhang C. YAP-1 Promotes Tregs Differentiation in Hepatocellular Carcinoma by Enhancing TGFBR2 Transcription. *Cell Physiol Biochem*. 2017;41(3):1189-1198. doi:10.1159/000464380

244. Liu S, Knochelmann HM, Lomeli SH, et al. Response and recurrence correlates in individuals treated with neoadjuvant anti-PD-1 therapy for resectable oral cavity squamous cell carcinoma. *Cell Rep Med*. Oct 19 2021;2(10):100411. doi:10.1016/j.xcrm.2021.100411
245. Geng J, Yu S, Zhao H, et al. The transcriptional coactivator TAZ regulates reciprocal differentiation of T(H)17 cells and T(reg) cells. *Nat Immunol*. Jul 2017;18(7):800-812. doi:10.1038/ni.3748
246. Stampouloglou E, Cheng N, Federico A, et al. Yap suppresses T-cell function and infiltration in the tumor microenvironment. *PLoS Biol*. Jan 2020;18(1):e3000591. doi:10.1371/journal.pbio.3000591
247. Lebid A, Chung L, Pardoll DM, Pan F. YAP Attenuates CD8 T Cell-Mediated Anti-tumor Response. *Front Immunol*. 2020;11:580. doi:10.3389/fimmu.2020.00580
248. Owonikoko TK, Dwivedi B, Chen Z, et al. YAP1 Expression in SCLC Defines a Distinct Subtype With T-cell-Inflamed Phenotype. *J Thorac Oncol*. Mar 2021;16(3):464-476. doi:10.1016/j.jtho.2020.11.006
249. Hu X, Zhang Y, Yu H, et al. The role of YAP1 in survival prediction, immune modulation, and drug response: A pan-cancer perspective. *Front Immunol*. 2022;13:1012173. doi:10.3389/fimmu.2022.1012173
250. Yin N, Liu Y, Weems C, et al. Protein kinase Ciota mediates immunosuppression in lung adenocarcinoma. *Sci Transl Med*. Nov 16 2022;14(671):eabq5931. doi:10.1126/scitranslmed.abq5931
251. Wang G, Lu X, Dey P, et al. Targeting YAP-Dependent MDSC Infiltration Impairs Tumor Progression. *Cancer Discov*. Jan 2016;6(1):80-95. doi:10.1158/2159-8290.CD-15-0224
252. Murakami S, Shahbazian D, Surana R, et al. Yes-associated protein mediates immune reprogramming in pancreatic ductal adenocarcinoma. *Oncogene*. Mar 2 2017;36(9):1232-1244. doi:10.1038/onc.2016.288
253. Yang R, Cai TT, Wu XJ, et al. Tumour YAP1 and PTEN expression correlates with tumour-associated myeloid suppressor cell expansion and reduced survival in colorectal cancer. *Immunology*. Oct 2018;155(2):263-272. doi:10.1111/imm.12949
254. Mills CD, Kincaid K, Alt JM, Heilman MJ, Hill AM. M-1/M-2 macrophages and the Th1/Th2 paradigm. *J Immunol*. Jun 15 2000;164(12):6166-73. doi:10.4049/jimmunol.164.12.6166
255. Chen P, Zhao D, Li J, et al. Symbiotic Macrophage-Glioma Cell Interactions Reveal Synthetic Lethality in PTEN-Null Glioma. *Cancer Cell*. Jun 10 2019;35(6):868-884 e6. doi:10.1016/j.ccell.2019.05.003
256. Nie P, Zhang W, Meng Y, et al. A YAP/TAZ-CD54 axis is required for CXCR2-CD44- tumor-specific neutrophils to suppress gastric cancer. *Protein Cell*. Jun 28 2023;14(7):513-531. doi:10.1093/procel/pwac045
257. Calvo F, Ege N, Grande-Garcia A, et al. Mechanotransduction and YAP-dependent matrix remodelling is required for the generation and maintenance of cancer-associated fibroblasts. *Nat Cell Biol*. Jun 2013;15(6):637-46. doi:10.1038/ncb2756
258. Panciera T, Citron A, Di Biagio D, et al. Reprogramming normal cells into tumour precursors requires ECM stiffness and oncogene-mediated changes of cell mechanical properties. *Nat Mater*. Jul 2020;19(7):797-806. doi:10.1038/s41563-020-0615-x
259. Meng KP, Majedi FS, Thauland TJ, Butte MJ. Mechanosensing through YAP controls T cell activation and metabolism. *J Exp Med*. Aug 3 2020;217(8)doi:10.1084/jem.20200053
260. Meli VS, Atcha H, Veerasubramanian PK, et al. YAP-mediated mechanotransduction tunes the macrophage inflammatory response. *Sci Adv*. Dec 2020;6(49)doi:10.1126/sciadv.abb8471
261. Basu D, Lettan R, Damodaran K, Strellec S, Reyes-Mugica M, Rebbaa A. Identification, mechanism of action, and antitumor activity of a small molecule inhibitor of hippo, TGF-beta, and Wnt signaling pathways. *Mol Cancer Ther*. Jun 2014;13(6):1457-67. doi:10.1158/1535-7163.MCT-13-0918
262. Song S, Xie M, Scott AW, et al. A Novel YAP1 Inhibitor Targets CSC-Enriched Radiation-Resistant Cells and Exerts Strong Antitumor Activity in Esophageal Adenocarcinoma. *Mol Cancer Ther*. Feb 2018;17(2):443-454. doi:10.1158/1535-7163.MCT-17-0560
263. Kandasamy S, Adhikary G, Rorke EA, et al. The YAP1 Signaling Inhibitors, Verteporfin and CA3, Suppress the Mesothelioma Cancer Stem Cell Phenotype. *Mol Cancer Res*. Mar 2020;18(3):343-351. doi:10.1158/1541-7786.MCR-19-0914
264. Liu-Chittenden Y, Huang B, Shim JS, et al. Genetic and pharmacological disruption of the TEAD-YAP complex suppresses the oncogenic activity of YAP. *Genes Dev*. Jun 15 2012;26(12):1300-5. doi:10.1101/gad.192856.112
265. Zhang H, Ramakrishnan SK, Triner D, et al. Tumor-selective proteotoxicity of verteporfin inhibits colon cancer progression independently of YAP1. *Sci Signal*. Oct 6 2015;8(397):ra98. doi:10.1126/scisignal.aac5418

266. Dasari VR, Mazack V, Feng W, Nash J, Carey DJ, Gogoi R. Verteporfin exhibits YAP-independent anti-proliferative and cytotoxic effects in endometrial cancer cells. *Oncotarget*. Apr 25 2017;8(17):28628-28640. doi:10.18632/oncotarget.15614
267. Condurat AL, Aminzadeh-Gohari S, Malnar M, et al. Verteporfin-induced proteotoxicity impairs cell homeostasis and survival in neuroblastoma subtypes independent of YAP/TAZ expression. *Sci Rep*. Mar 7 2023;13(1):3760. doi:10.1038/s41598-023-29796-2
268. Noland CL, Gierke S, Schnier PD, et al. Palmitoylation of TEAD Transcription Factors Is Required for Their Stability and Function in Hippo Pathway Signaling. *Structure*. Jan 5 2016;24(1):179-186. doi:10.1016/j.str.2015.11.005
269. Lu W, Wang J, Li Y, et al. Discovery and biological evaluation of vinylsulfonamide derivatives as highly potent, covalent TEAD autopalmitoylation inhibitors. *Eur J Med Chem*. Dec 15 2019;184:111767. doi:10.1016/j.ejmech.2019.111767
270. Kaneda A, Seike T, Danjo T, et al. The novel potent TEAD inhibitor, K-975, inhibits YAP1/TAZ-TEAD protein-protein interactions and exerts an anti-tumor effect on malignant pleural mesothelioma. *Am J Cancer Res*. 2020;10(12):4399-4415.
271. Kurppa KJ, Liu Y, To C, et al. Treatment-Induced Tumor Dormancy through YAP-Mediated Transcriptional Reprogramming of the Apoptotic Pathway. *Cancer Cell*. Jan 13 2020;37(1):104-122 e12. doi:10.1016/j.ccell.2019.12.006
272. Bum-Erdene K, Zhou D, Gonzalez-Gutierrez G, et al. Small-Molecule Covalent Modification of Conserved Cysteine Leads to Allosteric Inhibition of the TEAD-Yap Protein-Protein Interaction. *Cell Chem Biol*. Mar 21 2019;26(3):378-389 e13. doi:10.1016/j.chembiol.2018.11.010
273. Tang TT, Konradi AW, Feng Y, et al. Small Molecule Inhibitors of TEAD Auto-palmitoylation Selectively Inhibit Proliferation and Tumor Growth of NF2-deficient Mesothelioma. *Mol Cancer Ther*. Jun 2021;20(6):986-998. doi:10.1158/1535-7163.MCT-20-0717
274. Pobbati AV, Han X, Hung AW, et al. Targeting the Central Pocket in Human Transcription Factor TEAD as a Potential Cancer Therapeutic Strategy. *Structure*. Nov 3 2015;23(11):2076-86. doi:10.1016/j.str.2015.09.009
275. Holden JK, Crawford JJ, Noland CL, et al. Small Molecule Dysregulation of TEAD Lipidation Induces a Dominant-Negative Inhibition of Hippo Pathway Signaling. *Cell Rep*. Jun 23 2020;31(12):107809. doi:10.1016/j.celrep.2020.107809
276. Hagenbeek TJ, Zbieg JR, Hafner M, et al. An allosteric pan-TEAD inhibitor blocks oncogenic YAP/TAZ signaling and overcomes KRAS G12C inhibitor resistance. *Nat Cancer*. Jun 2023;4(6):812-828. doi:10.1038/s43018-023-00577-0
277. Li Q, Sun Y, Jarugumilli GK, et al. Lats1/2 Sustain Intestinal Stem Cells and Wnt Activation through TEAD-Dependent and Independent Transcription. *Cell Stem Cell*. May 7 2020;26(5):675-692 e8. doi:10.1016/j.stem.2020.03.002
278. Smith SA, Sessions RB, Shoemark DK, et al. Antiproliferative and Antimigratory Effects of a Novel YAP-TEAD Interaction Inhibitor Identified Using in Silico Molecular Docking. *J Med Chem*. Feb 14 2019;62(3):1291-1305. doi:10.1021/acs.jmedchem.8b01402
279. Jiao S, Wang H, Shi Z, et al. A peptide mimicking VGLL4 function acts as a YAP antagonist therapy against gastric cancer. *Cancer Cell*. Feb 10 2014;25(2):166-80. doi:10.1016/j.ccr.2014.01.010
280. Sun Y, Hu L, Tao Z, et al. Pharmacological blockade of TEAD-YAP reveals its therapeutic limitation in cancer cells. *Nat Commun*. Nov 8 2022;13(1):6744. doi:10.1038/s41467-022-34559-0
281. Seong BK, Fathers KE, Hallett R, et al. A Metastatic Mouse Model Identifies Genes That Regulate Neuroblastoma Metastasis. *Cancer Res*. 02 2017;77(3):696-706. doi:10.1158/0008-5472.CAN-16-1502
282. Cai Y, Chen K, Cheng C, et al. Prp19 Is an Independent Prognostic Marker and Promotes Neuroblastoma Metastasis by Regulating the Hippo-YAP Signaling Pathway. *Front Oncol*. 2020;10:575366. doi:10.3389/fonc.2020.575366
283. Wang M, Liu Y, Zou J, et al. Transcriptional co-activator TAZ sustains proliferation and tumorigenicity of neuroblastoma by targeting CTGF and PDGF-beta. *Oncotarget*. Apr 20 2015;6(11):9517-30. doi:10.18632/oncotarget.3367
284. Wang Q, Xu Z, An Q, et al. TAZ promotes epithelial to mesenchymal transition via the upregulation of connective tissue growth factor expression in neuroblastoma cells. *Mol Med Rep*. Feb 2015;11(2):982-8. doi:10.3892/mmr.2014.2818

285. Canzonetta C, Pelosi A, Di Matteo S, et al. Identification of neuroblastoma cell lines with uncommon TAZ+/mesenchymal stromal cell phenotype with strong suppressive activity on natural killer cells. *J Immunother Cancer*. 01 2021;9(1)doi:10.1136/jitc-2020-001313
286. Shim J, Goldsmith KC. A New Player in Neuroblastoma: YAP and Its Role in the Neuroblastoma Microenvironment. *Cancers (Basel)*. Sep 16 2021;13(18)doi:10.3390/cancers13184650
287. Chien YH, Iwashima M, Kaplan KB, Elliott JF, Davis MM. A new T-cell receptor gene located within the alpha locus and expressed early in T-cell differentiation. *Nature*. Jun 25-Jul 1 1987;327(6124):677-82. doi:10.1038/327677a0
288. Saito H, Kranz DM, Takagaki Y, Hayday AC, Eisen HN, Tonegawa S. Complete primary structure of a heterodimeric T-cell receptor deduced from cDNA sequences. *Nature*. Jun 28-Jul 4 1984;309(5971):757-62. doi:10.1038/309757a0
289. Petrie HT, Scollay R, Shortman K. Commitment to the T cell receptor-alpha beta or -gamma delta lineages can occur just prior to the onset of CD4 and CD8 expression among immature thymocytes. *Eur J Immunol*. Aug 1992;22(8):2185-8. doi:10.1002/eji.1830220836
290. Dudley EC, Girardi M, Owen MJ, Hayday AC. Alpha beta and gamma delta T cells can share a late common precursor. *Curr Biol*. Jun 1 1995;5(6):659-69. doi:10.1016/s0960-9822(95)00131-x
291. Saura-Esteller J, de Jong M, King LA, et al. Gamma Delta T-Cell Based Cancer Immunotherapy: Past-Present-Future. *Front Immunol*. 2022;13:915837. doi:10.3389/fimmu.2022.915837
292. Janeway CA, Jr., Jones B, Hayday A. Specificity and function of T cells bearing gamma delta receptors. *Immunol Today*. Mar 1988;9(3):73-6. doi:10.1016/0167-5699(88)91267-4
293. Lefranc MP, Rabbitts TH. The human T-cell receptor gamma (TRG) genes. *Trends Biochem Sci*. Jun 1989;14(6):214-8. doi:10.1016/0968-0004(89)90029-7
294. Lawand M, Dechanet-Merville J, Dieu-Nosjean MC. Key Features of Gamma-Delta T-Cell Subsets in Human Diseases and Their Immunotherapeutic Implications. *Front Immunol*. 2017;8:761. doi:10.3389/fimmu.2017.00761
295. McMurray JL, von Borstel A, Taher TE, et al. Transcriptional profiling of human Vdelta1 T cells reveals a pathogen-driven adaptive differentiation program. *Cell Rep*. May 24 2022;39(8):110858. doi:10.1016/j.celrep.2022.110858
296. Vantourout P, Hayday A. Six-of-the-best: unique contributions of $\gamma\delta$ T cells to immunology. *Nat Rev Immunol*. Feb 2013;13(2):88-100. doi:10.1038/nri3384
297. Mangan BA, Dunne MR, O'Reilly VP, et al. Cutting edge: CD1d restriction and Th1/Th2/Th17 cytokine secretion by human Vdelta3 T cells. *J Immunol*. Jul 1 2013;191(1):30-4. doi:10.4049/jimmunol.1300121
298. Sutton KS, Dasgupta A, McCarty D, Doering CB, Spencer HT. Bioengineering and serum free expansion of blood-derived gammadelta T cells. *Cytotherapy*. Jul 2016;18(7):881-92. doi:10.1016/j.jcyt.2016.04.001
299. Zoine JT, Knight KA, Fleischer LC, et al. Ex vivo expanded patient-derived $\gamma\delta$ T-cell immunotherapy enhances neuroblastoma tumor regression in a murine model. *Oncoimmunology*. 2019 2019;8(8):1593804. doi:10.1080/2162402X.2019.1593804
300. Jonus HC, Burnham RE, Ho A, et al. Dissecting the cellular components of ex vivo $\gamma\delta$ T cell expansions to optimize selection of potent cell therapy donors for neuroblastoma immunotherapy trials. *Oncoimmunology*. 2022;11(1):2057012. doi:10.1080/2162402X.2022.2057012
301. Raverdeau M, Cunningham SP, Harmon C, Lynch L. gammadelta T cells in cancer: a small population of lymphocytes with big implications. *Clin Transl Immunology*. 2019;8(10):e01080. doi:10.1002/cti2.1080
302. Ma C, Zhang Q, Ye J, et al. Tumor-infiltrating gammadelta T lymphocytes predict clinical outcome in human breast cancer. *J Immunol*. Nov 15 2012;189(10):5029-36. doi:10.4049/jimmunol.1201892
303. Peng G, Wang HY, Peng W, Kiniwa Y, Seo KH, Wang RF. Tumor-infiltrating gammadelta T cells suppress T and dendritic cell function via mechanisms controlled by a unique toll-like receptor signaling pathway. *Immunity*. Aug 2007;27(2):334-48. doi:10.1016/j.immuni.2007.05.020
304. Wu P, Wu D, Ni C, et al. gammadeltaT17 cells promote the accumulation and expansion of myeloid-derived suppressor cells in human colorectal cancer. *Immunity*. May 15 2014;40(5):785-800. doi:10.1016/j.immuni.2014.03.013
305. Silva-Santos B, Mensurado S, Coffelt SB. $\gamma\delta$ T cells: pleiotropic immune effectors with therapeutic potential in cancer. *Nat Rev Cancer*. 07 2019;19(7):392-404. doi:10.1038/s41568-019-0153-5

306. Coffelt SB, Kersten K, Doornebal CW, et al. IL-17-producing gammadelta T cells and neutrophils conspire to promote breast cancer metastasis. *Nature*. Jun 18 2015;522(7556):345-348. doi:10.1038/nature14282
307. Rei M, Pennington DJ, Silva-Santos B. The emerging Protumor role of gammadelta T lymphocytes: implications for cancer immunotherapy. *Cancer Res*. Mar 1 2015;75(5):798-802. doi:10.1158/0008-5472.CAN-14-3228
308. Mullen PJ, Yu R, Longo J, Archer MC, Penn LZ. The interplay between cell signalling and the mevalonate pathway in cancer. *Nat Rev Cancer*. Nov 2016;16(11):718-731. doi:10.1038/nrc.2016.76
309. Harly C, Guillaume Y, Nedellec S, et al. Key implication of CD277/butyrophilin-3 (BTN3A) in cellular stress sensing by a major human gammadelta T-cell subset. *Blood*. Sep 13 2012;120(11):2269-79. doi:10.1182/blood-2012-05-430470
310. Hsiao CC, Nguyen K, Jin Y, Vinogradova O, Wiemer AJ. Ligand-induced interactions between butyrophilin 2A1 and 3A1 internal domains in the HMBPP receptor complex. *Cell Chem Biol*. Jun 16 2022;29(6):985-995 e5. doi:10.1016/j.chembiol.2022.01.004
311. Silva-Santos B, Serre K, Norell H. gammadelta T cells in cancer. *Nat Rev Immunol*. Nov 2015;15(11):683-91. doi:10.1038/nri3904
312. Rincon-Orozco B, Kunzmann V, Wrobel P, Kabelitz D, Steinle A, Herrmann T. Activation of V gamma 9V delta 2 T cells by NKG2D. *J Immunol*. Aug 15 2005;175(4):2144-51. doi:10.4049/jimmunol.175.4.2144
313. Wrobel P, Shojaei H, Schitteck B, et al. Lysis of a broad range of epithelial tumour cells by human gamma delta T cells: involvement of NKG2D ligands and T-cell receptor- versus NKG2D-dependent recognition. *Scand J Immunol*. Aug-Sep 2007;66(2-3):320-8. doi:10.1111/j.1365-3083.2007.01963.x
314. Toutirais O, Cabillic F, Le Fric G, et al. DNAX accessory molecule-1 (CD226) promotes human hepatocellular carcinoma cell lysis by Vgamma9Vdelta2 T cells. *Eur J Immunol*. May 2009;39(5):1361-8. doi:10.1002/eji.200838409
315. Bauer S, Groh V, Wu J, et al. Activation of NK cells and T cells by NKG2D, a receptor for stress-inducible MICA. *Science*. Jul 30 1999;285(5428):727-9. doi:10.1126/science.285.5428.727
316. Dokouhaki P, Schuh NW, Joe B, et al. NKG2D regulates production of soluble TRAIL by ex vivo expanded human gammadelta T cells. *Eur J Immunol*. Dec 2013;43(12):3175-82. doi:10.1002/eji.201243150
317. Tokuyama H, Hagi T, Mattarollo SR, et al. V gamma 9 V delta 2 T cell cytotoxicity against tumor cells is enhanced by monoclonal antibody drugs--rituximab and trastuzumab. *Int J Cancer*. Jun 1 2008;122(11):2526-34. doi:10.1002/ijc.23365
318. Gertner-Dardenne J, Bonnafous C, Bezombes C, et al. Bromohydrin pyrophosphate enhances antibody-dependent cell-mediated cytotoxicity induced by therapeutic antibodies. *Blood*. May 14 2009;113(20):4875-84. doi:10.1182/blood-2008-08-172296
319. Riond J, Rodriguez S, Nicolau ML, al Saati T, Gairin JE. In vivo major histocompatibility complex class I (MHCI) expression on MHCIIow tumor cells is regulated by gammadelta T and NK cells during the early steps of tumor growth. *Cancer Immun*. Nov 2 2009;9:10.
320. Brandes M, Willmann K, Moser B. Professional antigen-presentation function by human gammadelta T Cells. *Science*. Jul 8 2005;309(5732):264-8. doi:10.1126/science.1110267
321. Altwater B, Pscherer S, Landmeier S, et al. Activated human gammadelta T cells induce peptide-specific CD8+ T-cell responses to tumor-associated self-antigens. *Cancer Immunol Immunother*. Mar 2012;61(3):385-96. doi:10.1007/s00262-011-1111-6
322. Holmen Olofsson G, Idorn M, Carnaz Simoes AM, et al. Vgamma9Vdelta2 T Cells Concurrently Kill Cancer Cells and Cross-Present Tumor Antigens. *Front Immunol*. 2021;12:645131. doi:10.3389/fimmu.2021.645131
323. Himoudi N, Morgenstern DA, Yan M, et al. Human gammadelta T lymphocytes are licensed for professional antigen presentation by interaction with opsonized target cells. *J Immunol*. Feb 15 2012;188(4):1708-16. doi:10.4049/jimmunol.1102654
324. Maniar A, Zhang X, Lin W, et al. Human gammadelta T lymphocytes induce robust NK cell-mediated antitumor cytotoxicity through CD137 engagement. *Blood*. Sep 9 2010;116(10):1726-33. doi:10.1182/blood-2009-07-234211
325. Caccamo N, Battistini L, Bonneville M, et al. CXCR5 identifies a subset of Vgamma9Vdelta2 T cells which secrete IL-4 and IL-10 and help B cells for antibody production. *J Immunol*. Oct 15 2006;177(8):5290-5. doi:10.4049/jimmunol.177.8.5290

326. Bansal RR, Mackay CR, Moser B, Eberl M. IL-21 enhances the potential of human gammadelta T cells to provide B-cell help. *Eur J Immunol*. Jan 2012;42(1):110-9. doi:10.1002/eji.201142017
327. Mensurado S, Blanco-Domínguez R, Silva-Santos B. The emerging roles of $\gamma\delta$ T cells in cancer immunotherapy. *Nat Rev Clin Oncol*. Jan 09 2023;doi:10.1038/s41571-022-00722-1
328. Pressey JG, Adams J, Harkins L, Kelly D, You Z, Lamb LS, Jr. In vivo expansion and activation of gammadelta T cells as immunotherapy for refractory neuroblastoma: A phase 1 study. *Medicine (Baltimore)*. Sep 2016;95(39):e4909. doi:10.1097/MD.0000000000004909
329. Dieli F, Vermijlen D, Fulfaro F, et al. Targeting human gammadelta T cells with zoledronate and interleukin-2 for immunotherapy of hormone-refractory prostate cancer. *Cancer Res*. Aug 1 2007;67(15):7450-7. doi:10.1158/0008-5472.CAN-07-0199
330. Meraviglia S, Eberl M, Vermijlen D, et al. In vivo manipulation of Vgamma9Vdelta2 T cells with zoledronate and low-dose interleukin-2 for immunotherapy of advanced breast cancer patients. *Clin Exp Immunol*. Aug 2010;161(2):290-7. doi:10.1111/j.1365-2249.2010.04167.x
331. Bennouna J, Bompas E, Neidhardt EM, et al. Phase-I study of Innacell gammadelta, an autologous cell-therapy product highly enriched in gamma9delta2 T lymphocytes, in combination with IL-2, in patients with metastatic renal cell carcinoma. *Cancer Immunol Immunother*. Nov 2008;57(11):1599-609. doi:10.1007/s00262-008-0491-8
332. Wilhelm M, Kunzmann V, Eckstein S, et al. Gammadelta T cells for immune therapy of patients with lymphoid malignancies. *Blood*. Jul 1 2003;102(1):200-6. doi:10.1182/blood-2002-12-3665
333. Hoeres T, Smetak M, Pretscher D, Wilhelm M. Improving the Efficiency of Vgamma9Vdelta2 T-Cell Immunotherapy in Cancer. *Front Immunol*. 2018;9:800. doi:10.3389/fimmu.2018.00800
334. Lamb LS, Pereboeva L, Youngblood S, et al. A combined treatment regimen of MGMT-modified gammadelta T cells and temozolomide chemotherapy is effective against primary high grade gliomas. *Sci Rep*. Oct 26 2021;11(1):21133. doi:10.1038/s41598-021-00536-8
335. Deniger DC, Switzer K, Mi T, et al. Bispecific T-cells expressing polyclonal repertoire of endogenous gammadelta T-cell receptors and introduced CD19-specific chimeric antigen receptor. *Mol Ther*. Mar 2013;21(3):638-47. doi:10.1038/mt.2012.267
336. Zhai X, You F, Xiang S, et al. MUC1-Tn-targeting chimeric antigen receptor-modified Vgamma9Vdelta2 T cells with enhanced antigen-specific anti-tumor activity. *Am J Cancer Res*. 2021;11(1):79-91.
337. Capsomidis A, Benthall G, Van Acker HH, et al. Chimeric Antigen Receptor-Engineered Human Gamma Delta T Cells: Enhanced Cytotoxicity with Retention of Cross Presentation. *Mol Ther*. Feb 7 2018;26(2):354-365. doi:10.1016/j.ymthe.2017.12.001
338. Ang WX, Ng YY, Xiao L, et al. Electroporation of NKG2D RNA CAR Improves Vgamma9Vdelta2 T Cell Responses against Human Solid Tumor Xenografts. *Mol Ther Oncolytics*. Jun 26 2020;17:421-430. doi:10.1016/j.omto.2020.04.013
339. Almeida AR, Correia DV, Fernandes-Platzgummer A, et al. Delta One T Cells for Immunotherapy of Chronic Lymphocytic Leukemia: Clinical-Grade Expansion/Differentiation and Preclinical Proof of Concept. *Clin Cancer Res*. Dec 1 2016;22(23):5795-5804. doi:10.1158/1078-0432.CCR-16-0597
340. Ferry GM, Agbuduwe C, Forrester M, et al. A Simple and Robust Single-Step Method for CAR-Vdelta1 gammadeltaT Cell Expansion and Transduction for Cancer Immunotherapy. *Front Immunol*. 2022;13:863155. doi:10.3389/fimmu.2022.863155
341. Sanchez Martinez D, Tirado N, Mensurado S, et al. Generation and proof-of-concept for allogeneic CD123 CAR-Delta One T (DOT) cells in acute myeloid leukemia. *J Immunother Cancer*. Sep 2022;10(9)doi:10.1136/jitc-2022-005400
342. Makkouk A, Yang XC, Barca T, et al. Off-the-shelf Vdelta1 gamma delta T cells engineered with glypican-3 (GPC-3)-specific chimeric antigen receptor (CAR) and soluble IL-15 display robust antitumor efficacy against hepatocellular carcinoma. *J Immunother Cancer*. Dec 2021;9(12)doi:10.1136/jitc-2021-003441
343. Ganesan R, Chennupati V, Ramachandran B, Hansen MR, Singh S, Grewal IS. Selective recruitment of gammadelta T cells by a bispecific antibody for the treatment of acute myeloid leukemia. *Leukemia*. Aug 2021;35(8):2274-2284. doi:10.1038/s41375-021-01122-7
344. de Weerd I, Lameris R, Ruben JM, et al. A Bispecific Single-Domain Antibody Boosts Autologous Vgamma9Vdelta2-T Cell Responses Toward CD1d in Chronic Lymphocytic Leukemia. *Clin Cancer Res*. Mar 15 2021;27(6):1744-1755. doi:10.1158/1078-0432.CCR-20-4576

345. Lameris R, Ruben JM, Iglesias-Guimaraes V, et al. A bispecific T cell engager recruits both type 1 NKT and Vgamma9Vdelta2-T cells for the treatment of CD1d-expressing hematological malignancies. *Cell Rep Med*. Mar 21 2023;4(3):100961. doi:10.1016/j.xcrm.2023.100961
346. de Weerd I, Lameris R, Scheffer GL, et al. A Bispecific Antibody Antagonizes Prosurvival CD40 Signaling and Promotes Vgamma9Vdelta2 T cell-Mediated Antitumor Responses in Human B-cell Malignancies. *Cancer Immunol Res*. Jan 2021;9(1):50-61. doi:10.1158/2326-6066.CIR-20-0138
347. de Bruin RCG, Veluchamy JP, Loughheed SM, et al. A bispecific nanobody approach to leverage the potent and widely applicable tumor cytolytic capacity of Vgamma9Vdelta2-T cells. *Oncoimmunology*. 2017;7(1):e1375641. doi:10.1080/2162402X.2017.1375641
348. Oberg HH, Peipp M, Kellner C, et al. Novel bispecific antibodies increase gammadelta T-cell cytotoxicity against pancreatic cancer cells. *Cancer Res*. Mar 1 2014;74(5):1349-60. doi:10.1158/0008-5472.CAN-13-0675
349. Dong T, Wu N, Gao H, et al. CD277 agonist enhances the immunogenicity of relapsed/refractory acute myeloid leukemia towards Vdelta2(+) T cell cytotoxicity. *Ann Hematol*. Oct 2022;101(10):2195-2208. doi:10.1007/s00277-022-04930-8
350. van Diest E, Hernandez Lopez P, Meringa AD, et al. Gamma delta TCR anti-CD3 bispecific molecules (GABs) as novel immunotherapeutic compounds. *J Immunother Cancer*. Nov 2021;9(11)doi:10.1136/jitc-2021-003850
351. Huang SW, Pan CM, Lin YC, et al. BiTE-Secreting CAR-gammadeltaT as a Dual Targeting Strategy for the Treatment of Solid Tumors. *Adv Sci (Weinh)*. Jun 2023;10(17):e2206856. doi:10.1002/advs.202206856
352. Marcu-Malina V, Heijhuurs S, van Buuren M, et al. Redirecting alphabeta T cells against cancer cells by transfer of a broadly tumor-reactive gammadeltaT-cell receptor. *Blood*. Jul 7 2011;118(1):50-9. doi:10.1182/blood-2010-12-325993
353. Straetemans T, Kierkels GJJ, Doorn R, et al. GMP-Grade Manufacturing of T Cells Engineered to Express a Defined gammadeltaTCR. *Front Immunol*. 2018;9:1062. doi:10.3389/fimmu.2018.01062
354. Johanna I, Straetemans T, Heijhuurs S, et al. Evaluating in vivo efficacy - toxicity profile of TEG001 in humanized mice xenografts against primary human AML disease and healthy hematopoietic cells. *J Immunother Cancer*. Mar 12 2019;7(1):69. doi:10.1186/s40425-019-0558-4
355. de Vries NL, van de Haar J, Veninga V, et al. gammadelta T cells are effectors of immunotherapy in cancers with HLA class I defects. *Nature*. Jan 2023;613(7945):743-750. doi:10.1038/s41586-022-05593-1
356. Schilbach KE, Geiselhart A, Wessels JT, Niethammer D, Handgretinger R. Human gammadelta T lymphocytes exert natural and IL-2-induced cytotoxicity to neuroblastoma cells. *J Immunother*. Sep-Oct 2000;23(5):536-48. doi:10.1097/O0002371-200009000-00004
357. Nishio N, Fujita M, Tanaka Y, et al. Zoledronate sensitizes neuroblastoma-derived tumor-initiating cells to cytotoxicity mediated by human gammadelta T cells. *J Immunother*. Oct 2012;35(8):598-606. doi:10.1097/CJI.0b013e31826a745a
358. Otto M, Barfield RC, Martin WJ, et al. Combination immunotherapy with clinical-scale enriched human gammadelta T cells, hu14.18 antibody, and the immunocytokine Fc-IL7 in disseminated neuroblastoma. *Clin Cancer Res*. Dec 1 2005;11(23):8486-91. doi:10.1158/1078-0432.CCR-05-1184
359. Schilbach K, Frommer K, Meier S, Handgretinger R, Eyrich M. Immune response of human propagated gammadelta-T-cells to neuroblastoma recommend the Vdelta1+ subset for gammadelta-T-cell-based immunotherapy. *J Immunother*. Nov-Dec 2008;31(9):896-905. doi:10.1097/CJI.0b013e31818955ad
360. Zeidan YH, Hannun YA. Translational aspects of sphingolipid metabolism. *Trends Mol Med*. Aug 2007;13(8):327-36. doi:10.1016/j.molmed.2007.06.002
361. Hanada K, Kumagai K, Yasuda S, et al. Molecular machinery for non-vesicular trafficking of ceramide. *Nature*. Dec 18 2003;426(6968):803-9. doi:10.1038/nature02188
362. Sterner E, Peach ML, Nicklaus MC, Gildersleeve JC. Therapeutic Antibodies to Ganglioside GD2 Evolved from Highly Selective Germline Antibodies. *Cell Rep*. Aug 15 2017;20(7):1681-1691. doi:10.1016/j.celrep.2017.07.050
363. Bieberich E, Freischutz B, Liour SS, Yu RK. Regulation of ganglioside metabolism by phosphorylation and dephosphorylation. *J Neurochem*. Sep 1998;71(3):972-9. doi:10.1046/j.1471-4159.1998.71030972.x
364. Simpson MA, Cross H, Proukakis C, et al. Infantile-onset symptomatic epilepsy syndrome caused by a homozygous loss-of-function mutation of GM3 synthase. *Nat Genet*. Nov 2004;36(11):1225-9. doi:10.1038/ng1460

365. Boukhris A, Schule R, Loureiro JL, et al. Alteration of ganglioside biosynthesis responsible for complex hereditary spastic paraplegia. *Am J Hum Genet.* Jul 11 2013;93(1):118-23. doi:10.1016/j.ajhg.2013.05.006
366. Li TA, Schnaar RL. Congenital Disorders of Ganglioside Biosynthesis. *Prog Mol Biol Transl Sci.* 2018;156:63-82. doi:10.1016/bs.pmbts.2018.01.001
367. Cutillo G, Saariaho AH, Meri S. Physiology of gangliosides and the role of antiganglioside antibodies in human diseases. *Cell Mol Immunol.* Apr 2020;17(4):313-322. doi:10.1038/s41423-020-0388-9
368. d'Azzo A, Tessitore A, Sano R. Gangliosides as apoptotic signals in ER stress response. *Cell Death Differ.* Mar 2006;13(3):404-14. doi:10.1038/sj.cdd.4401834
369. Irie RF, Giuliano AE, Morton DL. Oncofetal antigen: a tumor-associated fetal antigen immunogenic in man. *J Natl Cancer Inst.* Aug 1979;63(2):367-73.
370. Katano M, Sidell N, Irie RF. Human monoclonal antibody to a neuroectodermal tumor antigen (OFA-I-2). *Ann N Y Acad Sci.* 1983;417:427-34. doi:10.1111/j.1749-6632.1983.tb32884.x
371. Saito M, Yu RK, Cheung NK. Ganglioside GD2 specificity of monoclonal antibodies to human neuroblastoma cell. *Biochem Biophys Res Commun.* Feb 28 1985;127(1):1-7. doi:10.1016/so006-291x(85)80117-0
372. Pinho SS, Reis CA. Glycosylation in cancer: mechanisms and clinical implications. *Nat Rev Cancer.* Sep 2015;15(9):540-55. doi:10.1038/nrc3982
373. Julien S, Bobowski M, Steenackers A, Le Bourhis X, Delannoy P. How Do Gangliosides Regulate RTKs Signaling? *Cells.* Dec 6 2013;2(4):751-67. doi:10.3390/cells2040751
374. Cazet A, Bobowski M, Rombouts Y, et al. The ganglioside G(D2) induces the constitutive activation of c-Met in MDA-MB-231 breast cancer cells expressing the G(D3) synthase. *Glycobiology.* Jun 2012;22(6):806-16. doi:10.1093/glycob/cws049
375. Mansoori M, Roudi R, Abbasi A, et al. High GD2 expression defines breast cancer cells with enhanced invasiveness. *Exp Mol Pathol.* Aug 2019;109:25-35. doi:10.1016/j.yexmp.2019.05.001
376. Kailayangiri S, Altvater B, Meltzer J, et al. The ganglioside antigen G(D2) is surface-expressed in Ewing sarcoma and allows for MHC-independent immune targeting. *Br J Cancer.* Mar 13 2012;106(6):1123-33. doi:10.1038/bjc.2012.57
377. Longee DC, Wikstrand CJ, Mansson JE, et al. Disialoganglioside GD2 in human neuroectodermal tumor cell lines and gliomas. *Acta Neuropathol.* 1991;82(1):45-54. doi:10.1007/BF00310922
378. Cheresh DA, Klier FG. Disialoganglioside GD2 distributes preferentially into substrate-associated microprocesses on human melanoma cells during their attachment to fibronectin. *J Cell Biol.* May 1986;102(5):1887-97. doi:10.1083/jcb.102.5.1887
379. Schulz G, Cheresh DA, Varki NM, Yu A, Staffileno LK, Reisfeld RA. Detection of ganglioside GD2 in tumor tissues and sera of neuroblastoma patients. *Cancer Res.* Dec 1984;44(12 Pt 1):5914-20.
380. Yoshida S, Fukumoto S, Kawaguchi H, Sato S, Ueda R, Furukawa K. Ganglioside G(D2) in small cell lung cancer cell lines: enhancement of cell proliferation and mediation of apoptosis. *Cancer Res.* May 15 2001;61(10):4244-52.
381. Roth M, Linkowski M, Tarim J, et al. Ganglioside GD2 as a therapeutic target for antibody-mediated therapy in patients with osteosarcoma. *Cancer.* Feb 15 2014;120(4):548-54. doi:10.1002/cncr.28461
382. Peguet-Navarro J, Sportouch M, Popa I, Berthier O, Schmitt D, Portoukalian J. Gangliosides from human melanoma tumors impair dendritic cell differentiation from monocytes and induce their apoptosis. *J Immunol.* Apr 1 2003;170(7):3488-94. doi:10.4049/jimmunol.170.7.3488
383. Sarkar TR, Battula VL, Werden SJ, et al. GD3 synthase regulates epithelial-mesenchymal transition and metastasis in breast cancer. *Oncogene.* Jun 04 2015;34(23):2958-67. doi:10.1038/onc.2014.245
384. Nazha B, Inal C, Owonikoko TK. Disialoganglioside GD2 Expression in Solid Tumors and Role as a Target for Cancer Therapy. *Front Oncol.* 2020;10:1000. doi:10.3389/fonc.2020.01000
385. Cheresh DA, Pierschbacher MD, Herzig MA, Mujoo K. Disialogangliosides GD2 and GD3 are involved in the attachment of human melanoma and neuroblastoma cells to extracellular matrix proteins. *J Cell Biol.* Mar 1986;102(3):688-96. doi:10.1083/jcb.102.3.688
386. Wu ZL, Schwartz E, Seeger R, Ladisch S. Expression of GD2 ganglioside by untreated primary human neuroblastomas. *Cancer Res.* Jan 1986;46(1):440-3.
387. Corrias MV, Parodi S, Haupt R, et al. Detection of GD2-positive cells in bone marrow samples and survival of patients with localised neuroblastoma. *Br J Cancer.* Jan 29 2008;98(2):263-9. doi:10.1038/sj.bjc.6604179

388. Navid F, Sondel PM, Barfield R, et al. Phase I trial of a novel anti-GD2 monoclonal antibody, Hu14.18K322A, designed to decrease toxicity in children with refractory or recurrent neuroblastoma. *J Clin Oncol*. May 10 2014;32(14):1445-52. doi:10.1200/JCO.2013.50.4423
389. Sait S, Modak S. Anti-GD2 immunotherapy for neuroblastoma. *Expert Rev Anticancer Ther*. Oct 2017;17(10):889-904. doi:10.1080/14737140.2017.1364995
390. Mora J. Dinutuximab for the treatment of pediatric patients with high-risk neuroblastoma. *Expert Rev Clin Pharmacol*. 2016;9(5):647-53. doi:10.1586/17512433.2016.1160775
391. Dhillon S. Dinutuximab: first global approval. *Drugs*. May 2015;75(8):923-7. doi:10.1007/s40265-015-0399-5
392. Yu AL, Gilman AL, Ozkaynak MF, et al. Anti-GD2 antibody with GM-CSF, interleukin-2, and isotretinoin for neuroblastoma. *N Engl J Med*. Sep 30 2010;363(14):1324-34. doi:10.1056/NEJMoa0911123
393. Yu AL, Gilman AL, Ozkaynak MF, et al. Long-Term Follow-up of a Phase III Study of ch14.18 (Dinutuximab) + Cytokine Immunotherapy in Children with High-Risk Neuroblastoma: COG Study ANBL0032. *Clin Cancer Res*. 04 15 2021;27(8):2179-2189. doi:10.1158/1078-0432.CCR-20-3909
394. Mount CW, Majzner RG, Sundares S, et al. Potent antitumor efficacy of anti-GD2 CAR T cells in H3-K27M(+) diffuse midline gliomas. *Nat Med*. May 2018;24(5):572-579. doi:10.1038/s41591-018-0006-x
395. Majzner RG, Ramakrishna S, Yeom KW, et al. GD2-CAR T cell therapy for H3K27M-mutated diffuse midline gliomas. *Nature*. Mar 2022;603(7903):934-941. doi:10.1038/s41586-022-04489-4
396. Del Bufalo F, De Angelis B, Caruana I, et al. GD2-CART01 for Relapsed or Refractory High-Risk Neuroblastoma. *N Engl J Med*. Apr 06 2023;388(14):1284-1295. doi:10.1056/NEJMoa2210859
397. Kalinovskiy DV, Kibardin AV, Kholodenko IV, et al. Therapeutic efficacy of antibody-drug conjugates targeting GD2-positive tumors. *J Immunother Cancer*. Jun 2022;10(6)doi:10.1136/jitc-2022-004646
398. Kwon HY, Dae HM, Song NR, Kim KS, Kim CH, Lee YC. Valproic acid induces transcriptional activation of human GD3 synthase (hST8Sia I) in SK-N-BE(2)-C human neuroblastoma cells. *Mol Cells*. Jan 31 2009;27(1):113-8. doi:10.1007/s10059-009-0012-4
399. van den Bijgaart RJE, Kroesen M, Wassink M, et al. Combined sialic acid and histone deacetylase (HDAC) inhibitor treatment up-regulates the neuroblastoma antigen GD2. *J Biol Chem*. 03 22 2019;294(12):4437-4449. doi:10.1074/jbc.RA118.002763
400. Mabe NW, Huang M, Dalton GN, et al. Transition to a mesenchymal state in neuroblastoma confers resistance to anti-GD2 antibody via reduced expression of ST8SIA1. *Nat Cancer*. Jul 11 2022;doi:10.1038/s43018-022-00405-x
401. van den Bijgaart RJE, Kroesen M, Brok IC, et al. Anti-GD2 antibody and Vorinostat immunocombination therapy is highly effective in an aggressive orthotopic neuroblastoma model. *Oncoimmunology*. 09 20 2020;9(1):1817653. doi:10.1080/2162402X.2020.1817653
402. Theruvath J, Menard M, Smith BAH, et al. Anti-GD2 synergizes with CD47 blockade to mediate tumor eradication. *Nat Med*. 02 2022;28(2):333-344. doi:10.1038/s41591-021-01625-x
403. Richman SA, Nunez-Cruz S, Moghimi B, et al. High-Affinity GD2-Specific CAR T Cells Induce Fatal Encephalitis in a Preclinical Neuroblastoma Model. *Cancer Immunol Res*. 01 2018;6(1):36-46. doi:10.1158/2326-6066.CIR-17-0211
404. Moghimi B, Muthugounder S, Jambon S, et al. Preclinical assessment of the efficacy and specificity of GD2-B7H3 SynNotch CAR-T in metastatic neuroblastoma. *Nat Commun*. Jan 21 2021;12(1):511. doi:10.1038/s41467-020-20785-x
405. Majzner RG, Weber EW, Lynn RC, Xu P, Mackall CL. Neurotoxicity Associated with a High-Affinity GD2 CAR-Letter. *Cancer Immunol Res*. Apr 2018;6(4):494-495. doi:10.1158/2326-6066.CIR-18-0089
406. Heczey A, Louis CU, Savoldo B, et al. CAR T Cells Administered in Combination with Lymphodepletion and PD-1 Inhibition to Patients with Neuroblastoma. *Mol Ther*. Sep 06 2017;25(9):2214-2224. doi:10.1016/j.ymthe.2017.05.012
407. Gargett T, Yu W, Dotti G, et al. GD2-specific CAR T Cells Undergo Potent Activation and Deletion Following Antigen Encounter but can be Protected From Activation-induced Cell Death by PD-1 Blockade. *Mol Ther*. Jun 2016;24(6):1135-1149. doi:10.1038/mt.2016.63
408. Anderson J, Majzner RG, Sondel PM. Immunotherapy of Neuroblastoma: Facts and Hopes. *Clin Cancer Res*. Aug 2 2022;28(15):3196-3206. doi:10.1158/1078-0432.CCR-21-1356

409. Straathof K, Flutter B, Wallace R, et al. Antitumor activity without on-target off-tumor toxicity of GD2-chimeric antigen receptor T cells in patients with neuroblastoma. *Sci Transl Med.* 11 25 2020;12(571)doi:10.1126/scitranslmed.abd6169
410. Xu X, Huang W, Heczey A, et al. NKT Cells Coexpressing a GD2-Specific Chimeric Antigen Receptor and IL15 Show Enhanced In Vivo Persistence and Antitumor Activity against Neuroblastoma. *Clin Cancer Res.* 12 01 2019;25(23):7126-7138. doi:10.1158/1078-0432.CCR-19-0421
411. Heczey A, Courtney AN, Montalbano A, et al. Anti-GD2 CAR-NKT cells in patients with relapsed or refractory neuroblastoma: an interim analysis. *Nat Med.* 11 2020;26(11):1686-1690. doi:10.1038/s41591-020-1074-2
412. Heczey A, Xu X, Courtney AN, et al. Anti-GD2 CAR-NKT cells in relapsed or refractory neuroblastoma: updated phase 1 trial interim results. *Nat Med.* Jun 2023;29(6):1379-1388. doi:10.1038/s41591-023-02363-y
413. London WB, Bagatell R, Weigel BJ, et al. Historical time to disease progression and progression-free survival in patients with recurrent/refractory neuroblastoma treated in the modern era on Children's Oncology Group early-phase trials. *Cancer.* Dec 15 2017;123(24):4914-4923. doi:10.1002/cncr.30934
414. Chen L, Humphreys A, Turnbull L, et al. Identification of different ALK mutations in a pair of neuroblastoma cell lines established at diagnosis and relapse. *Oncotarget.* Dec 27 2016;7(52):87301-87311. doi:10.18632/oncotarget.13541
415. Schulte M, Köster J, Rahmann S, Schramm A. Cancer evolution, mutations, and clonal selection in relapse neuroblastoma. *Cell Tissue Res.* May 2018;372(2):263-268. doi:10.1007/s00441-018-2810-5
416. Yagi R, Chen LF, Shigesada K, Murakami Y, Ito Y. A WW domain-containing yes-associated protein (YAP) is a novel transcriptional co-activator. *EMBO J.* May 04 1999;18(9):2551-62. doi:10.1093/emboj/18.9.2551
417. Ahmed AA, Mohamed AD, Gener M, Li W, Taboada E. YAP and the Hippo pathway in pediatric cancer. *Mol Cell Oncol.* 2017;4(3):e1295127. doi:10.1080/23723556.2017.1295127
418. Ladisch S, Wu ZL. Detection of a tumour-associated ganglioside in plasma of patients with neuroblastoma. *Lancet.* Jan 19 1985;1(8421):136-8. doi:10.1016/s0140-6736(85)91906-3
419. Sariola H, Terävä H, Rapola J, Saarinen UM. Cell-surface ganglioside GD2 in the immunohistochemical detection and differential diagnosis of neuroblastoma. *Am J Clin Pathol.* Aug 1991;96(2):248-52. doi:10.1093/ajcp/96.2.248
420. Kushner BH, Cheung IY, Modak S, Basu EM, Roberts SS, Cheung NK. Humanized 3F8 Anti-GD2 Monoclonal Antibody Dosing With Granulocyte-Macrophage Colony-Stimulating Factor in Patients With Resistant Neuroblastoma: A Phase 1 Clinical Trial. *JAMA Oncol.* Dec 01 2018;4(12):1729-1735. doi:10.1001/jamaoncol.2018.4005
421. Blom T, Lurvink R, Aleven L, et al. Treatment-Related Toxicities During Anti-GD2 Immunotherapy in High-Risk Neuroblastoma Patients. *Front Oncol.* 2020;10:601076. doi:10.3389/fonc.2020.601076
422. Ozkaynak MF, Gilman AL, London WB, et al. A Comprehensive Safety Trial of Chimeric Antibody 14.18 With GM-CSF, IL-2, and Isotretinoin in High-Risk Neuroblastoma Patients Following Myeloablative Therapy: Children's Oncology Group Study ANBL0931. *Front Immunol.* 2018;9:1355. doi:10.3389/fimmu.2018.01355
423. Majzner RG, Mackall CL. Tumor Antigen Escape from CAR T-cell Therapy. *Cancer Discov.* Oct 2018;8(10):1219-1226. doi:10.1158/2159-8290.CD-18-0442
424. Terzic T, Cordeau M, Herblot S, et al. Expression of Disialoganglioside (GD2) in Neuroblastic Tumors: A Prognostic Value for Patients Treated With Anti-GD2 Immunotherapy. *Pediatr Dev Pathol.* 2018;21(4):355-362. doi:10.1177/1093526617723972
425. Schumacher-Kuckelkorn R, Hero B, Ernestus K, Berthold F. Lacking immunocytological GD2 expression in neuroblastoma: report of 3 cases. *Pediatr Blood Cancer.* Aug 2005;45(2):195-201. doi:10.1002/pbc.20301
426. Schumacher-Kuckelkorn R, Volland R, Gradehandt A, Hero B, Simon T, Berthold F. Lack of immunocytological GD2 expression on neuroblastoma cells in bone marrow at diagnosis, during treatment, and at recurrence. *Pediatr Blood Cancer.* Jan 2017;64(1):46-56. doi:10.1002/pbc.26184
427. Alter G, Malenfant JM, Altfeld M. CD107a as a functional marker for the identification of natural killer cell activity. *J Immunol Methods.* Nov 2004;294(1-2):15-22. doi:10.1016/j.jim.2004.08.008
428. Rubio V, Stuge TB, Singh N, et al. Ex vivo identification, isolation and analysis of tumor-cytolytic T cells. *Nat Med.* Nov 2003;9(11):1377-82. doi:10.1038/nm942

429. Betts MR, Brenchley JM, Price DA, et al. Sensitive and viable identification of antigen-specific CD8+ T cells by a flow cytometric assay for degranulation. *J Immunol Methods*. Oct 01 2003;281(1-2):65-78. doi:10.1016/S0022-1759(03)00265-5
430. Gao Y, Yang W, Pan M, et al. Gamma delta T cells provide an early source of interferon gamma in tumor immunity. *J Exp Med*. Aug 04 2003;198(3):433-42. doi:10.1084/jem.20030584
431. Zhang R, Banik NL, Ray SK. Combination of all-trans retinoic acid and interferon-gamma suppressed PI3K/Akt survival pathway in glioblastoma T98G cells whereas NF-kappaB survival signaling in glioblastoma U87MG cells for induction of apoptosis. *Neurochem Res*. Dec 2007;32(12):2194-202. doi:10.1007/s11064-007-9417-7
432. Gilman AL, Ozkaynak MF, Matthay KK, et al. Phase I study of ch14.18 with granulocyte-macrophage colony-stimulating factor and interleukin-2 in children with neuroblastoma after autologous bone marrow transplantation or stem-cell rescue: a report from the Children's Oncology Group. *J Clin Oncol*. Jan 01 2009;27(1):85-91. doi:10.1200/JCO.2006.10.3564
433. Stokes ME, Small JC, Vasciaveo A, et al. Mesenchymal subtype neuroblastomas are addicted to TGF- β R2/HMGCR-driven protein geranylgeranylation. *Sci Rep*. Jul 01 2020;10(1):10748. doi:10.1038/s41598-020-67310-0
434. Hamamura K, Tsuji M, Hotta H, et al. Functional activation of Src family kinase yes protein is essential for the enhanced malignant properties of human melanoma cells expressing ganglioside GD3. *J Biol Chem*. May 27 2011;286(21):18526-37. doi:10.1074/jbc.M110.164798
435. Ohkawa Y, Momota H, Kato A, et al. Ganglioside GD3 Enhances Invasiveness of Gliomas by Forming a Complex with Platelet-derived Growth Factor Receptor alpha and Yes Kinase. *J Biol Chem*. Jun 26 2015;290(26):16043-58. doi:10.1074/jbc.M114.635755
436. Yeh SC, Wang PY, Lou YW, et al. Glycolipid GD3 and GD3 synthase are key drivers for glioblastoma stem cells and tumorigenicity. *Proc Natl Acad Sci U S A*. May 17 2016;113(20):5592-7. doi:10.1073/pnas.1604721113
437. Ko K, Furukawa K, Takahashi T, et al. Fundamental study of small interfering RNAs for ganglioside GD3 synthase gene as a therapeutic target of lung cancers. *Oncogene*. Nov 2 2006;25(52):6924-35. doi:10.1038/sj.onc.1209683
438. Hamamura K, Furukawa K, Hayashi T, et al. Ganglioside GD3 promotes cell growth and invasion through p130Cas and paxillin in malignant melanoma cells. *Proc Natl Acad Sci U S A*. Aug 2 2005;102(31):11041-6. doi:10.1073/pnas.0503658102
439. Cao S, Hu X, Ren S, et al. The biological role and immunotherapy of gangliosides and GD3 synthase in cancers. *Front Cell Dev Biol*. 2023;11:1076862. doi:10.3389/fcell.2023.1076862
440. Ruan S, Raj BK, Lloyd KO. Relationship of glycosyltransferases and mRNA levels to ganglioside expression in neuroblastoma and melanoma cells. *J Neurochem*. Feb 1999;72(2):514-21. doi:10.1046/j.1471-4159.1999.0720514.x
441. De Maria R, Lenti L, Malisan F, et al. Requirement for GD3 ganglioside in CD95- and ceramide-induced apoptosis. *Science*. Sep 12 1997;277(5332):1652-5. doi:10.1126/science.277.5332.1652
442. Nardone G, Oliver-De La Cruz J, Vrbsky J, et al. YAP regulates cell mechanics by controlling focal adhesion assembly. *Nat Commun*. May 15 2017;8:15321. doi:10.1038/ncomms15321
443. Weng RR, Lu HH, Lin CT, et al. Epigenetic modulation of immune synaptic-cytoskeletal networks potentiates $\gamma\delta$ T cell-mediated cytotoxicity in lung cancer. *Nat Commun*. 04 12 2021;12(1):2163. doi:10.1038/s41467-021-22433-4

